


REPORT DOCUMENTATION PAGE			Form Approved OMB No. 0704-0188	
Public reporting burden for this collection of information is estimated to average 1 hour per response, including the time for reviewing instructions, searching existing data sources, gathering and maintaining the data needed, and completing and reviewing the collection of information. Send comments regarding this burden estimate or any other aspect of this collection of information, including suggestions for reducing this burden, to Washington Headquarters Services, Directorate for Information Operations and Reports, 1215 Jefferson Davis Highway, Suite 1204, Arlington, VA 22202-4302, and to the Office of Management and Budget, Paperwork Reduction Project (0704-0188) Washington, DC 20503.				
1. AGENCY USE ONLY (Leave Blank)	2. REPORT DATE September 1995	3. REPORT TYPE AND DATES COVERED Final		
4. TITLE AND SUBTITLE Paleoclimatic Reconstruction's from Owens Lake Core OL-92, Southeastern California		5. FUNDING NUMBERS		
6. AUTHORS Kristen Margaret Menking		AFRL-SR-BL-TR-98-		
7. PERFORMING ORGANIZATION NAME(S) AND ADDRESS(ES) University of California, Santa Cruz				
9. SPONSORING/MONITORING AGENCY NAME(S) AND ADDRESS(ES) AFOSR/NI 110 Duncan Avenue, Room B-115 Bolling Air Force Base, DC 20332-8080		10. SPONSORING/MONITORING AGENCY REPORT NUMBER		
11. SUPPLEMENTARY NOTES				
12a. DISTRIBUTION AVAILABILITY STATEMENT Approved for Public Release		12b. DISTRIBUTION CODE		
13. ABSTRACT (Maximum 200 words) See attached.				
19980115 191				
14. SUBJECT TERMS		15. NUMBER OF PAGES		
		16. PRICE CODE		
17. SECURITY CLASSIFICATION OF REPORT Unclassified	18. SECURITY CLASSIFICATION OF THIS PAGE Unclassified	19. SECURITY CLASSIFICATION OF ABSTRACT Unclassified	20. LIMITATION OF ABSTRACT UL	

OCT 20 1995
JAM

Copyright © by

Kirsten Margaret Menking

1995

Permission to reprint is granted for individuals to make single copies for personal use in research, study, or teaching and to use short quotes, figures, and tables from this dissertation for publication in environmental or scientific books and journals. There is no charge for these uses; the author requests only that the source be cited appropriately.

TABLE OF CONTENTS

Chapter 1: Introduction	1
Chapter 2: Climatic Signals in Clay Mineralogy and Grain-Size Variations in Owens Lake Core OL-92, Eastern California	8
Abstract.....	8
Introduction.....	9
Previous Work.....	10
Lacustrine Grain Size and its Relation to Climate Change	10
Clay Minerals in the Owens Lake System	11
Original Hypotheses.....	12
Grain-Size Analyses	13
Sample Types.....	13
Methods	14
Grain -Size Analysis of Point Samples.....	14
Sand, Silt, and Clay Contents of Channel Samples	15
Results of the grain-size analyses.....	16
Clay Mineralogical Analyses	20
Methods	20
X-Ray Diffraction Techniques.	20
Artificial mixtures.	20
Results of the X-Ray Diffraction Analysis	22
Results of the artificial clay-mixture experiments.....	28
Discussion.....	30

Comparison of grain size and clay-mineral variations to other paleoclimate proxies.....	36
Conclusions.....	38
Acknowledgments.....	39
Chapter 3: A Model of Runoff, Evaporation, and Overspill in the Owens River System of Lakes, Eastern California.....	
Abstract.....	40
Introduction.....	41
Tectonic and Climatic Setting	47
Previous work and constraints on Pleistocene paleoclimate in the Sierra Nevada region.....	49
Paleoclimatic evidence	49
Paleoclimatic calculations and models	55
Model.....	57
Theoretical Background	57
Lake Level Calculations.....	57
Isotopic Calculations	63
Construction of the Model.....	65
Lake hypsometries.....	66
Runoff.	66
Evaporation.....	68
Assumptions.....	68
Experiments	71
Steady-state Calculations.....	71
Sinusoidally Varying Runoff and Evaporation.....	79

Runoff and Evaporation Driven by the Marine Oxygen Isotopic Record	84
Sensitivity Analyses.....	87
Discussion and Conclusions.....	100
Acknowledgments.....	107
Chapter 4: Sub-Milankovitch Climatic Variations Recorded in Core	
OL-92, Owens Lake, Southeastern California	108
Abstract.....	108
Introduction.....	109
Location and Geologic Setting.....	112
The Owens Lake Core, Southeastern California.....	114
Methods	118
Results.....	119
Carbonate Content.....	123
Oxygen and Carbon Isotopic Values	125
Grain Size Analyses.....	125
Correlations and Time-Series Analysis	126
Discussion.....	128
Measurement error	136
Overspill from Mono Lake.....	136
Incorporation of detrital carbonate from the White and Inyo Mts.	143
Climatic Implications and Conclusions.....	149
Acknowledgments.....	152
References.....	153

LIST OF FIGURES

Fig. 1.1. Location Map.....	2
Fig. 2.1. Grain size of point and channel samples.....	17
Fig. 2.2. Mean grain size of point samples for top 200 m.....	18
Fig. 2.3. Typical X-ray diffraction scans from core OL-92.....	24
Fig. 2.4. Ratio of clay peak areas to quartz peak areas.....	25
Fig. 2.5. Smectite/quartz and plagioclase/K-feldspar with depth.....	26
Fig. 2.6. Relative abundances of clay minerals in clay-size fraction.....	27
Fig. 2.7. Artificial mixtures of clay and non-clays.....	29
Fig. 2.8. Comparison of Owens Lake records to marine isotopic record.....	35
Fig. 3.1. Location map.....	42
Fig. 3.2. Lake hypsometries used in the model.....	44
Fig. 3.3. Comparison of OL-92 records to marine isotopic record.....	45
Fig. 3.4. Area-volume relationships for lake chain.....	59
Fig. 3.5a. Lake response time for different basin geometries.....	62
Fig. 3.5b. Lake response time versus runoff and evaporation.....	62
Fig. 3.6. Response of Owens Lake to modern steady climate forcing.....	72
Fig. 3.7. Response time versus runoff for Owens Lake.....	74
Fig. 3.8. Response of lake chain to modern steady climate forcing.....	75
Fig. 3.9. Response of Owens Lake to drought conditions.....	77
Fig. 3.10. $\delta^{18}\text{O}$ values for different runoffs in Owens Lake.....	78
Fig. 3.11a. Climatic forcing functions, 100 year period.....	80
Fig. 3.11b. Lake level history for 100 year period climatic oscillations.....	80
Fig. 3.11c. Water residence time for 100-yr period climate.....	82

Fig. 3.11d. $\delta^{18}\text{O}$ value for 100 year period climatic oscillations.....	82
Fig. 3.12a. Climatic forcing functions, 20 kyr period.....	83
Fig. 3.12b. Lake level history for 20 kyr period climatic oscillations.....	83
Fig. 3.12c. Water residence time for 20-kyr period climate	85
Fig. 3.12d. $\delta^{18}\text{O}$ value for 20 kyr period climatic oscillations.....	85
Fig. 3.13a. Climatic forcing functions driven by marine isotopic record	88
Fig. 3.13b. Lake level history	88
Fig. 3.13c. Measured and modeled $\delta^{18}\text{O}$ values.....	89
Fig. 3.14. Sensitivity to atmospheric $\delta^{18}\text{O}$ value	91
Fig. 3.15. Sensitivity to calcification temperature	92
Fig. 3.16. Sensitivity to evaporation rate.....	94
Fig. 3.17. Sensitivity to amount of runoff.....	95
Fig. 3.18. Sensitivity to input Owens River isotopic value.....	96
Fig. 3.19. Residence time for different maximum runoffs.....	99
Fig. 3.20. Isotopic evolution of Owens Lake for different model runs.....	101
Fig. 3.21a. Isotopic values for best fit model.....	102
Fig. 3.21b. Modeled isotopic composition and measured carbonate content.....	102
Fig. 3.21c. Lake level history for best-fit model run.....	104
Fig. 4.1. Location map.....	113
Fig. 4.2. Age-depth model for core OL-92.....	115
Fig. 4.3. Comparison of Owens Lake proxies to marine isotopic record (3-m-channels).....	117
Fig. 4.4. Comparison of Owens Lake proxies to marine isotopic record (70-cm-channels	124

Fig. 4.5 Spectral analysis of 70-cm-channel records	129
Fig. 4.6. $\delta^{18}\text{O}$ versus $\delta^{13}\text{C}$ for OL-92 carbonates	133
Fig. 4.7. $\delta^{18}\text{O}$ versus $\delta^{13}\text{C}$ for two data subsets	134
Fig. 4.8a. 3.6x modern runoff in Mono, 1x modern runoff in Owens	140
Fig. 4.8b. 3.6x modern runoff in Mono, 3.6x modern runoff in Owens	140
Fig. 4.8c. 7x modern runoff in Mono, 1x modern runoff in Owens	141
Fig. 4.8d. 7x modern runoff in Mono, 4x modern runoff in Owens	141
Fig. 4.8e. 7x modern runoff in Mono, 7x modern runoff in Owens	142
White-Inyo carbonate rocks	145

LIST OF TABLES

Table 2.1. Grain-size statistics	19
Table 2.2. Mineral diffraction peaks.....	21
Table 3.1. Previous work on Owens chain lakes.....	51
Table 3.2. Paleo-temperature and -precipitation for last glacial maximum.....	54
Table 3.3. Hypsometric information.....	67
Table 3.4. Hydrologic parameters used in model.....	69
Table 4.1. Analysis results	120
Table 4.2. Correlation coefficients for whole sample suite	127
Table 4.3. Correlation coefficients for core subsections.....	127

Paleoclimatic reconstructions from Owens Lake Core OL-92, Southeastern California

KIRSTEN MARGARET MENKING

Earth Sciences Department, University of California, Santa Cruz

ABSTRACT

In 1992, the U.S. Geological Survey cored Owens Lake to obtain a continuous paleoclimate record for the Sierra Nevada region. Owens Lake heads a chain of closed-basin lakes which are separated by a series of bedrock sills, received their water primarily from Sierra Nevadan precipitation, and overflowed during wet periods. The core records the histories of cyclic glaciation of the Sierra Nevada and water-balance of Owens Lake over the past ~800 kyrs. A variety of paleoclimatic proxies have been studied, details of which may be found in Smith and Bischoff (1993). In this thesis, I report the results and interpretations of 1) grain-size and clay-mineralogical analyses performed on 3.5-m-long channel samples (~7500 years of sedimentation per sample) and point samples, 2) grain size, carbonate content, and oxygen isotopic measurements on 70-cm-long channel samples (~1500 years), and 3) a water-balance model used to infer the magnitude of runoff and evaporation changes necessary to fill the lakes in the Owens Lake system, and to determine the response time of the lake chain to climatic perturbations.

The channel sample analyses show that glacial periods are characterized by fine (~5 μm) mean grain size (overflowing lake), and by illite and feldspar in the <2 μm size fraction, interpreted to be glacial rock flour.

Interglacials are marked by coarser ($\sim 15\ \mu\text{m}$) grain size (lake surface below spillway) and by high smectite. Comparison of the $\delta^{18}\text{O}$ record from deep-sea sediments to the smectite percentage and mean grain size reveals striking similarities. The 70-cm-long samples display much higher-frequency water-balance oscillations superimposed upon the long-term glacial-interglacial cycles exhibited in the 3.5-m-long samples.

Results of the lake modeling work show that all of the lakes achieve steady-state volumes within a matter of decades, indicating that droughts or particularly wet periods of order several decades should have been recorded in the sediments of the Owens Lake core. Measured $\delta^{18}\text{O}$ values constrain a modeled lake level history which shows glacials as having experienced 7x modern runoff.

ACKNOWLEDGMENTS

I owe the completion of this thesis to many different people. Many thanks to Bob Kiefer, Jim Price, Carol Downing, Marion Hodges, Noland Wallace, Sue Neal, and Gary Lincoln for encouraging a girl to pursue math and science and for giving me the foundations necessary to achieve my goals many years later. A special thanks is due to Jim Madden for introducing me to geology. I also deeply appreciate the guidance and friendship of my undergraduate advisors Margi Rusmore and Scott Bogue, who solidified my interest in research and teaching, and in pursuing an advanced degree.

Thanks to my advisor, Bob Anderson, for being willing to supervise what turned out to be a paleoclimatic thesis, and for giving me a firm footing in the world of geomorphology as well. His excitement about science is contagious, and his quantitative skill very helpful to my research. In addition, he has always helped me to see the data from many different view points, thereby enhancing my interpretations. For his added perspective, I am extremely thankful. Bob Garrison and Shirley Dreiss both gave me very valuable criticism and feedback on ideas and a good grasp of sedimentology and hydrogeology.

Much of this thesis was carried out in conjunction with members of the U.S. Geological Survey. I am grateful to George Smith and Jim Bischoff for allowing me to become part of the Owens Lake project, and for taking me under their wings, sharing both their vast knowledge of the field area and paleoclimatic research, and their philosophies of research and data collection.

Many thanks to my labmates over the years, Nan Rosenbloom, Jeff Marshall, Rich McDonald, Eric Small, Jim Repka, Alex Densmore, Greg Dick,

Takahisa Furuichi (especially Taka for leaving us the CD-player!), and Lou Gilpin for their friendship, their help, and for allowing me to bounce ideas off onto them. Thanks also to Gretchen Zwart, Julie Blue, Barbara Bekins, Kirby Bunas, Mary Cummins, Daleth Foster, and Ornella Bonamassa-Cazzato for helping me through the difficult parts of graduate school.

Mike Torresan, Mark Johnsson, Dick Hay, Gabe Filipelli, Larry Benson, Fred Phillips, John Fitzpatrick, Jeff Fitts, Hanna Musler, Rob Franks, Kathy Vencill, Blair Jones, Jim Zachos, and Lisa Sloan all assisted me in my research in various ways, either through helping me with data collection or learning new techniques, or through assisting me with various technical and intellectual problems. Many thanks also to Jonathan Glen for many stimulating conversations about the data and life in general, and also for cooking vegetarian food with me on the Coleman camp stove in front of the motel room in Lone Pine where we spent our field season.

Finally, thanks to my family for their unwavering love and support, and to my granting agency, the National Defense Science and Engineering Graduate Fellowship Program, for their financial help.

CHAPTER I

Introduction

Many closed basins in the western U.S. exhibit shoreline features including beach gravels, wave-cut benches, and tufa deposits which indicate that large lakes once existed in what are presently arid regions (Smith and Street-Perrott, 1983; Benson and Thompson, 1987a; Benson and others, 1990). These closed basins have long been recognized for their usefulness in paleoclimatic studies because they act as traps for sediment and runoff from the surrounding mountains (Smith and Street-Perrott, 1983; Benson and Thompson, 1987a). Core studies, in conjunction with dating of shoreline deposits, have enabled the construction of lake-level histories for many of these basins, including the Lahontan system in northwest Nevada (Thompson and others, 1986; Benson and Thompson, 1987b; Lao and Benson, 1988), Lake Bonneville in western Utah (Currey and others, 1984; Oviatt and others, 1987; Oviatt and others, 1992), and the Owens Lake chain of lakes, southeastern California (Gale, 1914; Smith and Pratt, 1957; Smith, 1984; Jannik and others, 1991).

The latter system lies just to the south and east of the Sierra Nevada, and consists of five paleolakes separated by a series of bedrock sills. These lakes received their water primarily from precipitation on the Sierra Nevada (Smith, 1976; Phillips and others, 1992), and overflowed during extremely wet periods (Fig. 1.1). While the modern climate in the region does not support the existence of lakes in any valley but Owens, shoreline and core evidence suggests that all valleys contained significant lakes during parts of the Pleistocene (Smith and Street-Perrott, 1983; Benson and Thompson, 1987a; Smith and others, in press).

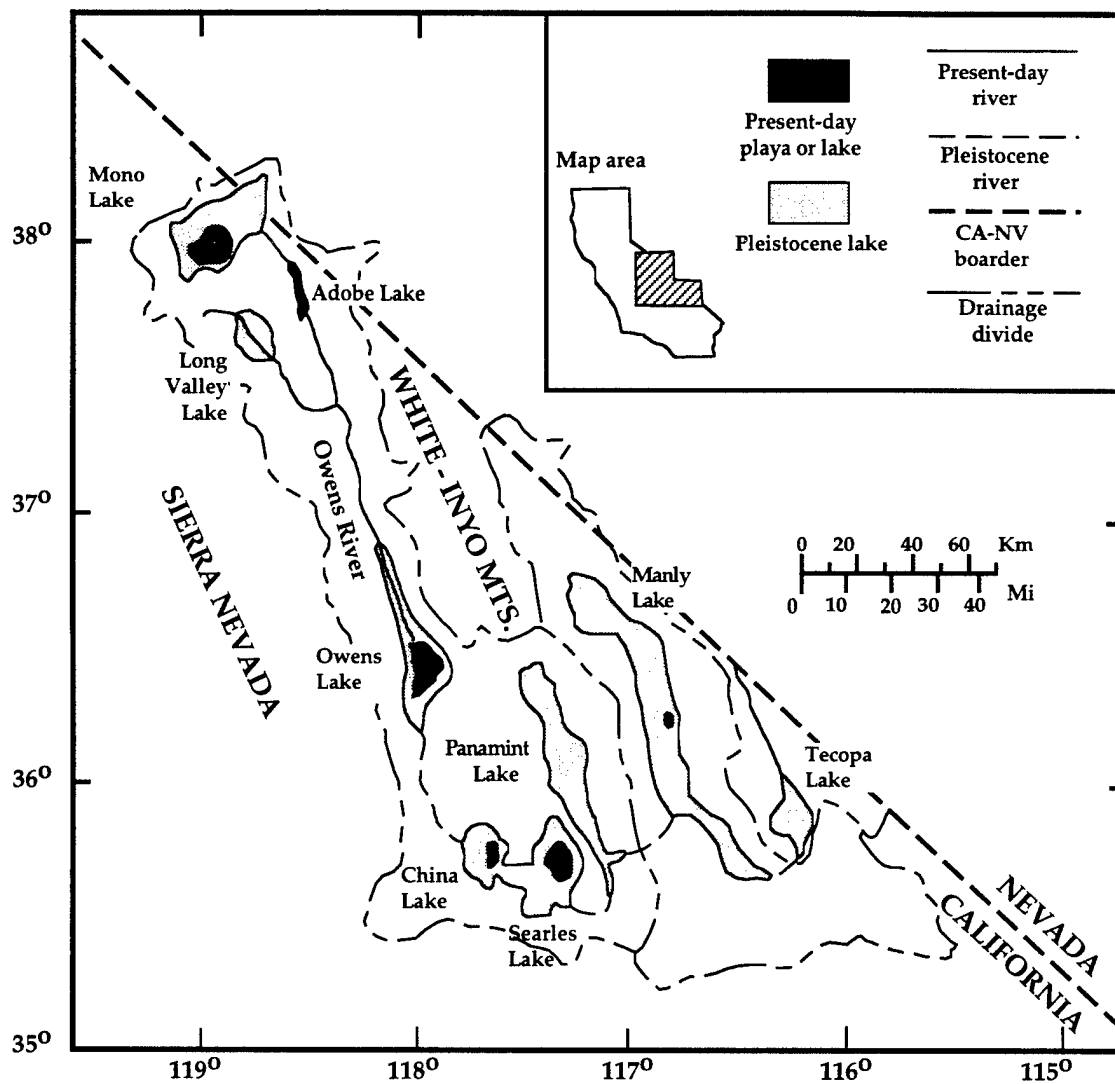


Fig. 1.1: Map of eastern California showing location of Owens Lake and surrounding Pleistocene pluvial lakes.

Paleoclimatic studies in this region are of great importance because of the heavy reliance of the city of Los Angeles on runoff from the eastern slope of the Sierra Nevada range. More than 390 million cubic meters (Los Angeles Department of Water and Power, unpublished data) of water are exported from the Owens Valley to Los Angeles each year by means of an aqueduct built in the 1910s (Smith and Street-Perrott, 1983). As urban demands for water continue to grow, knowledge of the impact of climate change on water supply becomes increasingly important.

In addition to the obvious public relevance of paleoclimatic inquiries in the Owens Lake system, many scientific questions of great interest may also be asked. These include 1) are lake highstands synchronous with glaciation in the Sierra Nevada, 2) are Sierra Nevada glaciations synchronous with global ice sheet growth, and 3) what combinations of runoff and evaporation are necessary to allow the growth of large lakes? Some work has already been done in this region in an attempt to answer these questions. However, past paleoclimate studies in this system have focused largely on the records contained in Searles and Panamint Lakes, downstream from Owens Lake and the Sierra Nevada (Smith and Pratt, 1957; Smith, 1984; Jannik and others, 1991; Phillips and others, 1992). As these lakes probably received most of their water through overflow from one lake to the next, they contain incomplete records of climate change. Previous work in the region also includes relative and absolute age-dating of glacial moraines in the Sierra Nevada (Blackwelder, 1931; Sharp, 1972; Birman, 1964; Gillespie, 1982; Phillips and others, 1990), themselves incomplete records of glaciation.

In the spring of 1992, the U.S. Geological Survey, under the direction of George Smith and James Bischoff, cored Owens Lake to obtain a continuous paleoclimate record for the Sierra Nevada region (Smith and Bischoff, in press). In choosing Owens Lake for the coring project, it was hoped that information would be gained both on the glacial history of the Sierra Nevada and on the water-balance history of the Owens Lake chain. Furthermore, the study aimed to tightly constrain the timing of climatic variations for comparison to the global record of glaciation (Smith and Bischoff, in press). This thesis is part of the larger USGS project and consists of three chapters which describe sedimentologic analyses undertaken on Owens Lake core OL-92, and a water-balance model used to assess how variations in climate in the eastern Sierra region might have affected lake level in the Owens Lake chain of pluvial lakes.

Chapter 2 (in press in *Geological Society of America Special Paper*) consists of grain-size and clay-mineralogical analyses conducted on 3.5-m-long channel samples from core OL-92. The clay analyses define episodes of glaciation in the Sierra Nevada through variation between two end-member compositions, illite and smectite. The illite, in conjunction with quartz and feldspar in the clay-size fraction, probably constitutes glacial rock flour, while the smectite probably comes from soils in the drainage basin or is formed authigenically within Owens Lake during interglacials. Grain size analyses reflect changes in lake level, with coarse grains deposited during lake low-stands when the shores of Owens Lake were close to the core site, and finer materials deposited during high-stands when the shoreline was far from the core site. The close correlation between clay mineralogical- and grain size-analyses provide the first direct evidence that Sierra Nevada glaciation and intense pluvial periods in the Owens Lake system

were synchronous. Furthermore, the clay and grain-size variations with depth/age in the core bear a strong resemblance to other Owens Lake paleoclimatic proxies (most notably carbonate content) and to the marine oxygen isotopic record. The latter reflects the variation in global ice volume over the last few million years, and the close correspondence of the Owens Lake proxies to the marine record indicates that the climate in the eastern Sierra Nevada region responded to global forcings, specifically the 20, 40 and 100 ka cycles in Earth's orbital parameters.

Chapter 3, written with Robert S. Anderson, describes a water-balance model for the Owens Lake chain of lakes. In the modeling effort we attempt to determine what combinations of evaporation, runoff, and overspill were necessary to create these large lakes, what effect drainage basin hypsometry has on water balance, and what the response time of each lake is to perturbations in climatic variables. The model uses lake hypsometries derived from 3 arc-second digital elevation models, and climatic information from a variety of sources. Modern values of precipitation and the pre-Los Angeles aqueduct elevation of Owens lake are used to constrain the modern runoff and evaporation values. The general temporal patterns of proxies such as carbonate percentage and mean grain size are used to constrain the modeled paleolakes. Importantly, an isotopic subroutine is used to calculate the $\delta^{18}\text{O}$ of the modeled Owens Lake, allowing more quantitative comparison with $\delta^{18}\text{O}$ values measured on core OL-92 carbonates (Benson and Bischoff, 1993).

Results of the modeling exercise suggest that all of the lakes achieve steady-state volumes within a matter of decades, indicating that droughts or particularly wet periods of order several decades should have been recorded in

the sediments of the Owens Lake core. Furthermore, $\delta^{18}\text{O}$ values also reach steady state, with periods of overflow showing depleted values close to Owens River water, and periods of low lake level showing enriched values. This rapid response to climatic forcings suggests that on long time-scales, the lake chain is perpetually at steady state. As a result, we might expect the sediments in the Owens Lake core to faithfully record climatic phenomena that operate with periods longer than a few hundred years. Using measured core carbonate $\delta^{18}\text{O}$ values to constrain lake-level fluctuations, we find that "maximum pluvial" lake stages require an increase in the flux of Owens River of 7x modern, given a decrease in evaporation rate to 70% of modern.

In Chapter 3, a hypothetical lake-level history is created for the Owens Lake system by modulating runoff and evaporation rates between modern and assumed glacial values using the $\delta^{18}\text{O}$ record from deep sea sediments (Imbrie and others, 1984) to scale the fluctuations. The resulting isotopic history is similar to that measured by Benson and Bischoff (1993) though it lacks several details, suggesting that the climate in the Owens Lake area was driven not only by long-term oscillations such as the 20, 40, and 100 ka orbital variations, but also by shorter-duration phenomena. The history motivates the study described in Chapter 4, which consists of analyses conducted on 70-cm-long channel samples taken from the top 155 kyrs of core sediments. These samples were taken to resolve shorter-period climatic phenomena than those observed in the 3.5-m-long channel samples and have been subjected to carbonate content, stable isotopic, and grain size measurements.

In general, there is strong agreement between the different analyses suggesting that the proxies are genetically related to one another. The marine

$\delta^{18}\text{O}$ record is mimicked even more closely at this higher resolution, showing several of the smaller scale fluctuations (e.g., isotope stage 3?) more clearly than in the more coarsely sampled results. However, the Owens Lake system, with a much shorter response time than the global climate system with its large ice sheets, shows considerably more complexity. Decreases in carbonate content and more depleted values of $\delta^{18}\text{O}$ indicate many short-duration excursions to wetter conditions during the dry interglacial stage 5 (50 ka to 120 ka in the Owens Lake core). In the intervals 13-30 ka, and 120-154 ka, carbonate content is very low (<1%) indicating that Owens Lake is large and overflowing into the China Lake basin. Oxygen isotopic values, however, vary widely (13-30 ka) or slowly increase (from 145 to 120 ka) which would suggest that Owens Lake was at a level below its spillpoint, and became increasingly evaporatively concentrated. Several possibilities are explored to explain the discrepancy between the carbonate content and oxygen isotopic data including measurement error, overflow of isotopically-enriched water from Mono Lake to Owens Lake during Owens Lake highstands, and incorporation of detrital carbonates from the White and Inyo Mts. into Owens Lake sediments during highstands.

CHAPTER 2

Climatic Signals in Clay Mineralogy and Grain-Size Variations in Owens Lake Core OL-92, Eastern California

KIRSTEN MARGARET MENKING

*Earth Sciences Department, Earth and Marine Sciences Bldg., University of California,
Santa Cruz*

ABSTRACT

Mean grain size and clay mineralogy of sediments in Owens Lake core OL-92 reflect climatic conditions in the Sierra Nevada region. Variations in mean grain size of mud within the core reflect climatic oscillations in the region; with relatively coarse sediments (mean grain size $\sim 15\ \mu\text{m}$ in diameter) probably deposited during Owens Lake lowstands and relatively fine sediments (mean grain size $\sim 5\ \mu\text{m}$ in diameter) deposited during highstands. The mineralogy of the clay-sized fraction, as determined by X-ray diffraction (XRD), also reflects the climatic history of cyclic glaciation. Mineral assemblages display two end-member XRD scans: Those having large illite, quartz, and feldspar peaks but a small smectite peak (interpreted to be glacial rock flour), and those with small illite, quartz, and feldspar peaks and a large smectite peak (interglacial sediments). On the basis of diffraction peak areas, illite and smectite probably constitute 70 percent or more of the mineralogy and are inversely abundant. In addition, core sections high in smectite correlate well with high mean grain size and carbonate content in Owens Lake sediments, while sediments rich in illite,

quartz, and feldspar (rock flour) correlate well with finer mean grain size and low carbonate content. Variations in clay mineralogy and grain size, which are strikingly similar to variations in deep-sea oxygen isotopic composition ($\delta^{18}\text{O}$), indicate that the lake-level variations and nature of sediments delivered to the lake vary in concert with global climate changes.

INTRODUCTION

This study is part of an on-going U.S. Geological Survey (USGS) project to examine sediments cored from Owens Lake in southeastern California. The purpose of the USGS study is to construct a more complete record of Pleistocene and Holocene climatic variations in the area than has been possible with the discontinuous and moderately age-constrained moraine record in the Sierra Nevada (Blackwelder, 1931; Sharp, 1972; Birman, 1964; Gillespie, 1982; Phillips and others, 1990) and the "filtered" climatic record in the Searles Lake core (Smith, 1984). Core OL-92 was taken from Owens Lake in the spring of 1992 by a USGS drilling crew. It measures 7.5 cm in diameter and was drilled to 323 m. Recovery was 80 percent. Sediments vary from an evaporite package at the top of the core to lacustrine clay-, silt-, sand-, and granule-sized clastic materials plus carbonate muds. Clastic sediments at the top of the core are predominantly clay- to silt-sized, and become interbedded silts and sands below about 200 m depth. Ages are constrained via magnetostratigraphy (Glen and Coe, in press), ^{14}C dating (Bischoff and others, in press (a)), and tephrochronology (Sarna-Wojcicki and others, 1993). Bischoff and others (in press (a)) constructed an age-versus-depth model based upon an assumption of a constant mass-accumulation rate for the core. This model agrees closely with the magnetostratigraphic record of Glen

and Coe (in press) and yields average mass-accumulation and sedimentation rates of 51.4 g/cm²/ky and 40.1 cm/ky, respectively. In this paper, I report the results of grain-size analyses and X-ray diffraction (XRD) analyses of clay minerals in the core and compare the relation of variations in grain size and clay mineralogy to other climate proxy records in the core. Furthermore, I make use of the age-versus-depth model of Bischoff and others (in press (a)) to compare the Owens Lake records to the $\delta^{18}\text{O}$ record that Imbrie and others (1984) derived from deep-sea sediments. Before proceeding to a description of the completed work, I briefly introduce previous work on lacustrine grain-size and clay-mineralogical analyses conducted both in the Owens Lake system of lakes and in other basins around the world.

PREVIOUS WORK

Lacustrine Grain Size and its Relation to Climate Change

Many workers have noted a relation between distance to the shoreline and grain size of materials deposited in lakes. Sarmiento and Kirby (1962) found that sediments from the center of Lake Maracaibo, Venezuela are substantially finer grained than those near the shores of the lake. Furthermore, a series of short cores (2-5.5 m long) reveal a coarsening-upward trend in one of the stratigraphic units, which possibly records a shallowing of the lake. Picard and High (1972, 1981) reported on the lithofacies of several lakes throughout the world. In general, they noted a progression from coarse sand and gravel at the shores of these lakes to fine muds near the centers. They also noted that sediments of particular sizes fell along concentric belts, generally parallel to the shores of the lakes. They attributed this pattern of deposition to the location of wave base and

wave agitation in the lakes. Sediments deposited below wave base are typically finer than those deposited above wave base, where wave energy is strong and fine grains are winnowed away.

Waitt (1980, 1985) interpreted a package of fining-upward rhythmites in bottom sediments from glacial Lake Missoula as evidence for periodic filling and catastrophic flooding of that lake. Failure of the ice dam confining Lake Missoula resulted in the instantaneous deposition of silt, which slowly fined upward to clay as the lake refilled. At least 40 filling and flood cycles are recorded by these bottom sediments. In each case, as the lake enlarged, deposits at any given site fined upward as the distance to the shorelines increased and as wave base moved away from the center of the lake.

In addition to the influence of wave-base location on sediment distribution, Boggs (1987) included river inflow that can send a plume of fine sediment far into the lake, long-shore currents, convective overturn of lake water due to thermal stratification, and density underflows. Smith (in press) also identified ice-rafting of pebbles and sand lenses as an important transport mechanism for coarse-grained material.

Clay Minerals in the Owens Lake System

Droste (1961a, b) first reported on the nature and relative abundances of clay minerals in the Owens chain of lakes. He identified montmorillonite (a smectite mineral), illite, chlorite, and kaolinite in about 20 samples each from 300- to 1,000-ft cores of Owens, China, Searles and Panamint Lakes taken in the 1950s. On the basis of mineralogic assemblages, Droste concluded that clays found in China and Searles Lakes had, to some extent, originated in the Owens Lake

drainage basin and had been transported by overspill into basins down the chain during pluvial-lake highstands. Lacustrine clay assemblages from pluvial lake lowstands, on the other hand, reflected their unique drainage basins (Droste, 1961b). He further noted that variations in clay mineralogy in a core from Owens Lake dominantly reflect variations in the proportion of montmorillonite to illite (Droste, 1961b) and that clay minerals constitute at least 70 percent of the clay-sized fraction (Droste, 1961a). Looking at samples of core sediments from Searles Lake, Hay and Moiola (1963) and Hay and others (1991) identified illite, montmorillonite, chlorite, and kaolinite in the clay-sized fraction; they stated that the silt and sand-sized fractions were dominated by microcline, orthoclase, albite, andesine, and quartz. Like Droste (1961b), they noted a variation in dominance of illite and montmorillonite in Searles Lake sediments, and Hay and Moiola (1963) suggested that the absence of montmorillonite in several samples was caused by its diagenetic destruction. Feth and others (1964) identified montmorillonite, kaolinite, and "micaceous clay minerals" (i.e., illite) in the $<4\text{-}\mu\text{m}$ fraction of sediments (Wentworth, 1922, convention) from various locations in the Sierra Nevada. Newton (1991) conducted XRD analyses on sediments from shallow cores ($<30\text{ m}$) from Owens and Mono Lakes. He interpreted the presence of quartz and feldspar in the $<4\text{-}\mu\text{m}$ fraction as indicative of glacial abrasion in the Sierra Nevada. Furthermore, he detected only trace amounts of clay minerals and concluded that the clay-size fraction was wholly rock flour.

ORIGINAL HYPOTHESES

Because of the proximity of Owens Lake to the Sierra Nevada and the fact that Owens Lake receives most of the runoff from the eastern side of the range,

the lake's sediments should contain a record of the cyclic glaciation experienced by the mountain range. From the results of the previous lacustrine grain-size studies (Picard and High, 1972, 1981; Sarmiento and Kirby, 1962; Waitt, 1980, 1985), I hypothesized that variations in lake level might manifest themselves by variations in grain size of sediments deposited at the core OL-92 site. In particular, I expected fine-grained deposition to characterize Owens Lake highstands, coarser grained materials to characterize lowstands, and grain-size variations that would generally reflect variations in the distance between the core site and the lake shores. Furthermore, I hypothesized that the lake sediments might alternate in mineralogy between glacial and nonglacial mineralogic end members. Following the lead of Newton (1991), I expected sediments characteristic of glacial periods to contain abundant quartz and feldspar in the clay-sized fraction because of the abrasive action of valley glaciers that produce vast amounts of rock flour. Interglacial sediments were expected to reflect less physical weathering and a concomitant increase in chemical weathering. As a result, smectite and other clay minerals were expected to outweigh the amounts of quartz and feldspar deposited during these periods. To test these hypotheses, I conducted grain-size and X-ray diffraction studies of core sediments.

GRAIN-SIZE ANALYSES

Sample Types

Two types of samples were taken from the core for grain-size analysis. Point samples, which represent about 2 to 3 cm of core length and which were cut out of the center of the core with a knife, were collected at the drill site at 1- to 2-m spacings (~2,500-5,000 years between samples). These samples were taken to

coincide with visually obvious changes in lithology, and each comprises about 60 g of bulk sediment. Because of the lengthy nature of analyses, a subset of these samples (1 sample about every 5 m) was chosen to undergo analyses of grain size, pore-water chemistry (Friedman and others, 1993), and geochemistry (Bischoff and others, in press (b)). The remainder were archived for future study. Channel samples were produced in the laboratory and represent integrated ribbons of sediment, each spanning ~3.5 m of core (~7,500 yrs of sedimentation) and comprising about 50 g of sediment. These samples were collected by pushing a long, thin, U-shaped spatula along the face of the split core. The spacing between point samples and the length of channel samples, were chosen to ensure good resolution of climatic fluctuations operating on time-scales of 10 ky or greater. Nearly 100 point and 100 channel samples were analyzed.

Methods

Grain -Size Analysis of Point Samples. About 10 g of each point sample was treated with Morgan's solution (weak acetic acid buffered to pH 5 with sodium acetate) and peroxide to remove carbonate and organic material (no attempt was made to remove biogenic silica, such as diatom tests). Samples sat in this solution for two days and were periodically stirred and were then boiled to remove excess peroxide. The remaining sediment was wet sieved to separate gravel, sand, and silt-plus-clay fractions. The clay and silt fraction of each sample was collected in a 1,000-ml graduated cylinder. Sands and gravels were poured into evaporating dishes, dried, and weighed.

Dried gravels and granules ($> \text{minus } 2 \Phi$; $> 2 \text{ mm}$; Wentworth, 1922, size conventions) were sieved at $0.5\text{-}\Phi$ intervals (Φ units are defined as minus log

base 2 of the grain size in millimeters). Sands (minus 1 to 4 Φ ; 0.0625 to 2 mm) were introduced into settling tubes and grain sizes were determined at 0.5- Φ intervals. To prevent flocculation, 5 ml of 5-percent sodium hexa-metaphosphate ("calgon") dispersant solution was added to each clay and silt solution ($>4 \Phi$; <0.0625 mm), and the graduated cylinders were topped off at 1,000 ml with deionized water. Each solution was agitated, after which 20 ml was removed with a pipette submerged to 20-cm depth (Folk, 1968). The 20-ml aliquot was dried in an oven, and the weight of silt and clay in each sample was determined by multiplying the dried mass value by 50. Each solution was re-agitated and another 20-ml sample drawn off. These aliquots were placed in a hydrophotometer and grain sizes were determined at 0.5- Φ intervals. For a more complete description of methods and instrumentation used, see Menking and others (1993a).

A few replicate measurements on sample splits were carried out to determine precision, and these analyses indicate an average precision of about $\pm 0.25 \Phi$. Torresan (1987) determined a precision of about $\pm 0.5 \Phi$ for the hydrophotometer used in these analyses, which is probably more indicative for the whole data set.

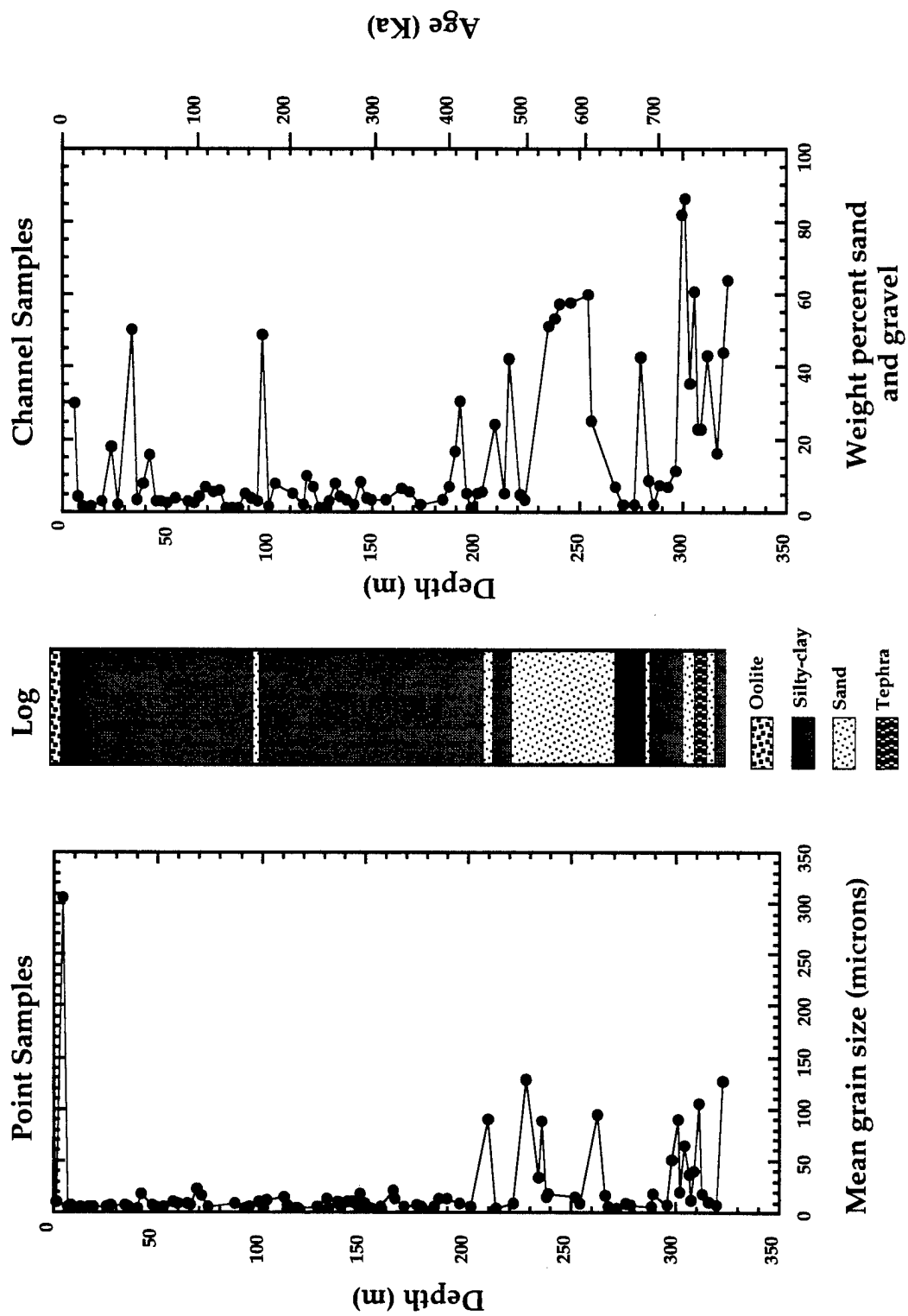
Sand, Silt, and Clay Contents of Channel Samples. Sand plus gravel, silt, and clay contents were determined on 91 of the 3.5-m-long channel samples. A 10-gram split of each sample was subjected to the same chemical treatments used on the point samples. Sand and gravel were separated from silt and clay by wet sieving. The sands and gravels were collected together in evaporating dishes and weighed after drying. Concentrations of coarse silt, fine silt, and clay in each

sample were determined by a scaled-down pipette analysis (Galehouse, 1971). Part of the clay-sized fraction of each channel sample was set aside for XRD analysis.

Results of the grain-size analyses

Grain-size analysis of point samples defines two distinct depositional regimes (Fig. 2.1). With the exception of a coarse-grained oolite layer at the top of the core, mean grain size between 7 and 200 m in depth fluctuates between 2 and 22 μm (clay- to silt-sized material). In contrast, mean grain size between 200 m and the base of the core at 323 m fluctuates between 10 μm (medium fine silt) and 30-130 μm (coarse silt to fine sand). Sand plus gravel, silt, and clay contents of the 3.5-m-long channel samples broadly mimic the point-sample trends; fine silts and clays predominate from the top of the core to 190 m depth, and coarser grained material predominates between 190 and 323 m depth (Fig. 2.1). Some mismatch exists between the percentage of sand in the channel samples and the mean grain size in microns of the point samples between 20 and 50 m in depth and again from 95 to 100 m. This mismatch is due to inadvertent oversight of a few coarse-grained layers in the subsampling of the point-sample sediments. This oversight, however, does not invalidate the conclusion that the top 200 m of the core are distinctly different from the lower 123 m. A closer examination of the top 200 m of the core reveals a crude periodicity in mean grain size with depth in the point-sample record (Fig. 2.2). Table 2.1 lists grain-size statistics (derived from point samples) for the top ~200 m of the core (excluding the very coarse oolite layer near the core top) and the bottom 123 m of the core. The difference in depositional style between these two core sections is evident in the

Fig. 2.1: Mean grain size in point samples and percentage of sand-, and gravel-sized grains in channel samples from core OL-92. Generalized lithologic log is based on the core log prepared by Smith (1993). Note the change in depositional style in the mean-grain-size record from predominantly silt and clay deposition between ~7 and 200 m to silt and sand deposition below 200 m. Channel samples and lithologic log show similar changes in depositional style at ~200 m depth. Mean grain size of point samples was determined by sieving, hydrophotometer, and settling tube. Percentage of sand and gravel was determined by sieving.



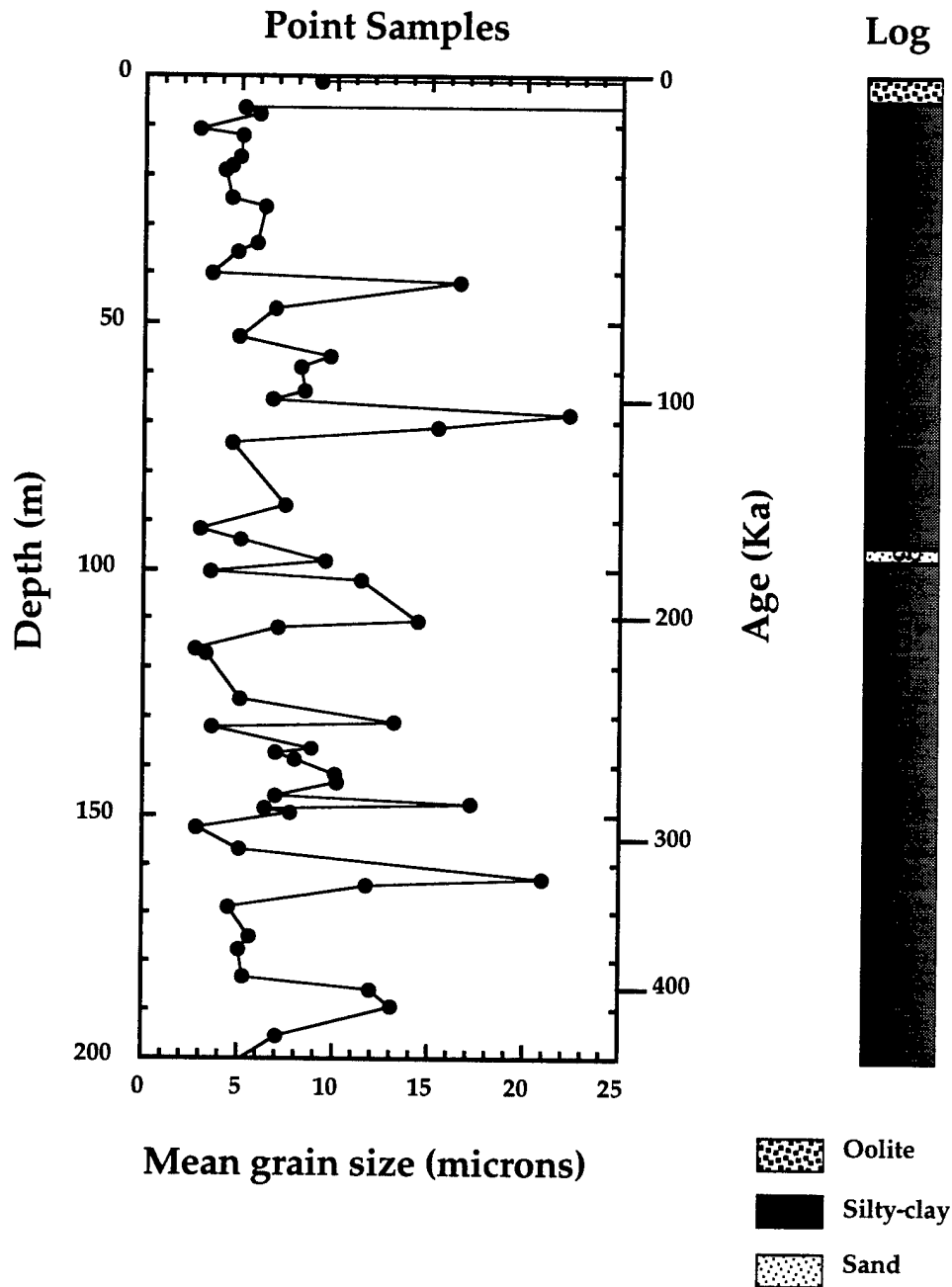


Fig. 2.2: Enlarged point-sample grain-size record and lithologic log for top 200 m of core OL-92. Mean grain size of point samples was determined by sieving, hydrophotometer, and settling tube. Note apparent periodicity in mean-grain-size variation with depth.

TABLE 2.1. Grain-size parameters for Core OL-92 between ~7 and 200 m and between 200 and 323 m (Statistical Parameters from Folk and Ward, 1957).

Statistical parameter	Core Depth	
	7-200 m	200-323 m
Mean grain size (Φ)	7.40 ± 0.79	5.73 ± 1.56
Mean sorting (Φ)	1.80 ± 0.43	1.90 ± 0.52
Mean skewness	0.16 ± 0.14	0.04 ± 0.25
Mean kurtosis	1.53 ± 0.39	1.41 ± 0.60
Φ refers to the phi grain-size scale in which Φ = minus log base 2 of the grain size in millimeters.		

mean grain size and skewness parameters, while the sorting and kurtosis are much the same in the two sections. All sediments are poorly sorted, whether they be the fine-grained sediments from the top of the core or the coarser grained sediments of the lower core. However, the poor sorting may be an artifact of the sampling technique because each point sample represents 2 to 3 cm of core length, and, therefore, may comprise more than one sedimentation unit, each with its own degree of sorting. Those sediments in the top 200 m of the core are positively skewed, implying a weighting toward fine grains. Sediments in the bottom 123 m show a nearly normal grain-size distribution. Both sections of the core are leptokurtic, meaning that the central part of the grain-size distribution is better sorted than the tails of the distribution (Folk and Ward, 1957).

CLAY MINERALOGICAL ANALYSES

Methods

X-Ray Diffraction Techniques. Channel-sample clays were mounted on glass microscope slides by using the filter-peel technique (Moore and Reynolds, 1989) and were step-scanned by X-ray diffractometer (XRD). All minerals were identified by reflection peak locations (Table 2.2), and some were further identified by various thermal and chemical treatments (Moore and Reynolds, 1989). To test for the presence of smectite minerals, samples were glycolated and then rescanned; changes in peak location and intensity were noted. To determine whether the 7-Å (angstrom) and 3.5-Å reflections were due to the presence of chlorite or kaolinite, clays were mounted on X-ray amorphous-tile slides and heated to 550°C for 1 hour. At this temperature, kaolinite becomes amorphous, causing a reduction in peak intensity in those samples containing it. The chlorite (001) peak also intensifies and shifts to 6.3 to 6.4 Å due to dehydroxylation of the inner brucite layer (Moore and Reynolds, 1989). Furthermore, a few samples were boiled in 1N HCl for 2 hours. This treatment dissolves chlorite but leaves kaolinite unaffected. An examination of the 7 Å peak before and after boiling in acid determines the presence of chlorite and/or kaolinite. For further description of methods and instrumentation used, see Menking and others (1993b).

Artificial mixtures. To determine the relative abundances of true clays and nonclays in the clay-sized fraction of the core, and thereby assess the relative proportions of glacial rock flour versus chemically derived clays in the core sediment, a series of artificial mixtures of various minerals was prepared

TABLE 2.2. Reflection peak locations used to identify minerals in the clay fraction of the core OL-92 channel samples

Mineral	(hkl)	$^{\circ}2\Theta$	\AA
Illite	(001)	4.4	10.1
Chlorite	(001)	6.2	14.2
	(002)	12.4	7.11
	(003)	18.8	4.72
	(004)	25.1	3.54
Smectite	(001)	5.2	17.0
Kaolinite	(001)	12.4	7.11
	(002)	25.1	3.54
Quartz	(100)	20.8	4.26
K-feldspar	(002)	27.5	3.24
Plagioclase	(002)	27.9	3.18

(hkl) refers to the mineralogical index used to describe crystal-face location.

$^{\circ}2\Theta$ refers to the angle the incident X-ray makes with the sample.

\AA refers to the wavelength in angstroms.

and analyzed by XRD. The <4- μm fractions of standard illite, smectite, plagioclase, and K-feldspar were separated by centrifugation of wet suspensions of commercially available standard mineral powders. Concentration of each mineral in suspension was determined by placing a known volume into a previously weighed aluminum vessel, drying the suspension in an oven heated to 60°C, and then reweighing the vessel. Once mineral concentrations were known, it was possible to mix suspensions to give known proportions of clay and nonclay minerals. The resulting mixtures were mounted on glass slides and were scanned with the XRD as described earlier. Areas of selected peaks were measured, and peak-area ratios of the artificial mixtures were compared to peak-area ratios of the channel sample sediments.

Results of the X-Ray Diffraction Analysis

XRD determinations of the clay mineralogy of channel samples show that illite, smectite, chlorite, and kaolinite are the primary clay minerals. Most samples also contain some clay-sized quartz, plagioclase, and K-feldspar. X-ray diffraction patterns are typically weak and fair to poor in quality (i.e., peaks often are only 2 to 3 times larger than background), which may indicate poorly crystallized materials. Attempts to determine whether clay minerals are dioctahedral or trioctahedral, on the basis of (060) reflections, were unsuccessful owing to weak reflections and to the overlapping ranges of (060) reflections in this mineralogically complex suite of samples. Shrinkage of some illite peaks upon glycolation indicates some illite/smectite mixed-layering.

The clay-size fractions are characterized by mixtures of two end-members. These consist of an endmember displaying small smectite but large illite, quartz,

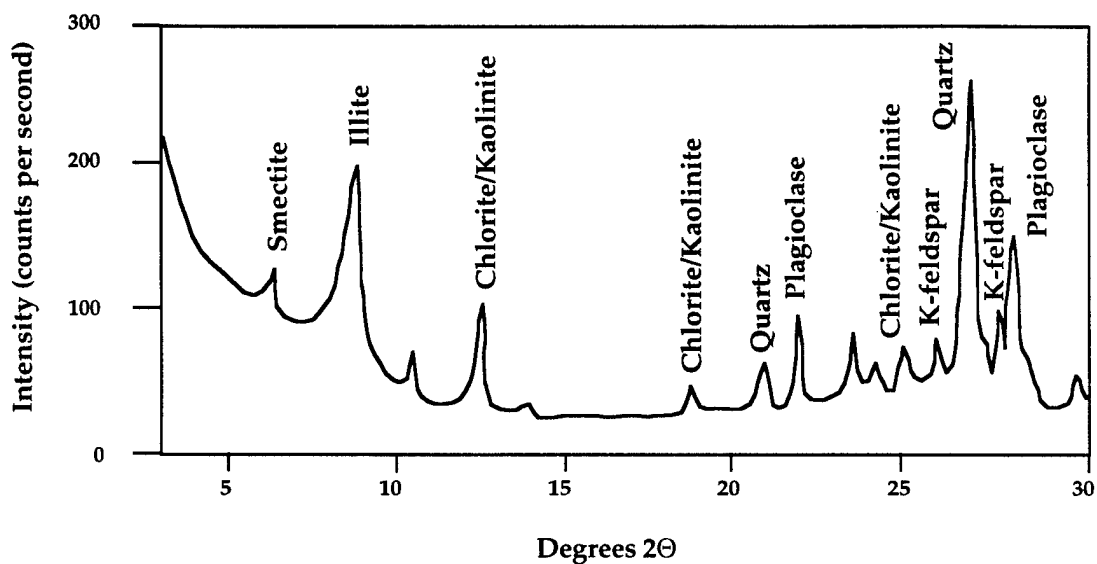
and feldspar peaks (Fig. 2.3a), and an endmember displaying large smectite but small illite, quartz, and feldspar peaks (Fig. 2.3b). After noting these two end-member compositions, I measured the peak areas of several clay and nonclay minerals in each sample to see if any regular pattern or periodicity existed in the deposition of clays and nonclays. Chlorite and kaolinite are both present but, due to overlapping reflection peaks, are not easily decoupled from one another. Therefore, I measured the combined chlorite-kaolinite reflection at 7.11 \AA ($12.4^\circ 2\theta$). In the Owens Lake core sediments, the ratios illite/quartz and chlorite-kaolinite/quartz correlate positively to each other and to the ratios K-feldspar/quartz and plagioclase/quartz (Fig. 2.4). The ratio smectite/quartz (Fig. 2.4), however, correlates positively sometimes to the other ratios, negatively sometimes, and sometimes does not correlate at all. Furthermore, the smectite/quartz and the plagioclase/K-feldspar ratios (Fig. 2.5) behave inversely; the smectite/quartz ratio shows a low value during the last glacial maximum ($\sim 20 \text{ ka}$, and 13 m depth in the core), whereas the plagioclase/K-feldspar ratio is high.

In addition, the multiplicative factors of Hallberg and others (1978), modified by Hay and others (1991), were used to determine the relative abundances ($\pm \sim 30$ weight percent) of clay minerals in the clay-sized fraction of the core samples. The results of this analysis (Fig. 2.6) show that smectite and illite are the dominant phases and that chlorite and kaolinite account for only about 10 to 20 percent of the clay mineralogy. Because of this, smectite and illite abundances vary inversely; smectite concentrations are very low in samples from the last glacial maximum ($\sim 13 \text{ m}$ depth, $\sim 21 \text{ ka}$), whereas illite concentrations are high. Furthermore, a strong periodicity in the smectite and illite curves is

Fig. 2.3: Typical X-ray diffraction scans from core OL-92. Tracings from air-dry mounts. All samples were scanned with a Norelco Step-Scanning X-Ray Diffractometer employing Cu Ka radiation, a $0.02^\circ 2\theta$ step size, and 5 second dwell time. A: Small smectite but large illite, quartz, and feldspar peak scan; sample from 78 m depth. Peak at $\sim 10.5^\circ 2\theta$ remains unidentified. Mineralogic assemblage is consistent with a glacial rock-flour source for the sediments. B: Large smectite but small illite, quartz, and feldspar peak pattern; sample from 192.13 m depth. Mineralogic assemblage is consistent with either a soil-clay origin or a combination of sediment eroded from the Sierra Nevada plus authigenic precipitation of smectite within Owens Lake.

a)

Typical Small Smectite and Large Illite, Quartz, and Feldspar Peaks



b)

Typical Large Smectite and Small Illite, Quartz, and Feldspar Peaks

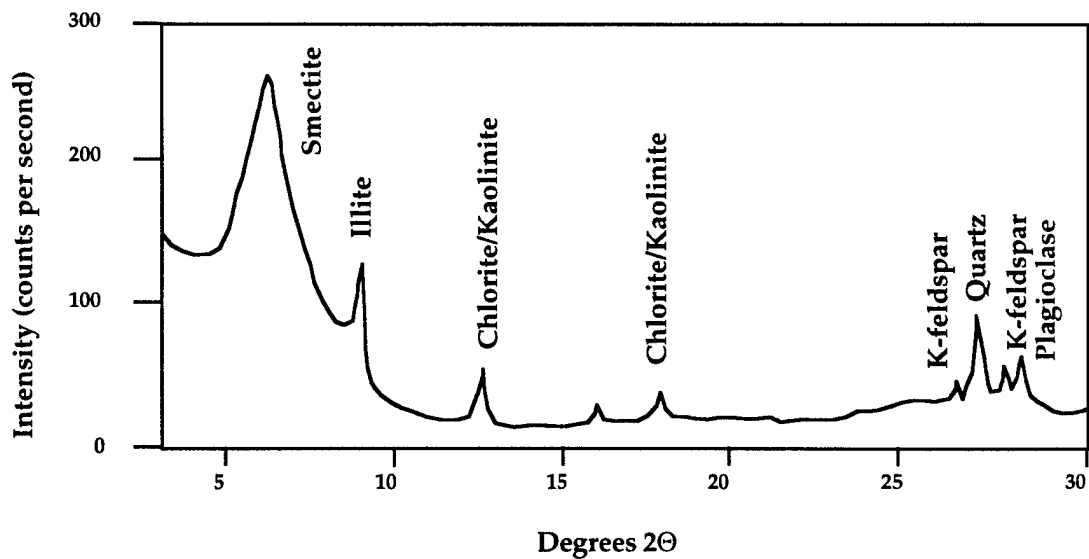


Fig. 2.4: Plot of normalized clay peak-area to quartz peak-area ratios from core OL-92; plot shows that the ratios of illite, chlorite-kaolinite, K-feldspar, and plagioclase to quartz exhibit similar behavior with depth. Lithology is also shown. Similarity of illite and chlorite-kaolinite curves to the plagioclase and K-feldspar curves may indicate a mechanical origin for much of the illite and chlorite. Extended plots show that the smectite/quartz ratio correlates positively sometimes (20 to 80 m), negatively sometimes (230 to 290 m), and not at all sometimes (60 to 110 m) to other clay minerals or feldspars.

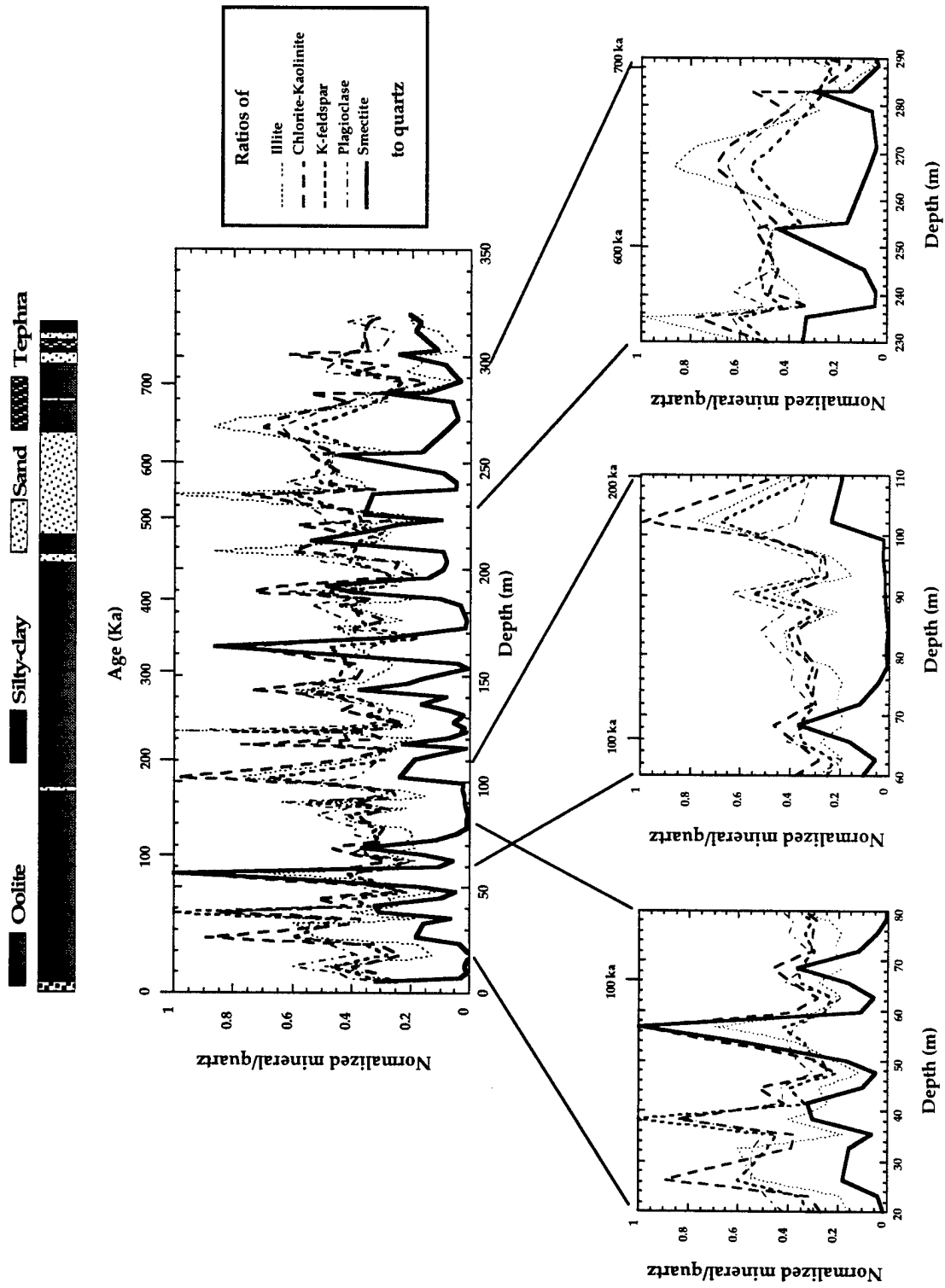
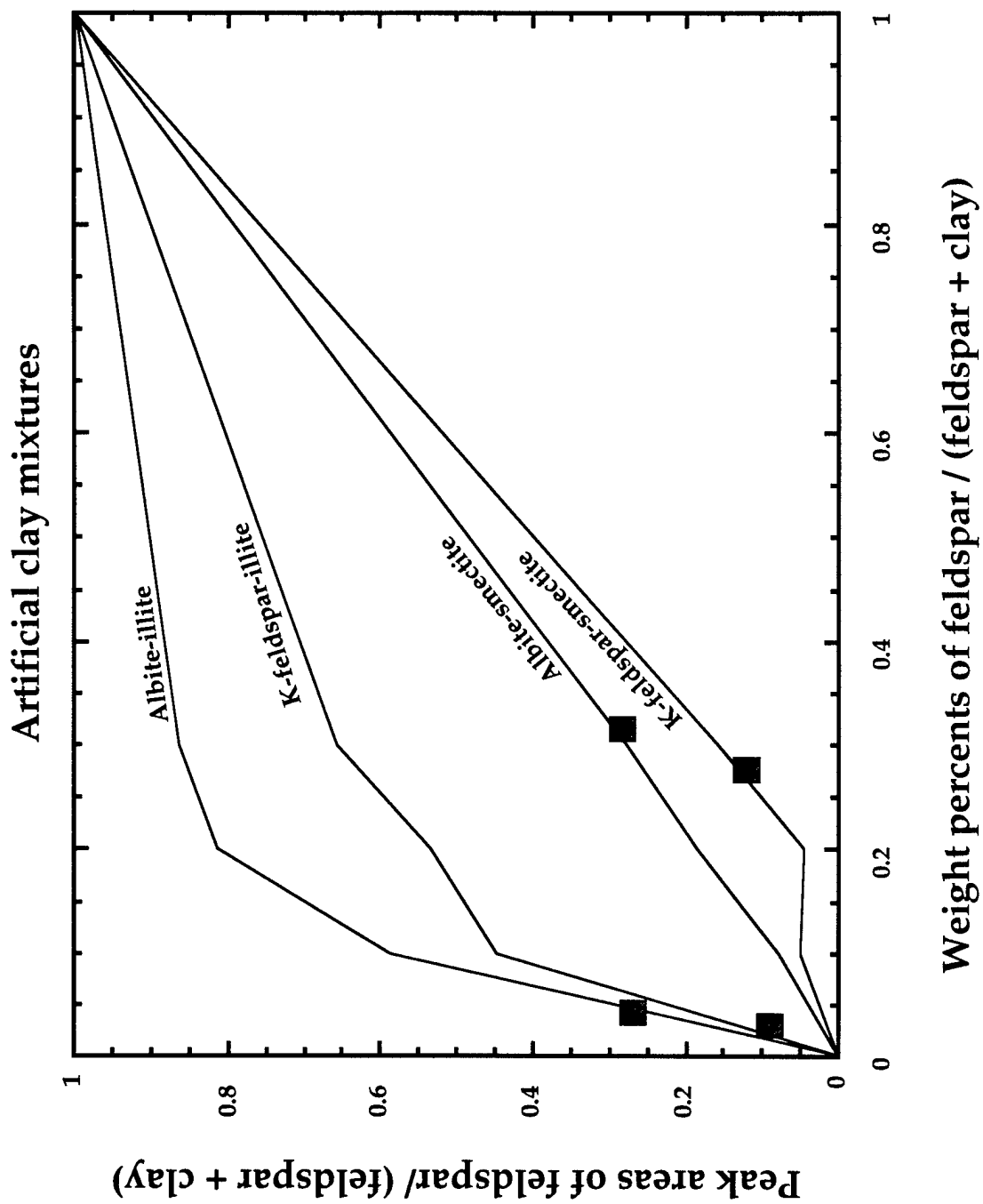


Fig. 2.5: Plot of normalized smectite/quartz and normalized plagioclase/K-feldspar ratios in core OL-92. Note inverse behavior of the two curves with depth (normalized plagioclase/K-feldspar axis is plotted inversely). High smectite/quartz values should correspond to low plagioclase/K-feldspar values if the smectite was produced by the chemical weathering of plagioclase (see discussion). Likewise, if smectite and K-feldspar are primarily authigenic precipitates formed when Owens Lake became saline, high smectite/quartz values should still correspond to low plagioclase/K-feldspar values (see discussion).



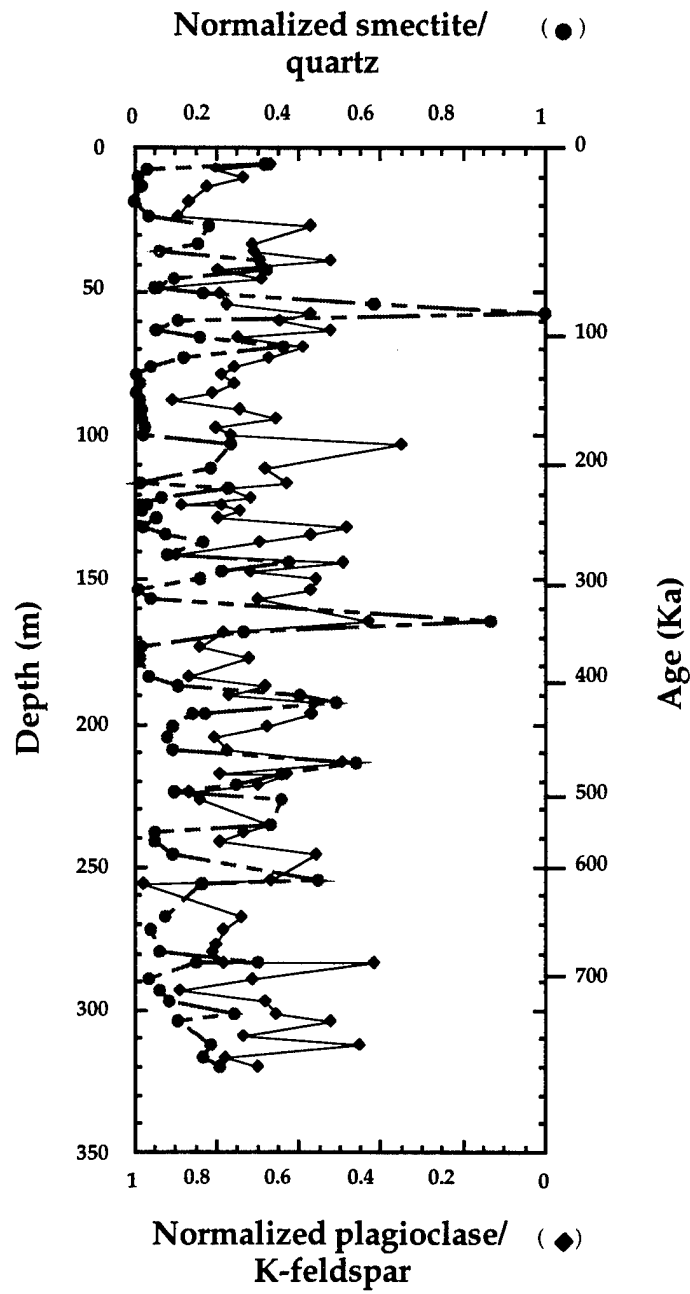
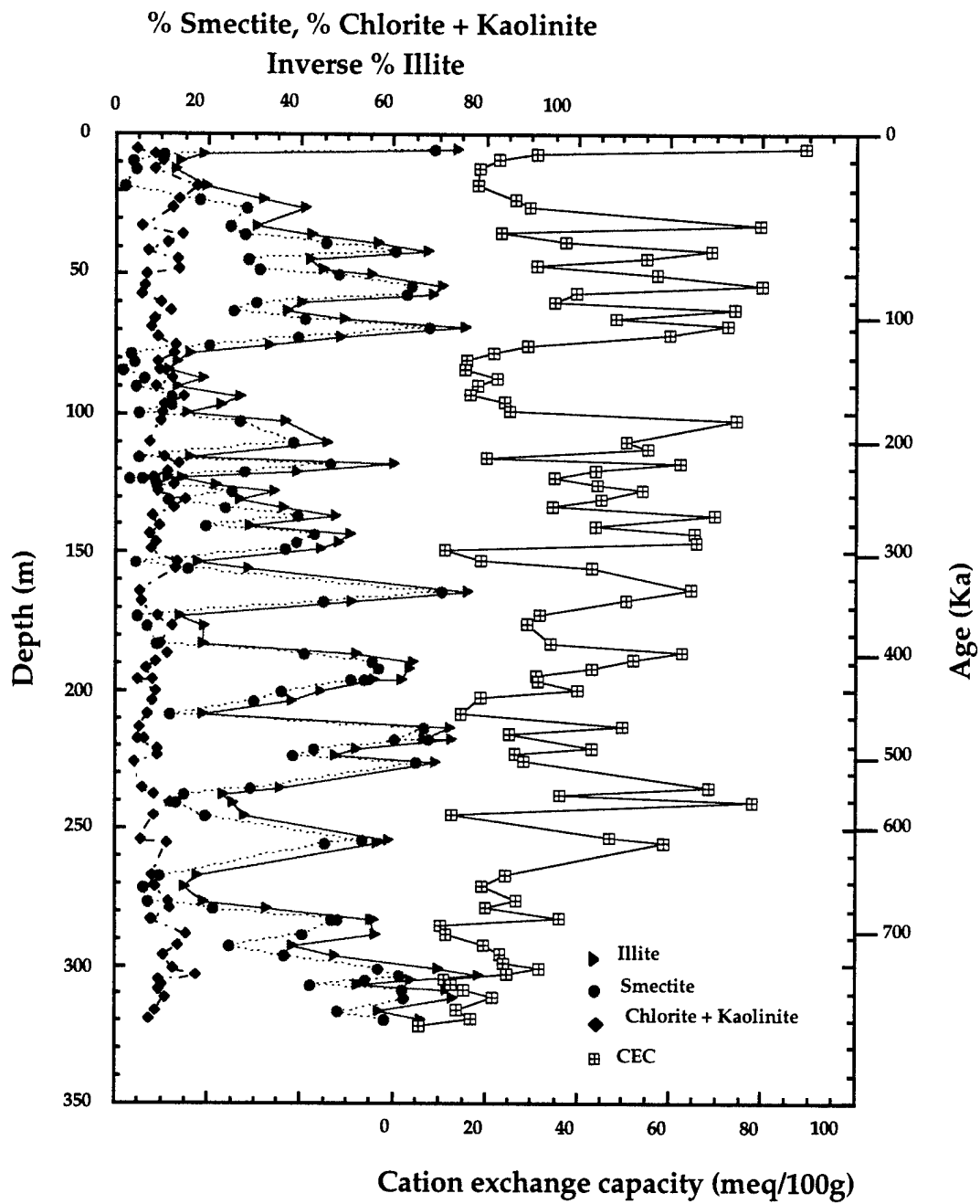


Fig. 2.6: Weight percentages of smectite and chlorite-kaolinite versus depth in core OL-92 as calculated by the methods of Hallberg and others (1978) and Hay and others (1991). Inverse weight percent of illite is also plotted. Smectite and illite are the dominant clay minerals and are, therefore, inversely abundant. Cation exchange capacity (CEC) of channel-sample sediments as determined by Bischoff and others (in press (b)) is also shown. CEC is high during periods in which mineralogy is dominated by smectite and low during periods dominated by illite, plagioclase and K-feldspar.



evident with depth. Cation exchange capacity (CEC) (Bischoff and others, in press (b)) follows the smectite curve (Fig. 2.6).

Results of the artificial clay-mixture experiments

The results of the artificial clay-mixture experiments are shown in Figure 2.7. The lines are derived from the artificial experiments; the gray boxes represent the mean peak-area ratios of Owens Lake channel sample sediments. I infer the concentration in weight-percent of each mineral in the channel-sample sediments by reading the graph. For example, the mean peak area of albite/(peak area of albite + peak area of illite) ratio for all $<4\text{-}\mu\text{m}$ sediments (value = 0.27) is represented by the grey box falling along the peak area of albite-illite line. This peak-area ratio value corresponds to a weight-percent feldspar/(feldspar+clay) value of ~ 0.05 or to an albite abundance relative to illite of ~ 5 percent. Thus, the average Owens Lake sample contains ~ 5 percent albite relative to illite. This does not mean that it contains 5 percent albite overall, because minerals other than albite and illite exist in each sample. Comparison of peak-area ratios for artificial mixtures to those for samples of unknown mineral abundances leads to the conclusion that no more than about 30 percent of the clay-sized fraction of any sample consists of nonclay minerals (K-feldspar, plagioclase, quartz). Thus, variations in smectite and illite concentrations represent most of the total variation in mineralogy. These results confirm the findings of Droste (1961b), and Hay and Moiola (1963).

Fig. 2.7: Plot of ratio of peak areas versus ratio of weight percents of feldspars to clay minerals for known mixtures of illite and smectite with albite and K-feldspar. Note nonlinearity of relations. Gray squares represent the mean peak-area ratios for channel-sample sediments from core OL-92, whose mineral weight abundances we want to determine. Boxes are plotted so they fall on their corresponding peak-area ratio versus weight-percent ratio lines (derived from artificial mixtures), and at their measured peak-area ratio values. Weight percent of feldspar to clay can be read off the graph. These peak area ratios suggest that no more than ~30 percent of any channel-sample sediment consists of nonclay minerals in the $<4\text{-}\mu\text{m}$ fraction.

DISCUSSION

Grain-size analyses of the top 200 m of the core indicate very fine deposition (clay- and silt-sized material with average size of $\sim 5 \mu\text{m}$) during the last glacial maximum (13-m depth in the core, $\sim 21 \text{ ka}$) and in other core sections that have been identified as representing glacial periods on the basis of several paleoclimatic proxies (see the following section on "Comparison of grain size and clay-mineral variations to other paleoclimate proxies"). In contrast, interglacial periods are marked by coarser deposition with a mean grain size of $\sim 15 \mu\text{m}$. Furthermore, the mean grain size of sediments deposited during interglacial periods varies more than that of sediments deposited during glacial periods. The mean sizes of sediments from glacial periods vary between values of 2 and $5 \mu\text{m}$, whereas those of interglacial periods vary between 11 and $23 \mu\text{m}$ (Fig. 2.2). Below 200 m, no correlation between grain size and climatic regime is apparent.

As suggested by Picard and High (1972, 1981), Smith (in press), and Boggs (1987), lacustrine grain size is a function of wave-base location, fluvial inflow rates that allow some plumes of fine sediment to penetrate far into a lake, long-shore currents, ice-rafting of pebbles and coarse sand lenses, and turbid underflows. In general, these processes, with the exception of turbid underflows and ice-rafting, result in a pattern of deposition of concentric rings of sediments increasing in grain size toward shore. The difference in grain size variability in the Owens Lake core, as well as the predominance of fine deposition during glacial periods and of coarser deposition during interglacial periods, might best be explained by these processes and by consideration of the hypsometry of the Owens Lake basin.

The slopes of the Owens Lake basin resemble those of a bathtub; there is little change in altitude for several kilometers and a rapid increase in altitude over a very small distance. A north-south transect between the core site and the north shore of the lake shows 4 m of elevation gain in ~17 km followed by 60 m of elevation gain over the next 8 km; the bulk of that 60-m elevation gain occurs within ~1 km. High lake levels, such as are thought to have characterized glacial periods, should have resulted in deposition of fine sediments at the core site, as the distance to the shoreline was large and the wave base would have existed far from the core site. During interglacial periods, when lake levels are thought to have been lower, mean grain size would have increased slowly until the lake level fell to the bottom of the bathtub at 1085 m. At this point, any further lowering of lake level would have allowed a large contraction of the lake, and shorelines and wave base would have rapidly neared the core site. As a result, coarser grains could be transported to the core site by waves and surface currents.

The bathtub morphology can also explain why the mean grain size in the interglacial sediments varies more than that in the glacial sediments. Because little change in distance between the core site and shorelines occurs after the lake level reaches the wall of the bathtub, further increases in lake level would lead to little change in wave-base location relative to the core site. Hence, a rather uniform grain size would be deposited at the core site regardless of fluctuations in lake level. During interglacials lake levels were lower, and fluctuations in lake level could have resulted in large variations in shoreline distance and wave base location relative to the core site. During this time, mean grain size of particles deposited at the core site might show large variations. The combination of lake-

level fluctuations and basin geometry appears to explain the observed variability in grain size. However, a derivation of absolute lake level from mean grain size may be problematic because turbid underflows, ice-rafting, aeolian transport, and other processes might also exert influence on grain size. Nevertheless, mean grain size appears to be a useful indicator of relative lake level.

Subtle variations in grain size between ~7- and 200-m depth, though mostly in the clay and silt size ranges, show a definite climatic signal; deposits were finer grained during glacial periods and coarser during interglacial periods. However, the abrupt transition from fine sediments above ~200 m, to silt- and sand-sized sediments below 200 m remains unexplained. The transition may be the result of climatic or tectonic factors, although Smith (in press) attributes the coarser section to earlier outwash from the Sherwin glaciation. However, aside from the size difference between the top and bottom sections of the core, both sections appear to represent poorly sorted lacustrine materials. As mentioned earlier, the poor sorting may be an artifact of the sampling technique.

Like Newton (1991), I interpret the presence of nonclay minerals (quartz, plagioclase, and K-feldspar) in the clay-sized fraction to be the result of glacial abrasion that produced large volumes of glacial flour in the Sierra Nevada. Indeed, it is rare to find quartz and feldspars in the clay-sized fraction of any sediment unless that sediment had a glacial origin (Moore and Reynolds, 1989). Of the true clay minerals, illite and chlorite are typically found as products of intense physical weathering of micas by glaciers in the absence of strong chemical weathering (Chamley, 1989, p. 58; Biscaye, 1965). Smectite and kaolinite, on the other hand, are more likely produced from the weathering of silicate minerals during soil formation, and they may, therefore, be more

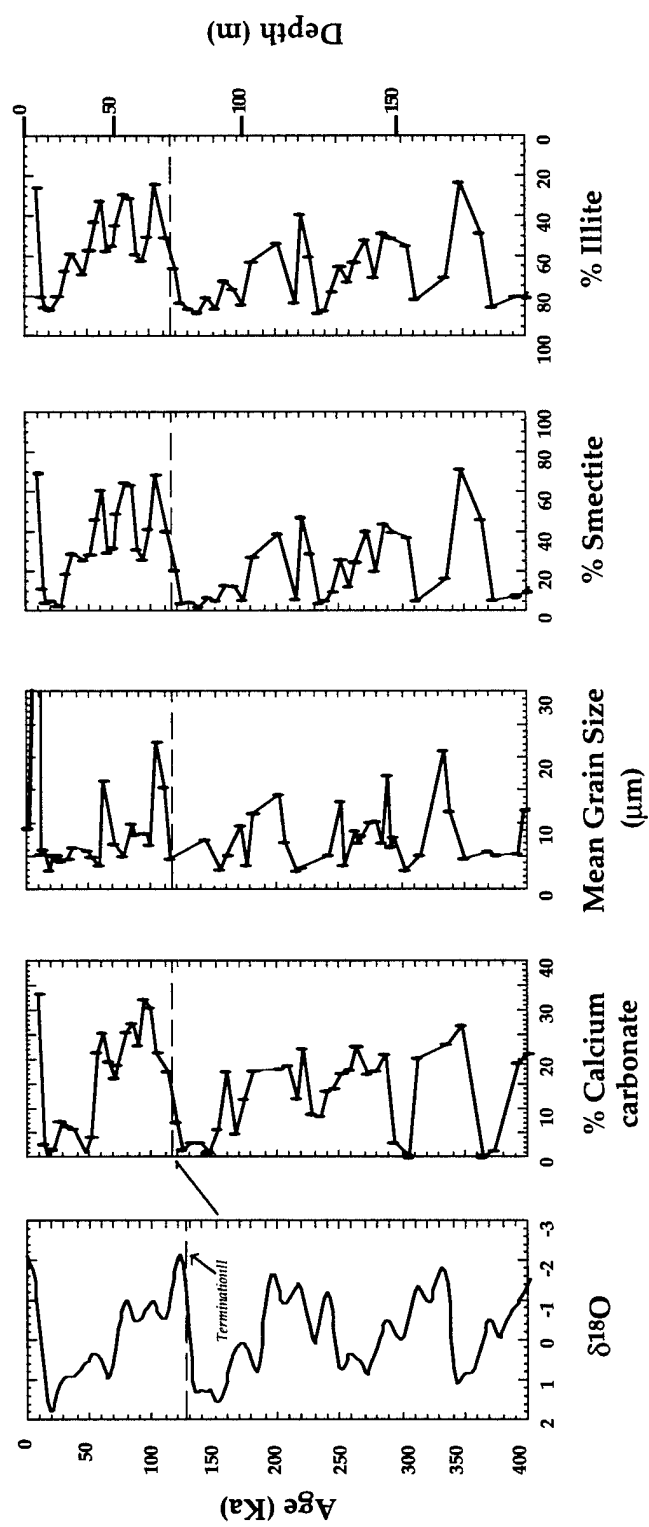
indicative of climates conducive to chemical weathering (Chamley, 1989, p. 7 and 13). Smectite is also a common weathering product of volcanic ash, so care must be taken to distinguish between true climatic variations and volcanic events (Chamley, 1989, p. 70).

Note that the illite/quartz and chlorite-kaolinite/quartz peak-area ratios correlate positively with the K-feldspar/quartz and plagioclase/quartz ratios in the Owens Lake samples (Fig. 2.4). Because feldspars may indicate immature, mechanically produced sediments, their correlation with illite and chlorite (though probably not kaolinite) may indicate a mechanical origin for these clays. In addition, samples having well-defined feldspar peaks always exhibit large illite peaks, while samples displaying weaker and fewer feldspar peaks show large smectite peaks. This peak distribution suggests that the illite is a low-grade alteration product of igneous muscovite or biotite, and that the illite plus feldspar XRD end-member represents glacial flour. The poor correlation of smectite/quartz to illite/quartz, K-feldspar/quartz, or plagioclase/quartz ratios (Fig. 2.4) suggests that smectite formed by a different process. Furthermore, the smectite/quartz ratio correlates negatively with the plagioclase/K-feldspar ratio. Because plagioclase is less resistant to chemical weathering than K-feldspar is (Loughnan, 1969), plagioclase/K-feldspar ratios should be lower in chemically weathered sediments than in those sediments unaltered by chemical processes. Because smectite is a chemical-weathering product, ratios of smectite/quartz should be high in those sediments that were chemically altered and low in those sediments that were unaltered. Therefore, smectite/quartz and plagioclase/K-feldspar ratios should, and do, behave inversely (Fig. 2.5).

An alternative explanation for the variation in sedimentation that is predominantly smectite or illite is that smectite may have formed authigenically in Owens Lake during periods of high salinity during low lake levels (interglacial periods). The curve of percent smectite versus depth (derived by using the multiplicative factors of Hallberg and others, 1978) closely follows the abundance of CaCO_3 (Bischoff and others, in press (b)) (Fig. 2.8), which may indicate an authigenic origin for much of the smectite in the core. Bischoff and others (in press (b)) also report the existence of a potentially authigenic acid-soluble Mg silicate whose abundance correlates with CaCO_3 abundance. The mineral that I describe as smectite may include or be this acid-soluble Mg silicate.

In addition to authigenic clay minerals, authigenic K-feldspar and zeolites are sometimes formed in saline lakes. Hay and others (1991) found authigenic K-feldspar in Searles Lake sediments, and Banfield and others (1991) found it in Abert Lake, Oregon. Even if Owens Lake smectite and K-feldspar are largely authigenic, the smectite/quartz and plagioclase/K-feldspar ratio curves would still vary inversely. In this instance, the varying smectite/quartz and plagioclase/K-feldspar values would result not from the differential chemical weathering of plagioclase and K-feldspar but from the periodic precipitation of K-feldspar and smectite in an authigenic setting. Presently, I cannot rule out either a detrital or authigenic origin for clay minerals and K-feldspars in the core, and my attempts at differentiating between detrital and authigenic K-feldspar by X-ray diffraction have proven unsuccessful. However, evidence for the high salinities necessary for authigenic K-feldspar precipitation is scant. The only evidence for high salinities is the evaporite minerals and oolites found between

Fig. 2.8: Comparison of deep-sea sediment $\delta^{18}\text{O}$ record and four different Owens Lake paleoclimatic proxies from core OL-92, plotted against age (derived using the age-vs.-depth model of Bischoff and others, this volume). $\delta^{18}\text{O}$ record of deep sea sediments from Imbrie and others (1984), calcium carbonate content from Bischoff and others (1993a or this volume), curves of mean grain size, smectite, and illite (plotted inversely) from this report. Note the strong similarity of Owens Lake proxies to oxygen isotopic record of the deep sea. Also note Termination II offset between the marine and Owens Lake records. This offset may result from an error in the age-depth curve determined for the core, or it may represent an actual time lag between global and local glaciations.



1- and 5-m depth. No other evaporite minerals exist in the core, and evidence of dissolution of evaporites is lacking.

No zeolites were found in the clay-sized fraction. These minerals are frequently found in saline lakes (Surdam, 1977) and in association with tephra layers that have been altered by saline brines. The absence of zeolites in the clay-size fraction of the Owens Lake core may indicate that authigenic mineral formation is not a significant process in the lake. However, Hay (1966) found four different zeolites in the silt-size fraction of sediments from a core of Owens Lake drilled in the 1950s, indicating that I may not have been looking for these minerals in the proper size fraction.

The initial hypothesis that the mineralogy of the $<4\text{-}\mu\text{m}$ (clay) fraction would reflect climate appears confirmed. Clay-sized particles are composed of varying proportions of rock flour and pedogenic or authigenic clays; most of the mineralogic variation occurs in the smectite and illite components of the sediments. CEC measurements confirm this mineralogic signal with values consistent with a variation in illite and smectite (Fig. 2.6).

COMPARISON OF GRAIN SIZE AND CLAY-MINERAL VARIATIONS TO OTHER PALEOCLIMATE PROXIES

Bulk grain size and clay mineralogy correlate to, and reflect, other paleoclimatic proxies in the Owens Lake core (Fig. 2.8). Glacial periods as represented by an overflowing Owens Lake, can be identified through combination of the following criteria: Fine mean grain size ($\sim 5\text{ }\mu\text{m}$), a dominance of illite, feldspar, and quartz over smectite in the clay-size fraction, very low CEC values that indicate rock flour (Bischoff and others, in press (b)), low carbonate and organic carbon

contents that indicate a fresh low-productivity lake (Bischoff and others, in press (b)), abundant fresh-water planktonic diatoms (Bradbury, 1993), and a decrease in pine pollen (Litwin and others, 1993). Coarser mean grain size ($\sim 15 \mu\text{m}$), clays dominated by smectite and high CEC values (Bischoff and others, in press (b)), high carbonate and organic carbon contents (Bischoff and others, in press (b)), greater frequency of saline diatoms (Bradbury, 1993) and ostracodes (Carter, 1993), and increases in pine pollen (Litwin and others, 1993) all correlate to reflect a somewhat saline, productive lake, probably during interglacial conditions.

Both carbonate content and mean grain size appear to reflect variations in lake level. For example, the last glacial maximum ($\sim 13 \text{ m}$, $\sim 21 \text{ ka}$) is marked in the core by very low carbonate contents, which indicate a very fresh overflowing Owens Lake (Bischoff and others, in press (b)). The dark muds deposited during the onset of the Holocene interglacial period, on the other hand, show very high percentages of carbonate content, which indicate a shallower lake in which the water reached saturation with respect to carbonate precipitation. Mean grain size also appears to reflect variations in lake level; coarse-grained materials were deposited during times of lake lowstands, when the shores of Owens Lake were closer to our core site, and fine-grained sediments were deposited during highstands, when the shoreline was farther from the core site.

Clay mineralogical variations do not indicate changes in lake level but reflect changes in the weathering environment in the Sierra Nevada or changes in salinity in Owens Lake. Comparison, by use of the age-versus-depth model of Bischoff and others (in press (a)), of the carbonate content, the mean grain size, and the smectite and illite contents of Core OL-92 sediments to the marine oxygen isotope record of Imbrie and others (1984) suggests that the climatic

conditions that led to glaciation in the Sierra Nevada and to lake-level changes in Owens Lake are the same as those that led to global climate cycles (Fig. 2.8). However, the age control on the Owens Lake core implies a time lag of about 10 ky between the marine and terrestrial records. For example, the deglaciation from isotope stage 6 to stage 5, known as "Termination II," occurs in the marine record at ~128 ka. The same feature is found in the Owens Lake core at ~120 ka. This time lag may be the result of an error of ~10 percent in dating or may represent a time lag between global ice-cap growth and lower latitude montane glacial response to global climatic fluctuations.

CONCLUSIONS

1. Variations in grain size of the sediments between ~7-200 m in Core OL-92 reflect variations in depth of Owens Lake. In particular, fine sediments (average grain size ~5 μm) were deposited at the core site during periods of high lake level, when the shores and wave base of Owens Lake were far from the site. Conversely, coarse sediments (average grain size ~15 μm) were deposited during lower lake stands, when the shores and wave base of Owens Lake more closely approached the core site. However, variations in grain size indicate only relative variations in lake level rather than absolute lake depths.
2. Alternations in clay mineralogy reflect cyclic glaciation in the Sierra Nevada. The clay-sized mineral assemblage dominated by illite, K-feldspar, and plagioclase most likely indicates rock flour produced during glacial periods. The assemblage dominated by smectite may represent either chemical weathering

processes on hillslopes active during interglacial periods or authigenic phyllosilicate formation within a shallow, saline Owens Lake.

ACKNOWLEDGMENTS

This work was supported by a National Defense Science and Engineering Graduate Fellowship. Hannah Musler and Jeff Fitts provided many hours of laboratory help, and Mark Johnsson and Mike Torresan provided much technical expertise. Discussions with Robert Anderson, James Bischoff, Jonathan Glen, and George Smith were very helpful. Many thanks to James Bischoff, Richard Hay, George Smith, and Joseph Smoot whose reviews improved the manuscript.

CHAPTER 3

A Model of Runoff, Evaporation, and Overspill in the Owens River System of Lakes, Eastern California

KIRSTEN M. MENKING and ROBERT S. ANDERSON

*Department of Earth Sciences and Institute of Tectonics,
University of California, Santa Cruz, CA 95064*

ABSTRACT

We present a numerical model of water balance for the Owens Lake chain of lakes, southeastern California. These lakes are separated by a series of bedrock sills, have received their water primarily from precipitation in the adjacent Sierra Nevada, and overflowed during extremely wet periods. While the modern climate in the region does not support the existence of lakes in any valley but Owens, shoreline and core evidence suggests that all valleys contained significant lakes during parts of the Pleistocene. Our modeling effort attempts to determine what combinations of runoff and evaporation were necessary to create these large lakes, what the response time of each lake is to perturbations in climatic variables, and whether the lakes are likely to have achieved steady-state with respect to long-term climatic fluctuations.

The model explicitly incorporates the hypsometry of each lake, derived from 3 arc-second DEM data. Runoff is applied and lake volume updated; detailed lake basin hypsometry is employed to calculate new depth and surface

area. Evaporative flux of water from each lake is calculated by multiplying lake surface area by an assumed evaporation rate. When lake volume exceeds the maximum volume dictated by the spillway elevation, excess volume is transferred to the next lake in the chain. The $\delta^{18}\text{O}$ of the model Owens Lake is also calculated for comparison with $\delta^{18}\text{O}$ values measured on carbonates from a core of Owens Lake.

Results suggest that all of the lakes achieve steady-state volumes within a matter of decades, indicating that droughts or particularly wet periods of order several decades to centuries should have been recorded in the sediments of the Owens Lake core, and that all lakes should achieve steady-state altitudes with respect to yet longer-period climate variations. Furthermore, modeled $\delta^{18}\text{O}$ values also reach steady state, with periods of overflow showing depleted values close to Owens River water, and periods of low lake level showing enriched values. "Maximum pluvial" lake stages require an increase in the flux of Owens River water, relative to modern values, of nearly an order of magnitude. Finally, comparison of a modeled lake-level history and oxygen isotopic composition to the lake-level reconstruction of Jannik and others (1991) and to the $\delta^{18}\text{O}$ record for the Owens Lake core (Benson and Bischoff, 1993) shows general agreement.

INTRODUCTION

A chain of Pleistocene lakes, headed by Owens Lake, lies to the south and east of the Sierra Nevada Mountains in southeastern California (Fig. 3.1). Abandoned shorelines found high above valley floors testify to the previous greatness of these lakes which are now all dry playas. The lake basins are

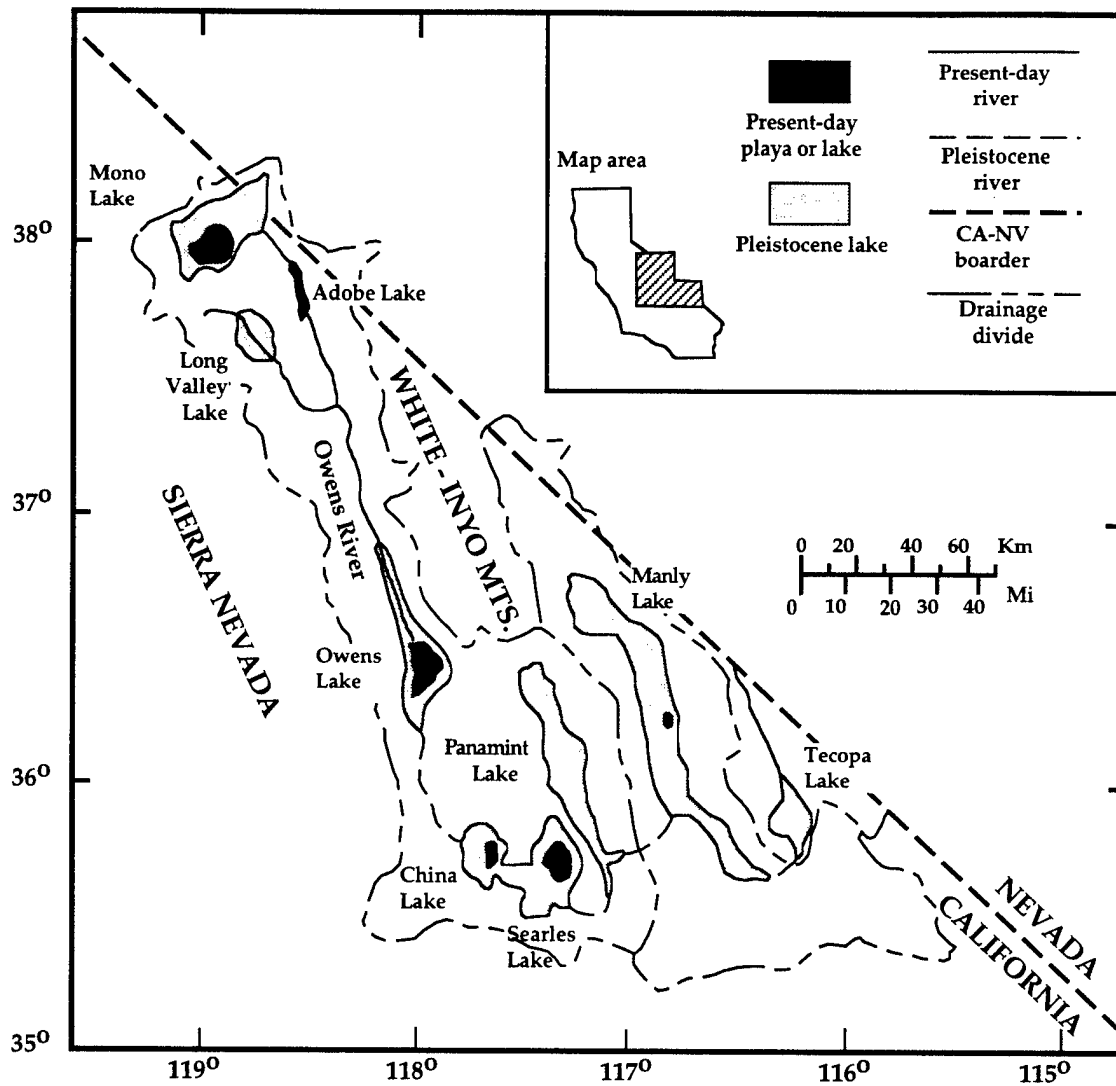


Fig. 3.1: Map of the Owens Lake chain of lakes in eastern California. Black areas represent modern lakes and playas. Grey areas represent the extents of Pleistocene pluvial lakes. Two of the three routes for introduction of water into Death Valley are shown (from overspill from Panamint Lake or from Tecopa Lake).

separated from each other by a series of bedrock sills (Fig. 3.2) and are thought to have received most of their water from precipitation in the Sierra Nevada (Smith, 1976; Smith and Street-Perrott, 1983). When Owens Lake exceeded its confines, it overflowed into the shallow China Lake basin, which rapidly filled and overspilled into the Searles Lake basin. During exceptionally wet periods, China and Searles Lakes coalesced, filled to a common sill level, and spilled into Panamint Valley and ultimately into Death Valley (Smith and Street-Perrott, 1983); surface area for the chain of lakes exceeded 9x the modern value. In this paper, we present a numerical water balance model used to address a number of questions including: what combinations of inflow, evaporation, and overspill are required to produce lakes with observed shoreline elevations? What is the characteristic response time of each lake if it is initially dry and then allowed to approach steady state, and what factors control this response time? Are lakes at steady-state with respect to long time-scale climatic fluctuations?

In 1992, the U.S. Geological Survey cored Owens Lake to obtain a continuous record of terrestrial paleoclimate in the Sierran region (Smith, 1993). Several paleoclimatic proxies, such as mean grain size (Menking, in press), oxygen isotopic composition (Benson and Bischoff, 1993), and carbonate content (Bischoff and others, in press (a)) bear strong resemblances to the oxygen isotopic record from deep-sea sediments (Fig. 3.3). These proxies suggest that glacial periods saw a fresh, isotopically depleted, overspilling Owens Lake while interglacial periods were marked by a shallow, saline, and isotopically enriched Owens Lake. In this paper, we use the measured carbonate oxygen isotopic composition determined by Benson and Bischoff (1993) as an additional

Fig. 3.2: Diagram of each lake's hypsometry and elevational relationship to the other lakes in the chain. Spillway elevations and basal elevations reported in table 1. When China Lake reached an altitude of 665 m, it spilled into the Searles Lake basin. Searles then filled to the China Lake spillway at 665 m, and the two lakes coalesced, filling to an ultimate level of 690 m. Further influx of water prompted spill into the Panamint Lake basin.

Lake Hypsometries Used in the Model

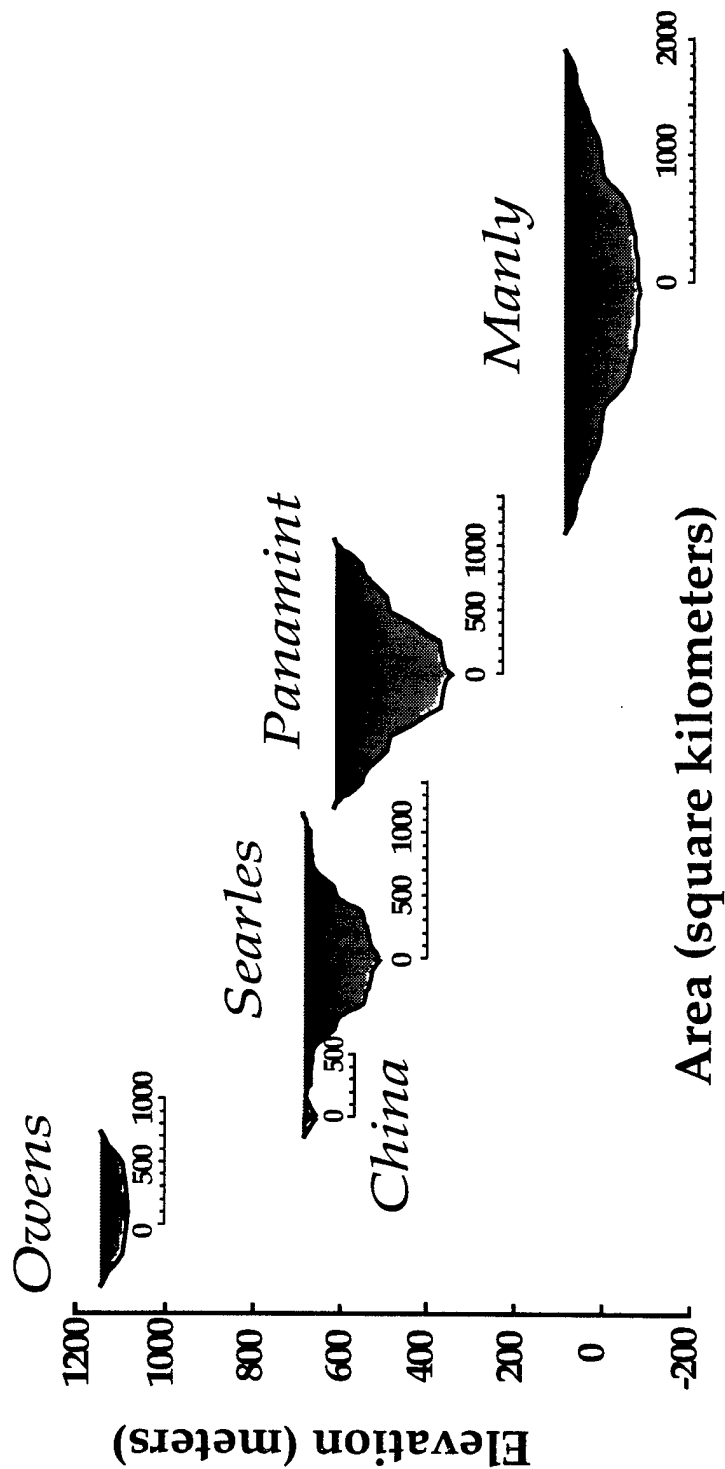
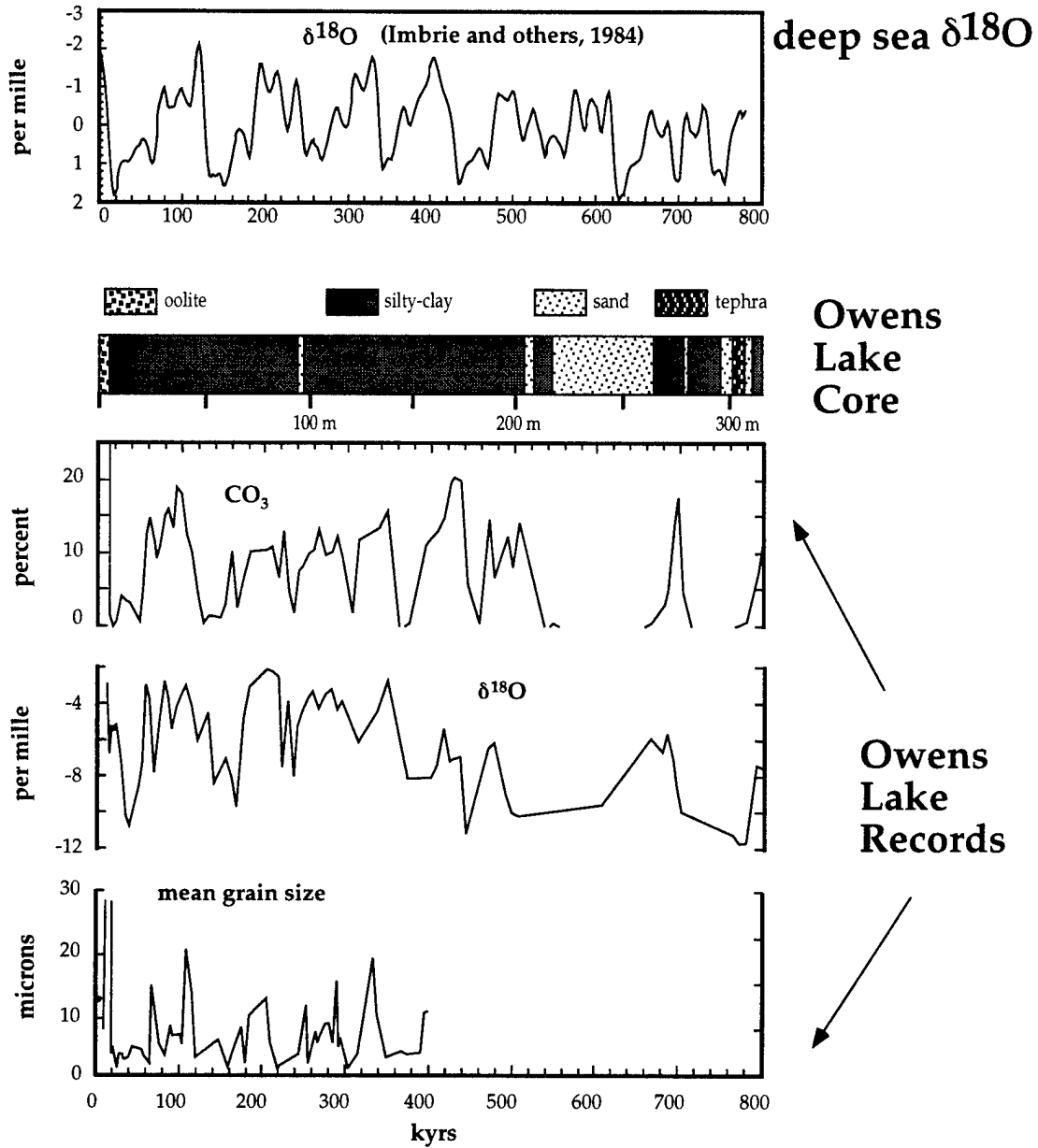


Fig. 3.3: Paleoclimatic proxies from the Owens Lake core compared to the marine oxygen isotopic record from Imbrie and others (1984). General agreement between the marine record and the Owens Lake records suggests that the regional climate in eastern California is being driven by the same processes that influence global climate. All three Owens Lake proxies are thought to reflect fluctuations in lake size. Carbonate content reflects changing salinity of Owens Lake; during glacial periods (such as at 20 ka) carbonate content is very low suggesting that Owens Lake is fresh and spilling over into the China Lake basin. In contrast, during interglacials (such as present and at 100 ka) carbonate content reaches >15% indicating that the lake is shallow and saline. Oxygen isotopic content of carbonates precipitated in equilibrium with lake water probably also reflect lake level. Benson and Bischoff (1993) have interpreted values more enriched than -4‰ as indicative of closed lake conditions. Finally, mean grain size at the core site is finest during glacial periods, and coarser during interglacials. The close correspondence of the grain size and carbonate content records indicate that both are responding to changes in lake size.



constraint on variations in runoff and evaporation necessary to create large Pleistocene lakes.

To investigate how the Owens chain of paleo-lakes responds to variations in climate, we perform a series of experiments with the water-balance model. We first conduct steady-state calculations in which we determine the response time of each lake to a constant input of runoff and constant evaporation rate. We next allow runoff and evaporation to oscillate sinusoidally between modern and assumed-maximum-glacial conditions with different periods of oscillation. To simulate maximum-glacial conditions, we use glacial-geologic and paleobotanical evidence of past temperature and precipitation rates for the southwestern Great Basin. These oscillatory climate experiments serve to confirm the response times determined in the steady-state experiments, and to explore whether water balance is controlled primarily by runoff or by evaporation. Finally, we drive runoff and evaporation with a more realistic forcing function, the $\delta^{18}\text{O}$ curve for deep sea sediments (Imbrie and others, 1984). We assess our reconstruction of water-balance history by tracking Owens Lake water oxygen isotopic composition for different model runs. Goodness of fit between modeled isotopic composition and the measured carbonate oxygen isotopic composition determined by Benson and Bischoff (1993) for the Owens Lake core is assessed visually. We also compare our modeled lake-level record to a lake-level history constructed by Jannik and others (1991), who used stratigraphic and Cl-accumulation evidence from cores of Searles and Panamint lakes. The model is run for the time period 200 ka to the present, such that two large glaciations (associated with isotope stages 2 and 6) and one large interglacial (isotope stage 5) are represented. Before proceeding to a description

of the model, we first outline the geologic and climatic setting of the study area, and review previously conducted work.

TECTONIC AND CLIMATIC SETTING

The Owens River system of lakes lies to the east and south of the Sierra Nevada Mts. in the Basin and Range tectonic province. Each lake resides in a downdropped fault-block valley bounded by essentially north-south trending ranges. Relief between valley floors and range crests is greater than 3000 m in some locations. All of the valleys are closed topographic basins with internal drainage networks. Extensive warping of previously-existing lake shorelines, visible fault scarps, modern seismic activity, and the presence of young volcanic cones and flows in many valleys are evidence of the continuing tectonic activity in the region (Bierman and others, 1991; Hollett and others, 1991; Smith, 1976; Densmore, 1994). In addition to volcanic deposits, each valley is filled with alluvial fan sediments derived from the surrounding ranges, fluvial deposits associated with the internal drainage network, and lacustrine deposits associated with the Owens chain of lakes.

Precipitation in the Owens Valley drainage basin is derived chiefly from the Pacific Ocean and falls primarily over the eastern flank of the Sierra Nevada, which receives some 60-80% of the rain and snow falling on the valley (Hollett and others, 1991). Most of the precipitation falls during the winter months (Benson and Thompson, 1987a; Smith, 1976), and average precipitation rates range from 13-15 cm/yr on the valley floor to more than 100 cm/yr at the crest of the Sierra. These mountains create a strong rain shadow, cutting the average annual precipitation in the White and Inyo Mountains to 18 to 35 cm/yr (Hollett

and others, 1991; California Water Atlas, 1979). Valleys to the east of Owens Valley are located not only in the rain shadow of the Sierra Nevada but also in the lee of other north-south trending ranges. As a result, regional precipitation tends to decrease with distance from the Sierra Nevada, with the lowest precipitation values, <10 cm/yr, being recorded in Death Valley (California Water Atlas, 1979). Those valleys containing paleo-lakes China, Searles, Panamint and Manly currently are marked by very low values of surface runoff, 0.63 cm or less per year. The western flank of the Owens Valley, by contrast, experiences runoff values between 0.63-100 cm/yr with runoff increasing with rising altitude (Langbein and others, 1949; Hollett and others, 1991).

Average monthly air temperature in the valleys ranges from less than 0°C in the winter to more than 30°C in the summer, with mean annual temperature near Owens Lake ~15°C (Hollett and others, 1991; Smith, 1976; Phillips and others, 1992). Winds blow predominantly up- and down-valley, with speeds of up to 50 km/hr. Relative humidity in the Owens drainage basin varies between less than 30% in the summer to more than 40% in winter, and evapotranspiration rates range from 30 to 100 cm/yr (Hollett and others, 1991). These climatic conditions favor the growth of alkaline scrub plant and meadow plant communities. Juniper and pine woodlands are found at higher elevations. Meyers (1962) and Smith and Street-Perrott (1983) report evaporation rates for lakes and reservoirs in several western states. Evaporation rate increases with distance from the Sierra Nevada, with the lowest average evaporation rates found in Owens Valley (75-110 cm/yr), and the highest found in Death Valley (180-220 cm/yr).

Modern climatic conditions do not support the existence of lakes in any valley except Owens. Prior to the construction of the Los Angeles aqueduct (1912) and the attendant diversion of Sierran runoff into the aqueduct, discharge into the Owens River maintained a 14 m deep, 290 km² area Owens Lake (Smith and Street-Perrott, 1983). As a result of the artificial diversions, this lake has since essentially desiccated. Paleo-shoreline evidence (Gale, 1914; Smith, 1976; Blackwelder, 1933 and 1954; Hunt and Mabey, 1966; Hooke, 1972) indicates that climatic conditions during some periods of the Pleistocene must have differed significantly from modern conditions. During what Smith (1984) terms extreme "pluvial" periods, Owens, China, Searles, and Panamint Lakes filled to overflowing, and Manly Lake, in Death Valley, filled to a depth of 173 m. At present, the combined surface area of all of the lakes (modern surface area being 0 km² in the case of China, Searles, Panamint, and Manly Lakes, and taken as the historical lake surface area [290 km²] for Owens Lake) represents only 1.1% of the total combined drainage area contributing to these lakes. At their maximum high-stand elevations, however, the five lakes covered 9.1% of the total combined drainage area. The climatic conditions required to maintain these large lakes are unclear, and provide the motivations for conducting this study.

PREVIOUS WORK AND CONSTRAINTS ON PLEISTOCENE

PALEOCLIMATE IN THE SIERRA NEVADA REGION

Paleoclimatic evidence

Gale (1914), Smith (1976), Blackwelder (1933 and 1954), Hunt and Mabey (1966), Hooke (1972), and Smith (1984) described geomorphic evidence for large lakes in the currently dry Owens, China, Searles, Panamint and Death Valleys.

This evidence consists of tufa towers and tufa shorelines, well-rounded beach gravels, deltaic deposits, beach-rock, and coquina shorelines incorporating fresh-water gastropods. Unfortunately, attempts at dating shoreline deposits have frequently been frustrated by a lack of datable material, or by post-depositional alteration of carbonate (Fitzpatrick and Bischoff, 1993; Smith, 1976). As a result, much of the information on timing of relative lake level stands has come from core evidence.

The drilling of several cores into Panamint and Searles Lakes in the 1950s (Smith and Pratt, 1957), and into Lake Manly in the 1990s (Lowenstein and others, 1994; Ku and others, 1994; Li and others, 1994; Roberts and others, 1994) showed a succession of high and low lake-level stands in these valleys with high lake levels marked by silt and clay deposition and low levels marked by evaporite deposition. Table 3.1 lists the core evidence for lake-level fluctuations. Jannik and others (1991) attributed low accumulation rates of chloride in Searles Lake to periods of overspill of Searles Lake into Panamint Valley, that overspill carrying the dissolved load of chloride into Panamint Lake where it was precipitated. In the 200 ka period relevant to this paper, they showed periods of low chloride accumulation in the Searles Lake core, and therefore overspill into Panamint Valley, occurring from 120-150 ka, and again from 10-24 ka. They did not determine any periods of overflow from Panamint Lake to Death Valley. On the other hand, Lowenstein and others (1994), Ku and others (1994), Li and others (1994) and Roberts and others (1994) found evidence for large lakes in Death Valley over the last 200 ka. These authors did not address the question of what was the source of the water in Death Valley during its large perennial lake cycles, however. There are three routes by which water entered Death Valley: through

TABLE 3.1: Core and Shoreline Evidence of Past Lake Levels for Several Owens Chain Lakes

Lake	Reference	Paleoclimatic Information	Evidence
Searles	Smith (1984)	Nine ~400 ka duration paleohydrologic regimes ranging from "wet" to "intermediate" to "dry." Some shorter duration fluctuations observed.	930 m KM3 Searles Lake core (3.2 Ma), sediments vary between deep lacustrine muds and evaporites
Searles and Panamint	Jannik and others (1991)	Overspill from Searles Lake to Panamint Valley from 120-150 ka, and again from 10-24 ka. No overspill to Death Valley from 0-200 ka.	Accumulation of chloride in cores from Searles and Panamint Lakes. Chronology of cores established with ^{36}Cl .
Manly	Lowenstein and others (1994) Ku and others (1994) Li and others (1994) Roberts and others (1994)	Saline pan from 0-10 ka, shallow saline lake from 10-30 ka, saline pan with two small lake cycles from 30-60 ka, mudflat from 98-120 ka, perennial saline lake from 120-128 ka, large perennial lake from 128 to 186 ka, saline lake alternating with salt pan from 186-193 ka. Lake Manly at its deepest (~174 m) at 185 ka. This stage lasted until 130 ka.	Core stratigraphy varies from black deep-lacustrine muds to halite beds. Fabrics in halite beds distinguish saline pan from saline lake environments. Tufa shoreline ages and core chronology established with U-series methods.

overspill from Panamint Valley to the west, from the Amargosa River to the south, and from the Tecopa Lake system to the east. At present, the relative importance of these sources is not known (Lowenstein, personal communication). Given the Cl accumulation evidence of Jannik and others (1993), which suggests that Searles Lake spilled over into Panamint Valley from 120-150 ka, but not earlier, it appears as though the large lake that existed in

Death Valley at 186 ka may have been produced by runoff from the Tecopa and Amargosa entrances to Death Valley, rather than by overspill from Panamint Valley.

In 1992, the U.S. Geological Survey cored Owens Lake to obtain a continuous record of terrestrial paleoclimate in the Sierran region (Smith, 1993). Unlike Searles Lake (Smith, 1984), which underwent several filling and desiccation cycles captured in sedimentologic variations between deep lacustrine clays and evaporites, Owens Lake appears to have contained water for at least 786 ka. A close examination of the sediments in the 323-m-long core OL-92 (the base of the core is at the Bruhnes/Matuyama magnetic reversal at 786 ka) reveals no evidence for a desiccation event at any time except at approximately 5 ka when a 1-2 m thick section of oolites formed. There are no thick evaporite packages or playa assemblages, and there exists no evidence for dissolution of evaporite minerals. Nevertheless, there exists evidence for substantial lake level variations in such paleoclimatic proxy records as mean grain size (Menking, *in press*), carbonate content (Bischoff and others, *in press (a)*), and oxygen isotopic composition of inorganically precipitated carbonate (Benson and Bischoff, 1993) (Fig. 3.3).

Geochemical calculations performed by Bischoff and others (*in press (a)*) and by Benson and Bischoff (1993) on OL-92 sediments may constrain periods of closed- and open-lake conditions. Bischoff and others (*in press (a)*) used calcium carbonate accumulation rates to argue that Owens Lake remained closed for periods lasting up to 50 kyrs, separated by shorter (20-30 kyr) durations of overflow. They noted, however, that discrepancies exist between their calculated timing of overflow events and the stratigraphic evidence of overflow into the

Searles Lake basin. In particular, from 50-120 ka, these authors found no evidence for overflow, while Bischoff and others (1985) reported stratigraphic evidence for overflow events during this period from a core from Searles Lake. Furthermore, Bradbury (1993) identified several fresh-water diatom species in the Owens Lake core which would indicate spillover between 80-90 ka. Nevertheless, Bischoff and others' (in press (a)) calculations of overflow from Owens Lake compare favorably to Jannik and others' (1991) estimations of overflow of Searles Lake into Panamint Valley, with the former authors suggesting overflows between ~10 and 50 ka, and again between ~110 and 150 ka. Benson and Bischoff (1993) interpreted oxygen isotopic compositions of lacustrine carbonates more enriched than -4‰ (PDB) as indicative of closed lake conditions. If correct, then Owens Lake spilled into the China and Searles basins from 10 to 55 ka, 61-75 ka, 84-94 ka, and 110-176 ka. As the geochemical analyses conducted by Bischoff and others (in press (a)) and by Benson and Bischoff (1993) were performed on samples with an 8 kyr resolution, caution is warranted in ruling out short episodes of overflow in the intervening periods.

The lake records described above require that climate during some parts of the Pleistocene must have been very different from modern. Many workers have addressed the questions of what temperatures and precipitation rates prevailed during glacial periods in the southwestern Great Basin, Table 3.2. The Sierra Nevada are dotted with evidence of multiple Pleistocene (Phillips, 1990) and Holocene (Birman, 1964; Burbank, 1991) glacial advances, and the location of past glacial equilibrium line altitudes calls for a lowering of mean annual temperature by 5°C relative to modern values (Porter, 1983). Several other workers (Dohrenwend, 1984; Spaulding and Graumlich, 1986; Stamm, 1991) have

TABLE 3.2: Paleo-Temperature and Paleo-Precipitation Estimates for the Last Glacial Maximum

<u>Reference</u>	<u>Paleoclimatic Information</u>	<u>Evidence</u>
Porter (1983)	Mean annual temperature (MAT) during glaciations 5 °C colder than modern.	Glacial equilibrium line altitudes 800 m lower than modern in Sierra Nevada.
Dohrenwend (1984)	Either no increase in precipitation and 7 °C lowering of MAT relative to modern, or 370 mm increase in precipitation and 5.5 °C lowering of MAT.	Nivation hollow threshold altitude depressed during glaciations; hollows identified in Sierra Nevada and White Mts., among other ranges.
Spaulding and Graumlich (1986)	≤40% increase in precipitation and ~5 °C decrease in temperature in Mojave Desert during last glacial maximum. No increase in precipitation above 36 °N latitude.	Packrat middens
Stamm (1991)	70% increase in precipitation and 6 °C decrease in MAT at Lake Lahontan, ~350 km north of the Owens chain of lakes.	Solutions to a local climate model constructed for the southwestern U.S. Boundary conditions come from global climate models.

estimated similar regional decreases in temperature for the last glacial maximum. In addition to temperature variations, precipitation is also thought to have increased by 40% (Spaulding and Graumlich, 1986) to 70% (Stamm, 1991) during parts of the Pleistocene.

Paleoclimatic calculations and models

Various models have been constructed to address the effects of changing climate on the water balance of closed-basin lakes. Smith and Street-Perrott (1983) assessed the amount of Owens River discharge necessary to fill successively each lake in the chain, assuming that none of the four lakes down-river from Owens received any water from its own local drainage basin; with various evaporation values, the flow in the Owens River would have to be increased by 5x to >10x modern in order to fill Lake Manly to its high-stand level. Phillips and others (1992) reconstructed lake-surface-area histories for the Owens lake-chain based upon oxygen-isotopic values of carbonates from a core of Searles Lake and upon a water-balance model which related oxygen-isotopic composition of Searles Lake water to different steady climate forcings. They found an episode of overspill from Searles to Panamint at 18-24 ka and from Panamint to Manly Lake at ~140 ka (p. 135). The model of Orndorff and Craig (1994) determines snowpack, runoff, and lake extent for the Owens chain of lakes from temperature, precipitation, and topographic data. This regional climate model was constructed to compare estimates of past temperature and precipitation rates from paleobotanical and glacial-geologic evidence to known extents of lakes, and allows spatial variability in temperature, precipitation, windfield, and topography. Orndorff (personal communication) has informed us that the model predicts a 3.5-fold increase in runoff in the Owens Lake region during the last glacial maximum. Finally, Hostetler and Benson (1994) constructed a predictive model of oxygen and deuterium isotopes for Pyramid Lake, Nevada, based upon several climatic variables including air temperature, relative humidity, windspeed, solar and thermal radiative fluxes, amount of

precipitation falling on the watershed, and isotopic composition of precipitation. Given these variables, they calculated the volume of the lake at any time step, the amount of water evaporating from the lake's surface, and the isotopic composition both of the evaporated water and of the remaining lake water.

The model described in this paper is different from that of Smith and Street-Perrott (1983) and Orndorff and Craig (1994) because it allows us to explore transience in lake levels as climate changes, as well as to determine the time required to reach steady-state-lake conditions given a particular suite of paleoclimatic variables. These authors were confined to looking at end-member, steady-state climatic scenarios, and thus could not generate a lake-level history for the Owens Lake chain of lakes. Furthermore, we make use of the new oxygen isotopic data set from Owens Lake carbonates (Benson and Bischoff, 1993) to constrain our modeled estimates of lake level history, rather than the Searles Lake isotopic record used by Phillips and others (1991). Because Searles received its input runoff from overspill from Owens Lake, the Searles Lake record is an incomplete record of climate change in the region. Finally, the model of Hostetler and Benson (1994), while excellent at predicting modern isotopic values in lakes, requires meteorological data that we presently have no way of constraining for Pleistocene paleoclimates. We therefore use a more simplified and general approach to determine to first order the relative importance of changes in runoff and evaporation on lake size. Though our modeling approach differs from the approaches employed by Orndorff and Craig (1994), Smith and Street-Perrott (1983), Benson and Hostetler (1994) and Phillips and others (1992), we draw on their works as sources of climatic data and for comparison of results.

MODEL

Theoretical Background

Lake Level Calculations. The water balance of a closed-basin lake can be described by the following equation (Mifflin and Wheat, 1979; Phillips and others, 1992; Benson and Hostetler, 1994):

$$\frac{dV}{dt} = \alpha P A_B - E A_L + G_{in} - G_{out} \pm V_{spill} \quad (1)$$

where P is the precipitation rate, A_B is the drainage basin area, α is a runoff coefficient, E is the lake evaporation rate, A_L is the lake surface area, G_{in} and G_{out} are the fluxes of groundwater into and out of the lake, and V_{spill} is the volume of water spilled into or out of the lake basin. As we have no way of constraining either G_{in} or G_{out} for the Owens chain of lakes, we ignore these terms. Danskin (personal communication) has informed us that the quantity of water entering or leaving Owens Lake through the groundwater system is small (<10%) compared to the flux of surface water into the lake/aqueduct system. This is primarily due to the fact that the permeability of the sediments underlying Owens Lake is quite low. Looking at Mono Lake however, a possible analog for Owens Lake when it contained water, Rogers (1993) estimated that the groundwater contribution of inflow might be as high as 28% of the total. We ignore groundwater contributions to the water balance of Owens Lake through time, although we realize that such contributions may have been larger during wet periods of the Pleistocene, perhaps more akin to the situation in the Mono Basin. Phillips and others (1992, p. 59) make the same assumption of negligible groundwater contribution for Searles Lake based upon the observation that the basin is arid and that runoff into Searles Lake came primarily from overspill from China Lake rather than from precipitation over Searles' drainage basin. The same

assumption can be applied to China, Panamint, and Manly Lakes. For a steady state lake which is neither gaining nor losing water by spillover, equation 1 simplifies to (Benson and Paillet, 1989),

$$\alpha P A_B = E A_L \quad (2)$$

in which the lake surface area, A_L , is easily predicted from known parameters. Any perturbation in runoff or evaporation rate will result in a new steady-state lake area.

We would like to know how long a particular lake system takes to respond to changes in climatic forcing (step-changes in runoff and evaporation rates), i.e., we seek the system-response time constant, t . Casting lake area in terms of lake volume, equation 1 becomes a non-linear non-homogeneous differential equation which can be solved to determine the response time of a lake to climatic perturbations. For the Owens chain of lakes, area and volume are approximately related by the expression

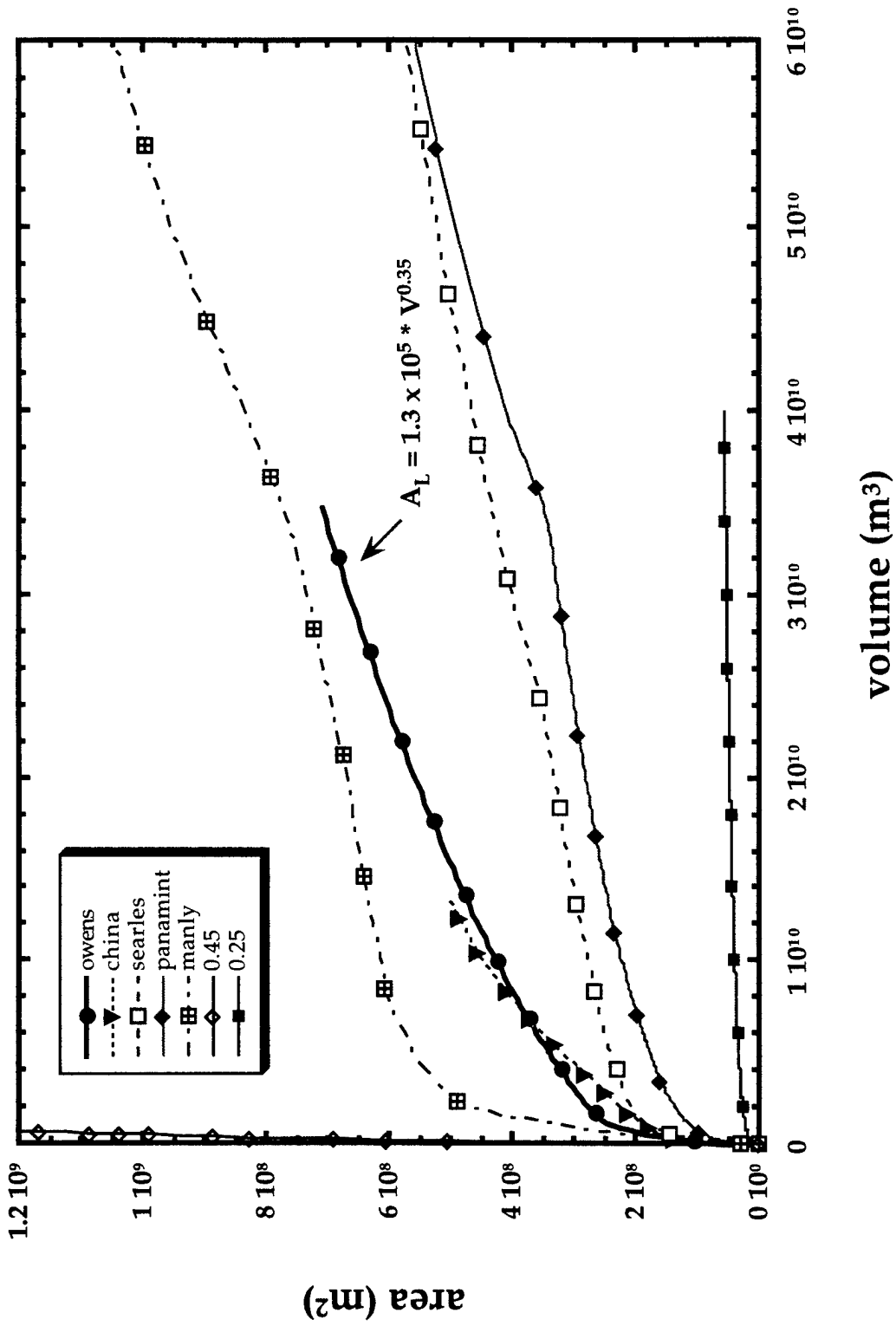
$$A_L = m * V^q \quad (3)$$

where m is a constant, and q is a power less than one (Fig. 3.4). Substituting equation 3 into equation 1, ignoring both the groundwater fluxes into and out of the lake, and additions by overspill, defining $C = \alpha P A_B$ (corresponding to total basin runoff), and $a = m * E$, yields

$$\frac{dV}{dt} + a * V^q = C \quad (4)$$

Fig. 3.4: Area-volume relationships for each lake in the Owens chain. The relationship generally can be characterized by the equation $A_L = m * V^q$ where A_L is the area of the lake, V is the volume of the lake, m is a constant, and q is a power < 1 . The dashed line parallel to the Owens Lake area-volume curve represents the best fit to the equation above for Owens Lake. Also shown are two hypothetical area-volume relationships for different values of the power q . Low q values give rise to very small increases in lake surface area for large changes in volume. High q values create lakes whose surface areas change rapidly with small increases in volume.

Area-volume relationships for the Owens Lake chain



At steady state, $a * V_{ss}^q = C$ or $V_{ss} = \left(\frac{C}{a}\right)^{\frac{1}{q}}$, where V_{ss} is the volume of the lake at steady state. As will be shown below in the section on steady-state climate experiments, the volume versus time behavior of an initially dry lake subjected to steady climate forcing appears to be approximated well by

$$V = V_{ss} * \left(1 - e^{-\frac{t}{\tau}}\right) \quad (5)$$

where t is a time constant dependent on amount of runoff, evaporation rate, and basin geometry. Differentiation of equation 5 and substitution into equation 4 yields:

$$\frac{1}{\tau} V_{ss} e^{-\frac{t}{\tau}} + C \left(1 - e^{-\frac{t}{\tau}}\right)^q = C \quad (6)$$

In order to solve this equation for t , we must define what we mean by steady state. We arbitrarily assume that we have reached steady state when the volume of the lake has reached 95% of its asymptotic steady state volume, V_{ss} . Rewriting equation 5 as

$$\frac{V}{V_{ss}} = \left(1 - e^{-\frac{t}{\tau}}\right) = 0.95 \quad (7)$$

and substituting this into equation 6 to solve for t gives:

$$\tau = \left[\frac{0.05}{1 - (0.95)^q} \right] * \frac{C^{\frac{1}{q}-1}}{(m * E)^{\frac{1}{q}}} \quad (8)$$

Once we have determined t , rearrangement of equation 7 reveals how long it takes an empty lake to achieve a steady-state volume in the face of steady climate forcing:

$$t = -\tau * \ln(0.05) \quad (9)$$

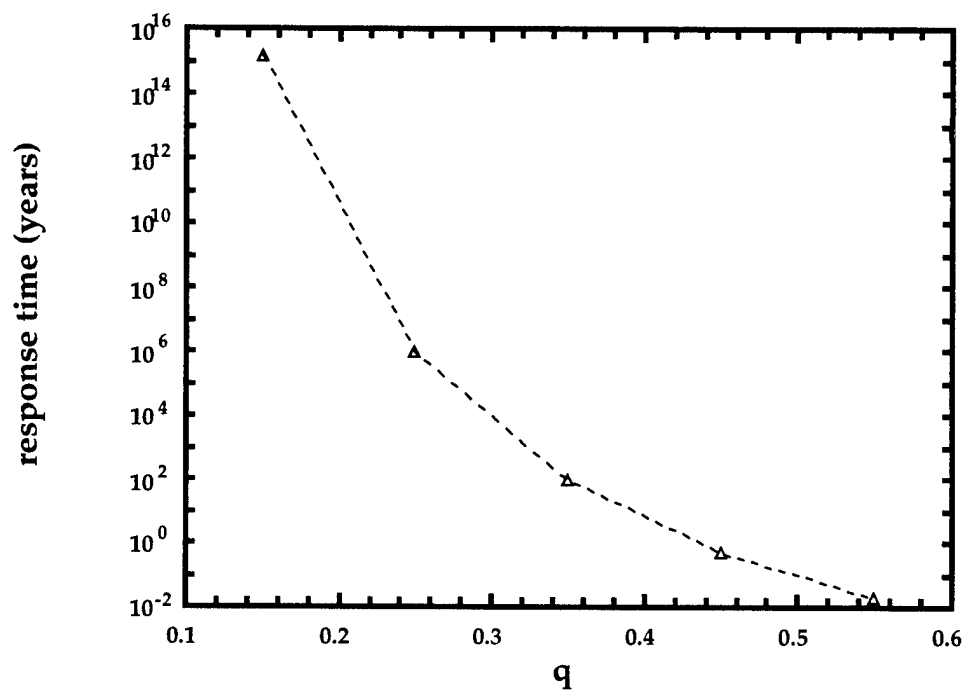
Equation 8 provides insight into the relative importance of climatic and geometric parameters in determining the response of a lake to climatic forcings. Because lake surface area is equivalent to lake volume raised to some power q , lake response time is extremely sensitive to basin geometry. In Figure 3.4, we show the five Owens chain- and two hypothetical-lake area-volume relationships. The smaller the q value, the smaller the increase in surface area per change in volume. The effect of these different geometries on response time is shown in Figure 3.5a. The lake with q value of 0.15 has an extremely long response time, reflecting the fact that its surface area-to-volume ratio is very low, and that it takes a long time for evaporation from the lake's surface to balance inflow. The converse is true for the lake with $q=0.55$. Owens Lake, with its q value of 0.35, has an intermediate response time. It should take approximately 100 years for the lake to reach 95% of its steady-state size.

In Figure 3.5b we explore the importance of changes in runoff and evaporation rate on response time for Owens Lake. For the same evaporation rate and basin geometry, small amounts of runoff are quickly balanced by

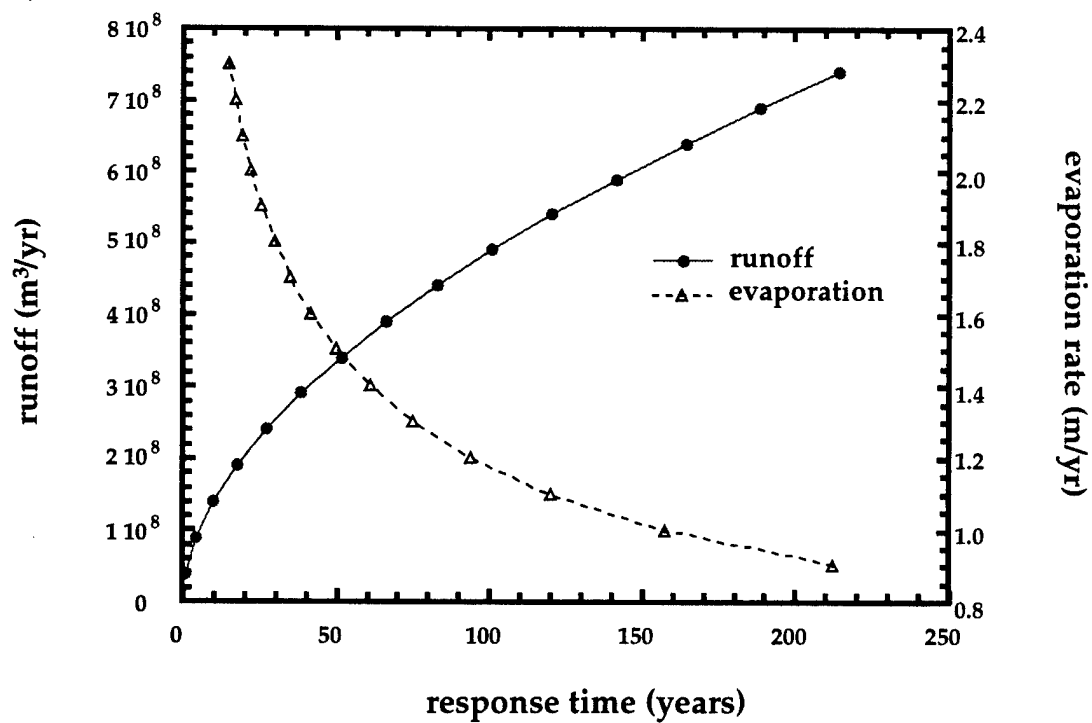
Fig. 3.5a: Relationship of lake response time to lake hypsometry. Evaporation and runoff are specified as modern values for Owens Lake. Shown are response times for different q values. The smaller the q value, the longer it takes evaporation from the lake's surface to balance inflow.

Fig. 3.5b: Relationship between lake response time and amount of runoff flowing into the lake and evaporation rate. For the runoff curve, basin hypsometry and evaporation rate remain constant. For the evaporation curve, basin hypsometry and runoff remain constant.

a) Response time of a lake for different geometries



b) Response time versus amount of runoff and evaporation



evaporation while larger amounts of runoff require substantially longer times to reach steady state. The response time shows the opposite behavior for changes in evaporation rate when runoff rate and basin geometry are held constant; increases in evaporation rate cause decreases in t . Examination of Figures 3.5a and b shows that the hypsometry of the lake is of primary importance in determining the response time. Climatically reasonable changes in runoff and evaporation lead to changes in response time of order tens of years, while changes in hypsometry could cause changes in response time of orders of magnitude. However, hypsometric changes, such as might result from tectonic factors or changes in sedimentation in the basin, occur over time periods much longer than climatic change, and therefore do not present a problem when trying to model water balance.

Isotopic Calculations. In addition to modeling volume changes with different climatic forcings, we can also model the oxygen isotopic composition of Owens Lake water through time for comparison to the isotopic values measured on carbonates in the Owens Lake core (Benson and Bischoff, 1993). We use the equations of Gonfiantini (1986) which describe the evolution of oxygen isotopic composition in a water sample subjected to evaporation:

$$\delta = \left(\delta_0 - \frac{a}{b} \right) f^b + \frac{a}{b} \quad (10)$$

where

$$a = \frac{(h * \delta_a) + \Delta \epsilon + \frac{\alpha - 1}{\alpha}}{1 - h + \Delta \epsilon} \quad (11)$$

$$b = \frac{h - \Delta\epsilon + \frac{\alpha - 1}{\alpha}}{1 - h + \Delta\epsilon} \quad (12)$$

and

$$\Delta\epsilon = (1 - h) * \left(\frac{\rho_i}{\rho} - 1 \right) \quad (13)$$

h = relative humidity

ρ_i and ρ are resistance coefficients which describe the relative efficiencies of transport of the rare and common isotopic species

α = fractionation factor for water/vapor system,

$$\ln(\alpha) = \frac{1.137 * 10^3}{T^2} - \frac{0.4156}{T} - 2.0667 * 10^{-3} \text{ (Hostetler and Benson, 1994)}$$

δ_a = the oxygen isotopic composition of the atmosphere over the lake

δ_0 = the initial oxygen isotopic composition of the lake water

f = the fraction of liquid remaining after evaporation

We employ this relationship to keep track of the oxygen isotopic composition of Owens Lake water through time, using the modern $\delta^{18}\text{O}$ value of Owens River water for the input precipitation, -16‰ (Hay and others, 1991), an atmospheric isotopic value of -21‰ (value used by Hostetler and Benson (1994) to model isotopic evolution of Pyramid Lake), and an empirically derived value of r_i/r of 1.0141 (Gonfiantini, 1986). We further assume that the relative humidity of the atmosphere over the lake is 35%. For comparison, the Owens Valley experiences relative humidities in excess of 40% during the winter and smaller than 30% in the summer. In order to facilitate comparison of the modeled $\delta^{18}\text{O}$ values with the measured carbonate $\delta^{18}\text{O}$ values of Benson and Bischoff (1993), we convert

the water oxygen isotopic composition to an equivalent calcium carbonate isotopic composition using the following equations (Friedman and O'Neil, 1977):

$$1000\ln(\alpha) = \frac{2.76 \cdot 10^6}{T^2} - 2.89 \quad (14)$$

$$\delta^{18}O_{calcite} = [(\delta^{18}O_{water} + 1000) * \alpha] - 1000 \quad (15)$$

where α is the fractionation factor for the water-calcite system, and T is the calcification temperature, here taken to be the modern mean annual temperature near Owens Lake, 15°C.

Construction of the Model

The water balance model described in this paper is a finite difference computer model written in the Fortran computer language. In each model timestep, runoff is applied to Owens Lake and its volume is updated. We next employ a detailed lake basin hypsometry to calculate the new depth and surface area of the lake. Once surface area has been established, the evaporative flux of water from the lake is calculated by multiplying surface area by an assumed evaporation rate. When Owens Lake's volume exceeds the maximum volume dictated by its spillway elevation, the excess volume is transferred to the next lake in the chain (China Lake). The overspilled volume represents the runoff into the next lake and the model then goes through the same process of updating that lake's volume, determining the new depth and surface area, and calculating an evaporative flux and overspilled flux from the lake. The volume, surface area,

and depth calculations are conducted for each lake in sequence of its position within the lake chain before the next timestep begins. The model timestep is one year, and different experiments are run for timespans of several hundred years to 200 kyrs. The $\delta^{18}\text{O}$ of the model Owens Lake is also calculated for comparison with $\delta^{18}\text{O}$ values measured on carbonates from core OL-92 which was taken in 1992. The following sections describe the hypsometric and climatic data used in the exercise.

Lake hypsometries. We use U.S. Geological Survey 3 arc-second digital elevation data to construct altitude versus area hypsometries for each lake. We delineate drainage basins for each of the five lakes using Geographical Information System software, and calculate the area contained within each 1 m contour, yielding an area-elevation relationship for each lake. Next we determine the volume of the lake at each 1 m contour by averaging the surface area at that contour with the surface area of at the contour below, and multiplying that average by the contour interval. Figure 3.2 shows the hypsometries determined for each lake. Hypsometric data such as valley floor elevation, spillway elevation, maximum lake depth at spill elevation, and maximum volume attainable by each lake are found in Table 3.3.

Runoff. In the model, we lump changes in runoff coefficient, α , and precipitation rate, P , into changes in the product of these values, αP , because we cannot constrain changes in the individual parameters in the past. Using unpublished Los Angeles Department of Water and Power records of yearly discharge through the Owens River aqueduct system since 1932, we determine

TABLE 3.3: Hypsometric information for each modeled lake

	<u>Owens</u>	<u>China</u>	<u>Searles</u>	<u>Panamint</u>	<u>Manly</u>
lake base (m) ¹	1081	657	493	317	-86
spill elevation (m) ¹	1145	665	690	609	87 ³
max depth (m) ¹	64	8	197	292	173
max lake area (km ²) ²	610	195	650	780	1560
max lake volume (km ³) ²	25	1.2	76	117	153

¹from Smith and Street-Perrott, 1983

²determined from the 3 arc second DEMs and ArcInfo

³maximum shoreline elevation

the mean annual runoff that would be available to Owens Lake were it not diverted to be $3.98 \times 10^8 \text{ m}^3/\text{yr}$.

Langbein and others (1949) reported a set of empirical curves relating runoff in the United States to mean annual air temperature and precipitation. Benson and Thompson (1987a) have suggested for various reasons that these curves are inaccurate for reconstructing climate in the Great Basin. In spite of their warnings, in order to make a first approximation, we make use of these curves to estimate what runoff during the last glacial maximum might have been, and then refine our estimates later when we compare our modeled isotopic values to the measured isotopic values of Benson and Bischoff (1993). Based upon geologic and climate-model evidence for a 5°C cooling (Porter, 1983; Dohrenwend, 1984; Spaulding and Graumlich, 1986; Stamm, 1991) and 70%

increase in precipitation (Stamm, 1991), average runoff in the Owens Valley would have increased by ~10-fold over modern.

Evaporation. The product of the instantaneous surface area of each lake with the annual evaporation rate determines the evaporative flux of water out of the lake at each time step. We use the evaporation rates suggested by Smith and Street-Perrott (1983) for both modern conditions and for a 5°C cooler annual climate, with the exception of the modern Owens Lake evaporation value. We determine this value by solving the steady state lake equation for evaporation rate given the historic lake size and mean annual runoff values. Lakes to the south and east of Owens Lake have progressively larger evaporation rates, reflecting both their decreasing elevations and rain shadow effects. Table 3.4 lists the measured modern and inferred glacial runoff and evaporation rates for each of the lakes in the model.

Assumptions

We make the following set of simplifying assumptions to facilitate the modeling. First, we ignore tectonic activity in each drainage basin, taking modern curves for our paleo-hypsometries. By making this assumption, we assume that the maximum volume of each lake has remained constant over the 200 kyrs represented by the model. Bierman and others (1991) report vertical displacement rates on range-bounding faults in Owens Valley of ~0.3 mm/yr. For a 200 kyr model run, this translates into 60 m of subsidence. However, as Owens Lake has received ~0.4 mm/yr of sediment over the last 800 ka, subsidence rates appear to be approximately matched by sedimentation rates (at

TABLE 3.4: Hydrologic parameters for each lake for fixed runoff and evaporation case

	<u>Owens</u>	<u>China</u>	<u>Searles</u>	<u>Panamint</u>	<u>Manly</u>
average modern runoff (m^3/yr) ¹	3.98×10^8	0	0	0	0
average modern evaporation rate (m/yr) ²	1.34 ^s	1.41	1.65	1.65	1.97
inferred glacial runoff (m^3/yr)	3.98×10^9	0	0	0	0
inferred glacial evaporation rate (m/yr) ³	0.94	0.99	1.15	1.15	1.38

least in Owens Valley), and we can assume that the lake hypsometry has not changed significantly. Similar sedimentation rates have been reported for Searles (0.2 mm/yr, Phillips and others, 1992), and Panamint (0.4 mm/yr, Jannik and others, 1991) Valleys, with a somewhat higher rate (~1 mm/yr) reported for Death Valley (Ku and others, 1994). Subsidence rates in these valleys are poorly constrained (Ellis, personal communication). However, Hodges and others (1989), citing previous work, state that between 0 and 2 km of vertical movement has occurred along the Hunter Mtn. fault zone in northern Panamint Valley. The subsidence of Panamint Valley, relative to Hunter Mtn. itself is thought to have occurred over the last 3-3.6 Ma, giving maximum subsidence rates on order 0.5-0.6 mm/yr for Panamint Valley, in general agreement with sedimentation rates in the valley. Hooke (1972) used tilted fan segments in Death Valley to estimate a

vertical slip rate of 7 mm/yr on the Black Mountain fault. If this slip rate were indicative of subsidence of the entire valley, then Death Valley would have to be subsiding much more rapidly than it is filling with sediment. In this case, our assumption of a constant hypsometry over the last 200 kyrs would be invalid. However, as Death Valley is the last lake in the chain and does not overflow, the position of the valley floor relative to the spillway is unimportant in our modeling exercises.

We set runoff contributions from all drainage basins other than Owens Valley to zero. Spaulding and Graumlich (1986) analyzed pack-rat middens to determine the spatial and temporal distribution of temperature and precipitation over the last ~25 ka in the southwestern U.S. They inferred a decrease in mean annual precipitation during the last glacial maximum for regions in the lee of the Sierra Nevada, while localities to the south experienced enhanced precipitation. These data would tend to confirm the calculations of Smith (1976), which show that high lake-level stands in the China, Searles, Panamint and Manly Lake basins must have been derived by overspill from Owens Lake rather than by increased precipitation on each lake's individual drainage basin.

We ignore groundwater fluxes into or out of each lake for reasons mentioned above. We further neglect any dependence of evaporation rate on lake salinity, assuming in all of our calculations that fresh water is evaporating. Salts tend to decrease the thermodynamic activity of water, thereby slowing the evaporation rate (Gonfiantini, 1986), but this effect is very small and can be neglected unless waters are exceptionally saline (Gonfiantini, 1986). There is no evidence in core OL-92 that Owens Lake ever reached salinities high enough for evaporation to have been inhibited. Since Owens Lake is presently a dry playa,

we have no information regarding the lake's previous thermal structure. We therefore assume that the lake is an unstratified, homogeneous water body with no gradients in temperature or isotopic composition with depth. Finally, we assume simple Rayleigh distillation of lake water with a relative humidity of 35% in the overlying atmosphere. Sensitivity analyses below will address some of our assumptions.

EXPERIMENTS

In order to develop our understanding of the dynamics of the 5-lake system, we report a series of experiments employing both steady and variable climatic forcing, and displaying each lake's depth through time. In addition, for Owens Lake, we continuously monitor the oxygen isotopic composition of lake water for comparison to the data set of Benson and Bischoff (1993). In the first set of experiments (steady-state calculations), we use modern climate data to assess the response time of lakes to dramatic increases and decreases in precipitation. In the second set of experiments (sinusoidally varying runoff and evaporation), we allow runoff and evaporation to vary sinusoidally with time between modern and hypothetical glacial values. In the final set of experiments (runoff and evaporation driven by the marine $\delta^{18}\text{O}$ record), we use the $\delta^{18}\text{O}$ record of deep sea sediments (Imbrie and others, 1984) to drive runoff and evaporation between modern and assumed glacial values.

Steady-state Calculations

We conduct a series of steady-state experiments to determine the response time of each lake to variations in runoff and evaporation. Figure 3.6 shows the

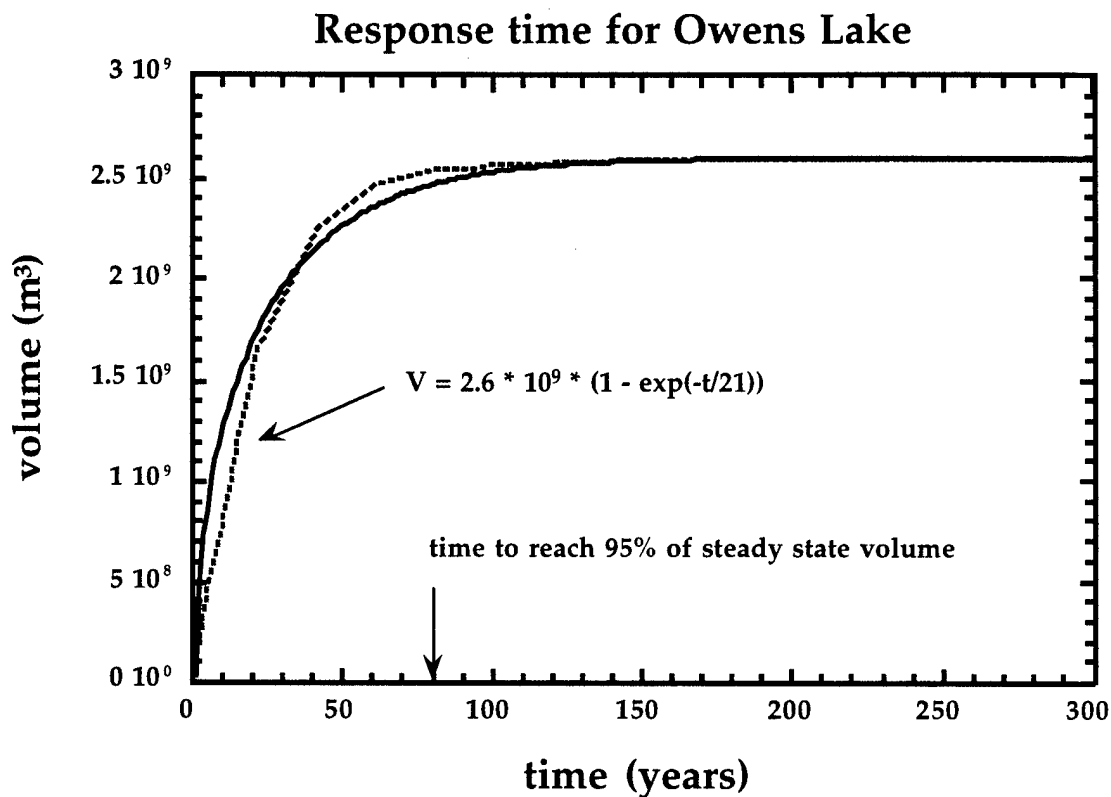


Fig. 3.6: Volume of Owens Lake with time, given an initially empty lake basin subjected to modern climatic conditions: $3.98 \times 10^8 \text{ m}^3/\text{yr}$ of runoff, evaporation rate of 1.34 m/yr . Note that the lake achieves a steady-state volume in about a century. Therefore, climate changes occurring with timescales of centuries or longer should be reflected in the sediments of the Owens Lake core.

history of Owens Lake volume, given an initially empty basin subjected to modern climatic conditions. This curve appears to follow the form

$$V = V_{ss} * (1 - e^{-t/\tau}) \quad (16)$$

where V is the volume of the lake at any particular timestep, V_{ss} is the steady state volume, t is time, and τ is a time constant dependent on basin geometry, amount of runoff, and evaporation rate. The lake achieves a steady-state volume in approximately one century. Holding evaporation rate constant, we explore the relationship between Owens Lake response time and amount of runoff (Fig. 3.7). For a fixed evaporation rate, response time increases as runoff increases. This agrees with the derivation of response time in equations 8 and 9 above. In fact, the only difference between Figure 3.7 and Figure 3.5b is that to create Figure 3.7 we use the actual hypsometry of Owens Lake rather than an idealized hypsometry of the form $A_L = m * V^q$ used in Figure 3.5b. At runoff values >210% of modern, Owens Lake exceeds the confines of its basin and spills into China Lake. Below ~40% of modern runoff, Owens Lake becomes ephemeral, with evaporation removing all runoff that has entered the lake during each annual timestep. Similar plots for the other lakes in the chain show similar behavior: all lakes have response times of approximately one century. In Figure 3.8, we show the response of all lakes in the chain to steady state climatic forcing over the Owens Lake drainage basin (no local precipitation falls on any of the other lake basins), with runoff equal to 10x modern and evaporation equal to modern values. The spilling over and successive filling of each lake in the chain is readily

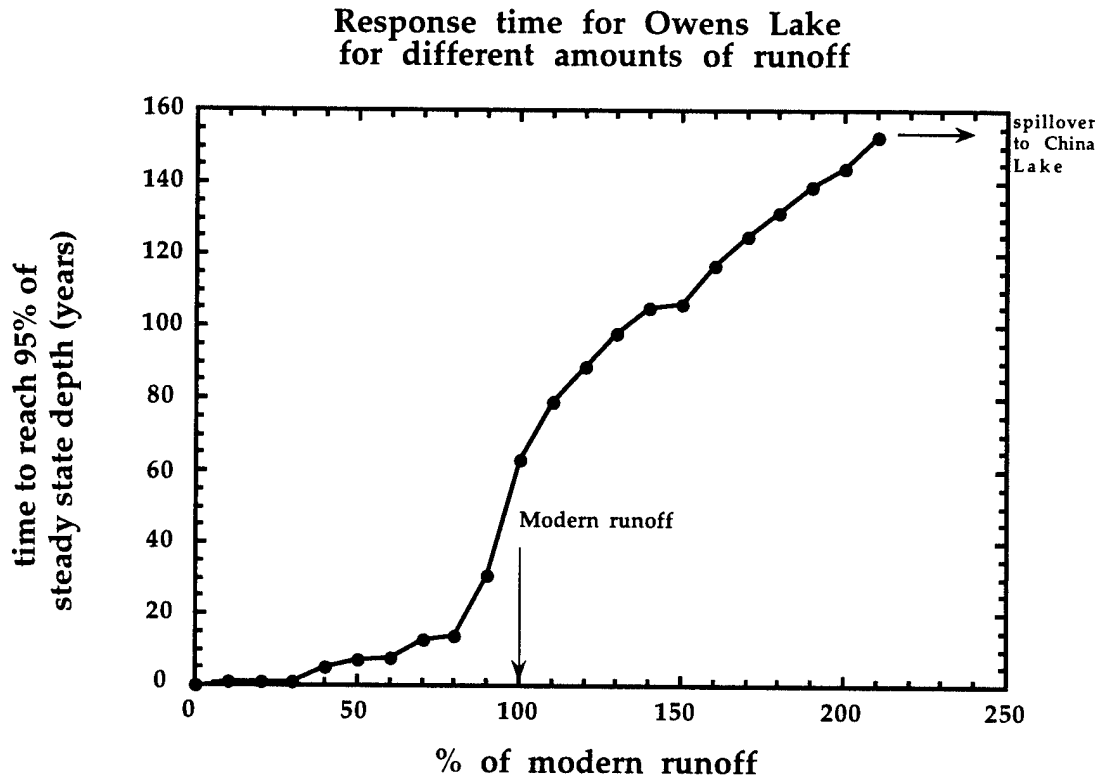
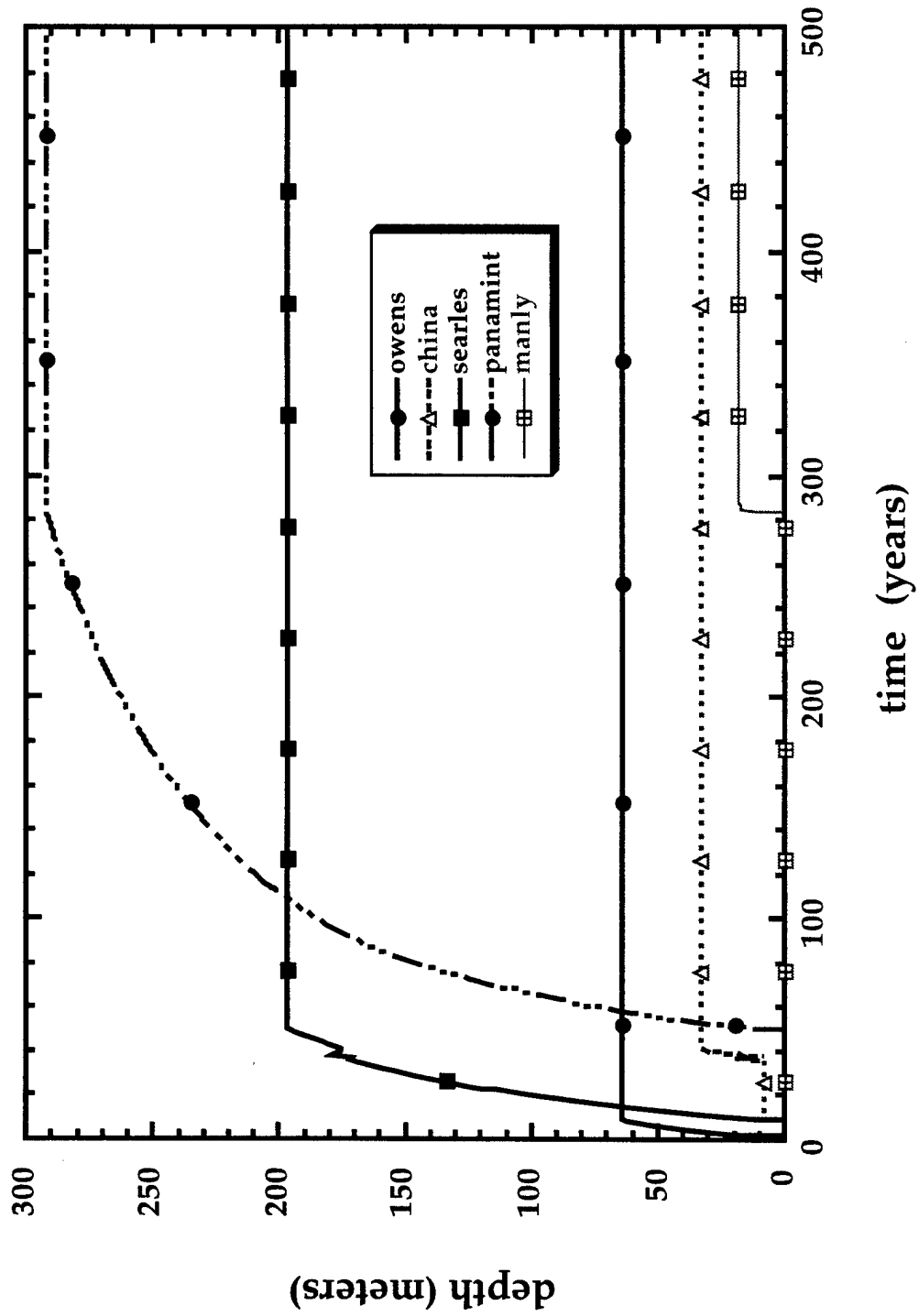


Fig. 3.7: Relationship between lake response time (here defined as the time necessary to reach 95% of the steady state volume) and amount of runoff for Owens Lake. Evaporation rate remains constant at 1.34 m/yr while runoff varies between 0% and 210% of modern, with modern runoff = $3.98 \times 10^8 \text{ m}^3/\text{yr}$. The higher the amount of runoff, the longer the lake takes to respond (see equations 8 and 9). This results from the fact that the steady-state lake size for a higher runoff lake is larger than for a lower runoff lake. Above 210% of modern runoff, Owens Lake exceeds its confines and flows into China Lake.

Fig. 3.8: Response of the lake chain system to an input of water to Owens Lake. All lakes are initially empty and receive water solely by overspill from one basin to the next. Likewise, all lakes are subjected to modern evaporation rates (see Table 2). Owens Lake receives 10 x modern runoff and rapidly fills to its spill point. China then instantaneously fills to its spill point and introduces water to Searles Lake. At 20 years, Searles has reached the China Lake spill point and the two lakes coalesce and grow to a combined spillover level. The maximum depth acquired by China Lake, then, is 30 m during periods when it is attached to Searles Lake, and 8 m when the two lakes are separated. The jump from 8 to 30 m is readily apparent at 20 years into the model run. The jaggedness of the lake depth versus time curves at 20 years for both the China and Searles Lake records is an artifact of the way these lakes are "welded" together in the model; it is not reflective of a short term climatic phenomenon. The combined Searles-China lake spills into Panamint Valley at 25 years. Because of the enormity of the Panamint Valley basin, it takes another 250 years for Panamint Lake to reach its spill point and flow into Death Valley. A small (<20 m) lake forms in Death Valley and the whole chain achieves steady state at ~280 years.

Response of lake chain to 10x modern runoff in the Owens Valley drainage basin



apparent. It takes the entire lake chain about 280 years to respond to this climate forcing.

Figures 3.7 and 3.8 indicate that for long term changes in climate, such as 20, 40 and 100 kyr variations induced by orbital cycles, the lake chain is perpetually in steady state. However, for short timescale phenomena, such as annual to decadal fluctuations in runoff and evaporation, steady state will not have been achieved by the time the forcing changes. In Figure 3.9, we depict the desiccation of Owens Lake that would occur if the lake were at its maximum high-stand volume and then ceased to receive further runoff. The modern evaporation rate dries the lake completely within 50 years. Stine (1994) has found evidence for two extreme droughts in California which lasted more than 200 years prior to 1112 A.D. and for more than 140 years prior to 1350 A.D. Inasmuch as the response time for Owens Lake is on the order of one century, we might expect to find evidence of these drought events in the Owens Lake core. At present, these events have not been identified.

Finally, the oxygen isotopic composition of Owens Lake water for different amounts of runoff is depicted in Figure 3.10. Higher runoffs lead to more depleted lake water values (i.e., values more similar to the initial Owens River value of -16‰), while lower runoff leads to more enriched lake water values. The degree of enrichment of lake water reflects the relative importance of runoff and evaporation rates on lake volume. For high runoff (5x and 10x modern runoff), Owens Lake is overflowing to the China Lake basin, and the residence time of water in the lake is very short. As a result, water does not remain in Owens Lake long enough for significant evaporative enrichment to occur. In contrast, for lower runoff (0.5x, 1x, and 2x modern), Owens Lake

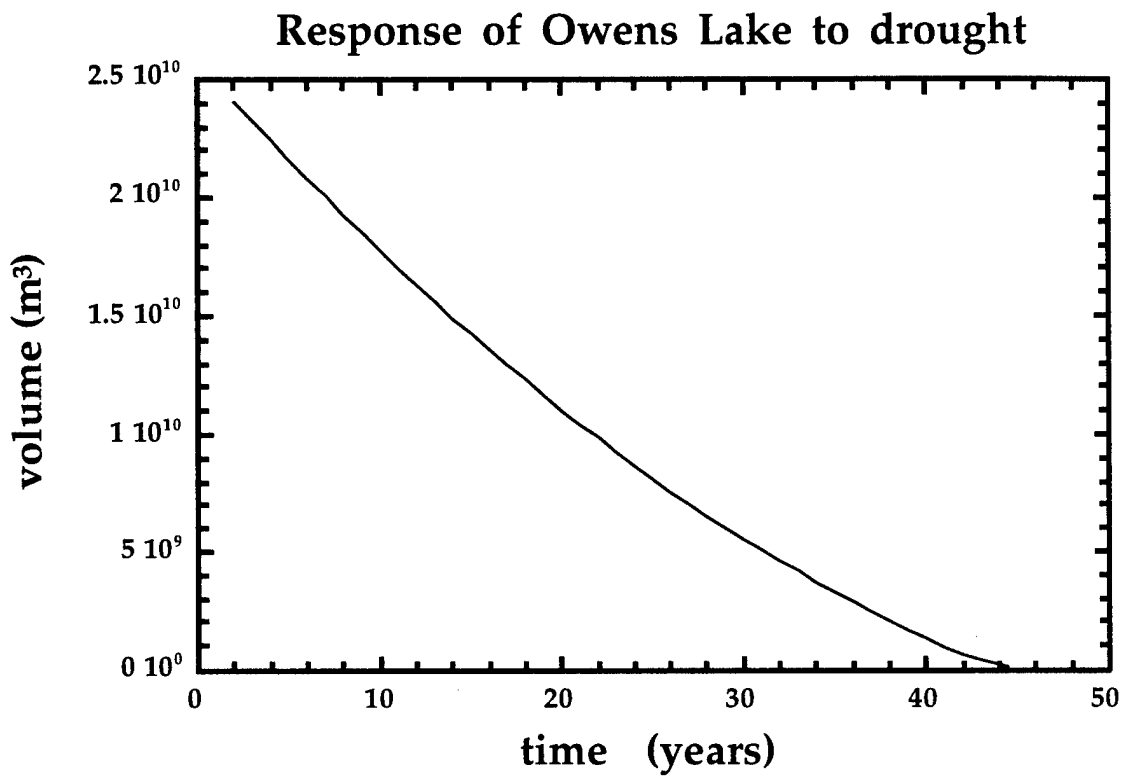


Fig. 3.9: Response of Owens Lake to drought conditions. Lake begins model run at its highstand volume. Modern evaporation rate removes water from lake. No runoff comes into the lake.

Modeled oxygen isotopic composition of Owens Lake water for different amounts of runoff

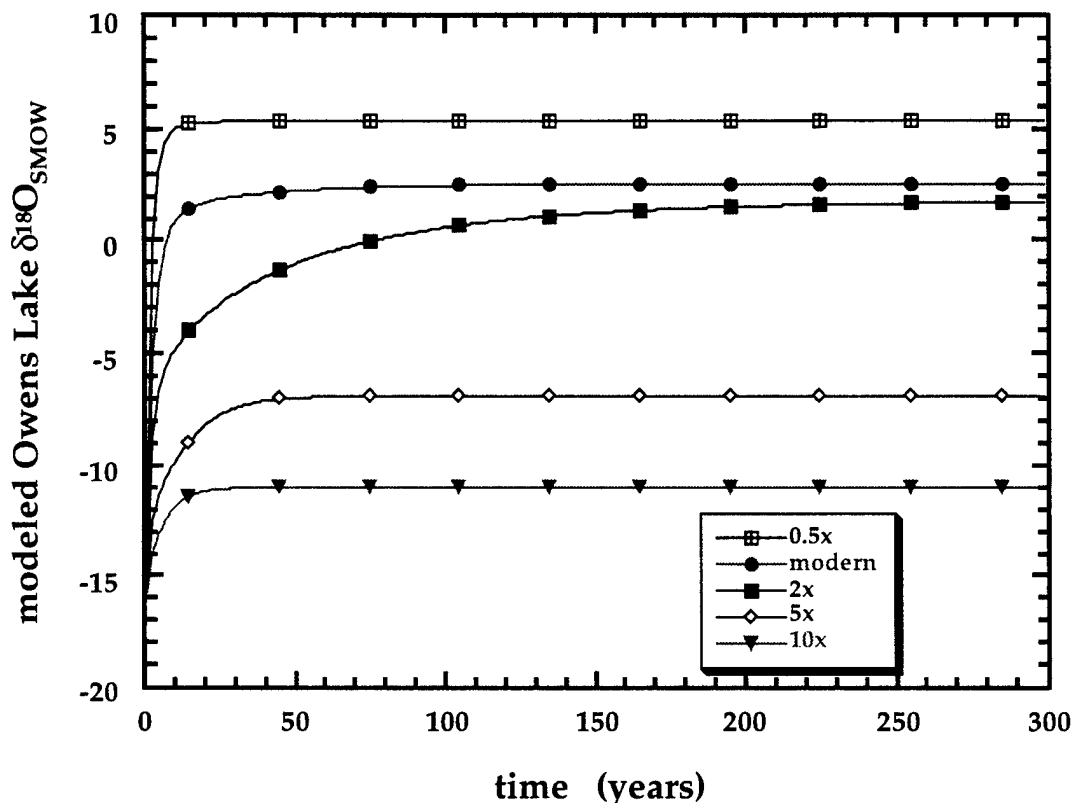


Fig. 3.10: Oxygen isotopic composition of Owens Lake water for different amounts of runoff (modern = $3.98 \times 10^8 \text{ m}^3/\text{yr}$, 0.5x modern, 2x modern, 5x modern, and 10x modern), reported in SMOW units. In all cases, evaporation rate = 1.34 m/yr. Isotopic composition of the input Owens River water is -16‰ . The lake quickly reaches isotopic steady state, with larger amounts of runoff requiring more time to equilibrate. The higher the amount of runoff, the more depleted the lake water at steady state. The steady-state isotopic value for the 2x modern case eventually reaches $\sim 1.8\text{‰}$ which is very similar to the value for modern runoff of $\sim 2.3\text{‰}$.

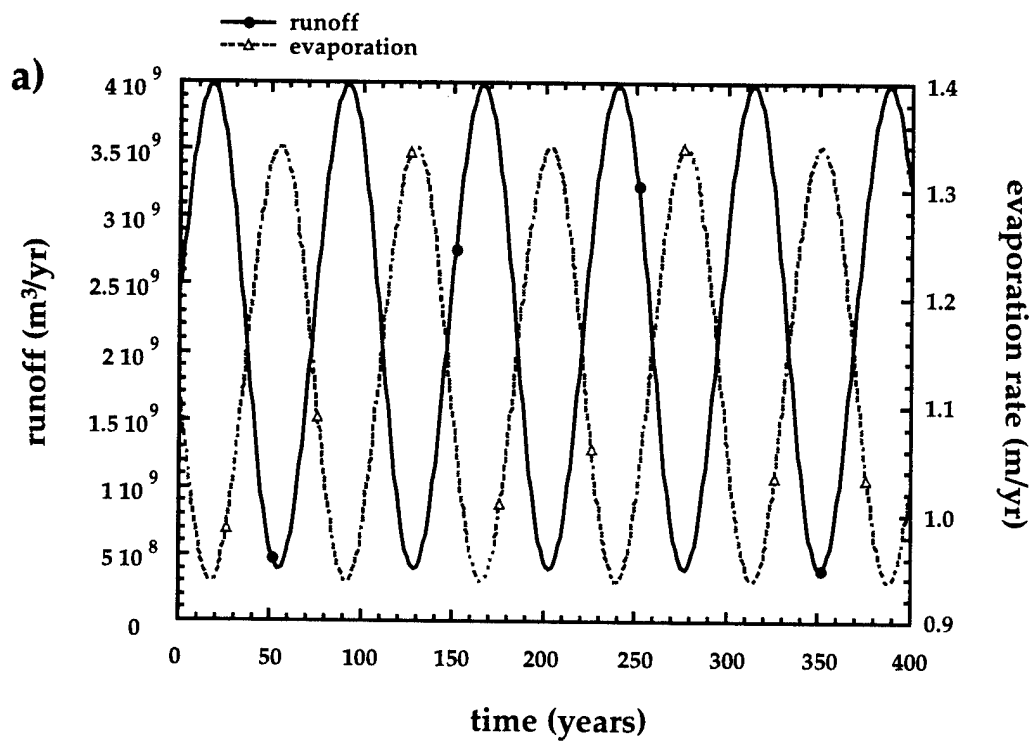
remains below its spill level, and evaporation causes a 15-20‰ enrichment over the input water isotopic value. In all cases, however, lake isotopic composition reaches a steady state value in roughly 50 years or less. Thus, climatic variations of the sort described by Stine (1994), with durations of 140 to >200 years, should also be recorded in the isotopic composition of carbonate minerals precipitated in equilibrium with Owens Lake water.

Sinusoidally Varying Runoff and Evaporation

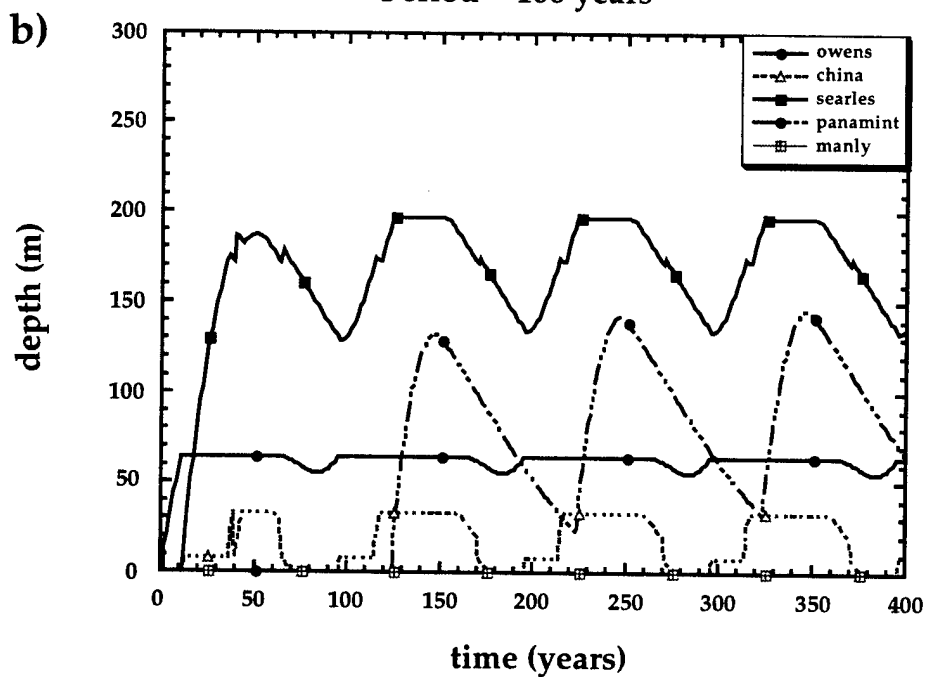
To illustrate how the Owens Lake system might respond to fluctuations in climatic parameters, we next conduct a series of experiments in which runoff and evaporation are driven sinusoidally with different periods, 100 years and 20 kyrs. In the first experiment, αP in the Owens Lake drainage basin varies between modern values and 10 times modern with a period of 100 years. We choose this period in order to confirm the response time determinations from the steady state climate experiments. If the response time of the lake chain is in fact ~280 years for a 10x modern runoff forcing, then none of the lakes in this experiment should achieve their steady state sizes. For all lakes in this experiment, evaporation is driven between modern and 70 percent of modern values. The minimum evaporation values are taken from Smith and Street-Perrott (1983), who estimated the decrease in evaporation rate associated with a 5°C cooling in the area. Figure 3.11a shows the runoff and evaporation forcing functions at Owens Lake over the 1000 year long model run; we have specified that the maximum runoff conditions prevail during periods also dominated by minimum evaporation rates, i.e., that the two forcings are 180° out of phase. Figure 3.11b shows the lake depth histories corresponding to this climatic forcing. Note that

Fig. 3.11a: Climatic forcing functions for oscillating climate with 100 year period. All lakes are initially empty and lakes down-chain from Owens receive water solely by overspill from one basin to the next. Runoff varies between modern and 10x modern values. Evaporation varies between modern and 0.7x modern values and is shown only for Owens Lake.

Fig. 3.11b: Lake depth versus time for oscillating climate with 100 year period. Note that Owens Lake never reaches its modern depth of 14 m, even though the runoff and evaporation rates go through modern values every 50 years. Likewise, large lakes persist in the China, Searles, and Panamint Lake basins even though these lakes should be completely dry during periods marked by modern climatic conditions. The persistence of large lakes in these basins indicates that the lake system has not achieved steady state.



Lake level history for sinusoidally driven climate.
Period = 100 years



while the climatic forcing goes through modern values every 100 years (Fig. 3.11a), Owens Lake never reaches its modern depth of 14 m. Instead, its surface altitude hovers around the spillpoint elevation, declining only by ~10 m during minimum runoff and maximum evaporation conditions. Likewise, in spite of the observation that modern climatic conditions lead to no lakes in any basin but Owens Valley, large modeled lakes persist in Searles and Panamint Valleys given these parameters. These results suggest that the system of lakes has not reached steady state values for lake depth, volume, and surface area. Remembering the response time calculations detailed above, in which we determined that response to climatic perturbation occurs within about a century, the behavior shown in Figure 3.11b is explicable as a transient response, i.e., the time scale of the forcing is too short for the lakes to attain their steady state values.

Figure 3.11c depicts residence time for water in the lake (calculated by dividing instantaneous lake volume by instantaneous inflow rate). Residence time is longest at 75 years and every 100 years thereafter, corresponding to intermediate values of runoff and evaporation (Fig. 3.11a). In Figure 3.11d we show the evolution of the oxygen isotopic value of Owens Lake through time (here reported in ‰ units relative to SMOW). The most enriched values occur immediately after the longest residence time periods, perhaps indicating again that the lake chain has not reached steady-state.

In the second experiment (Fig. 3.12), runoff and evaporation vary between the same extremes as in the first experiment, but the period of fluctuation is changed to 20 kyrs, and the model run time is adjusted to 40 kyrs. Owens Lake rapidly reaches its spill point, retreating from this value only at 13 and 33 ka, when modeled runoff declines and evaporation increases. China, Searles, and

Fig. 3.11c: Residence time for water in Owens Lake for oscillating climate with 100 year period (calculated by dividing lake volume by inflow rate). Comparison of residence time to isotopic composition of lake water (Fig. 3.8c) shows that Owens Lake water becomes most enriched shortly after residence time reaches maximum values.

Fig. 3.11d: Oxygen isotopic value of Owens Lake water through time for oscillating climate with 100 year period (here reported SMOW units). Lake water becomes most enriched at ~80 years and every 100 years thereafter. Comparison of the isotopic values to the lake level history shows that the isotopic enrichment occurs when Owens Lake is below its spill point.

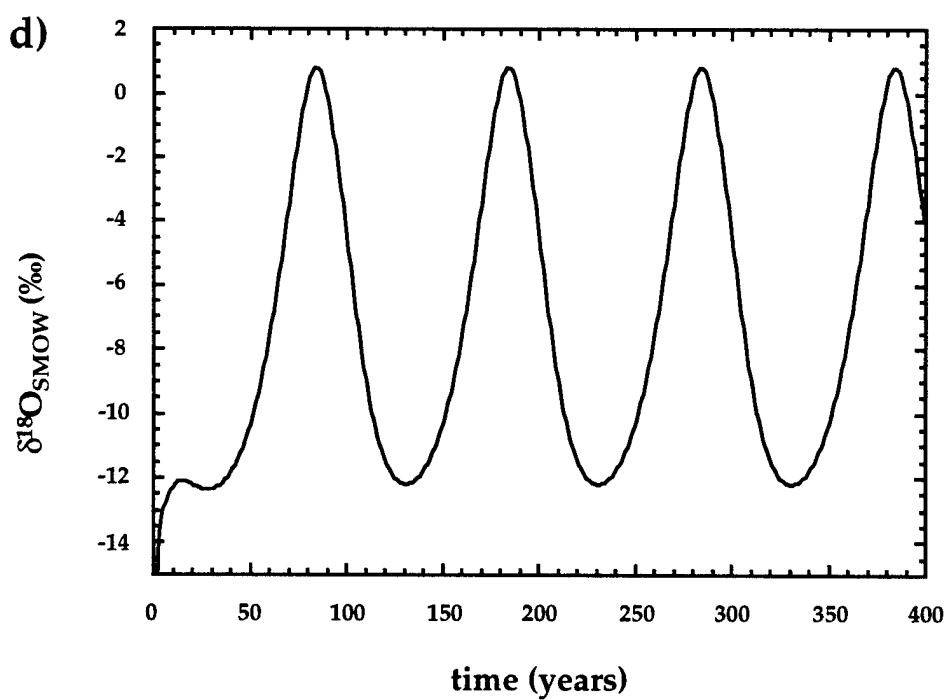
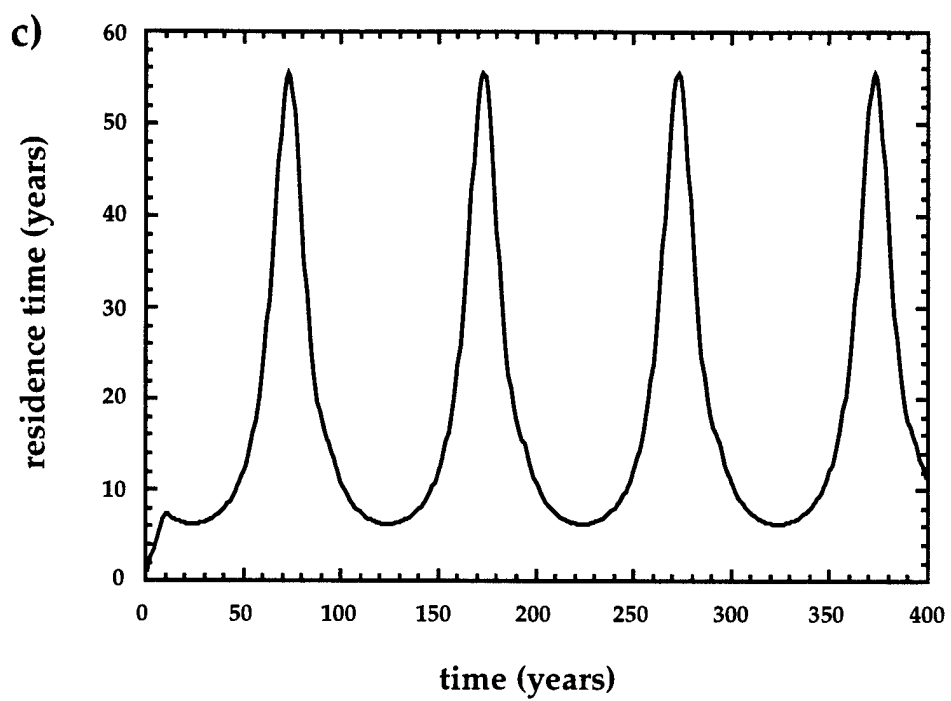
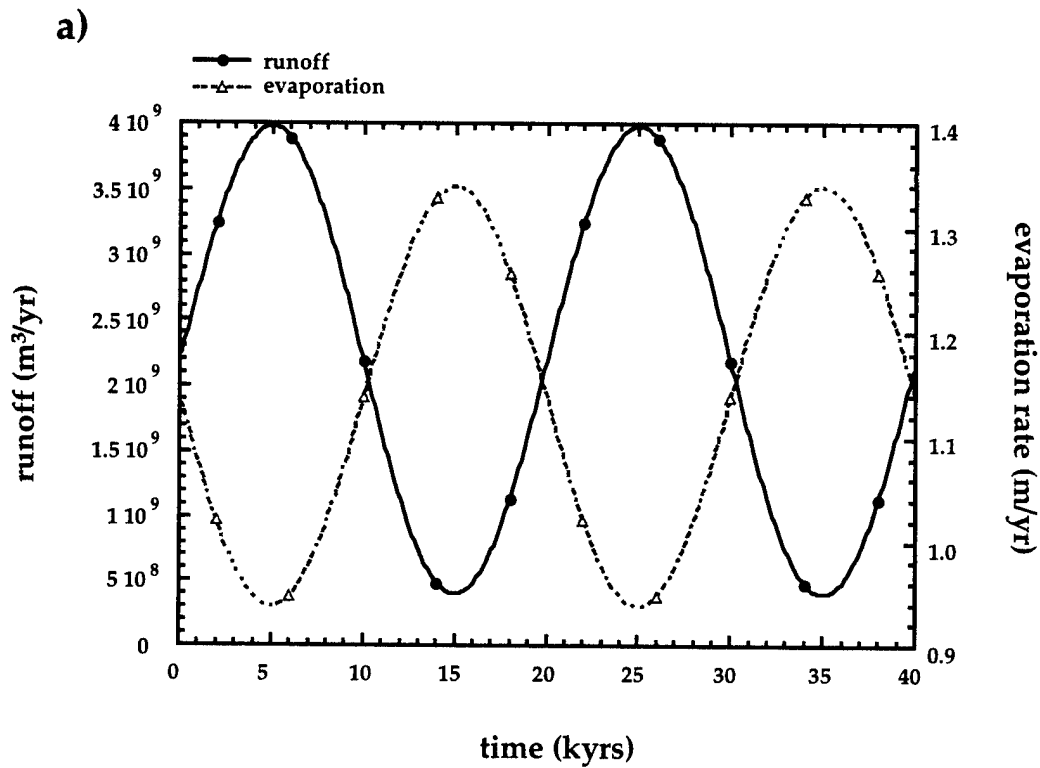
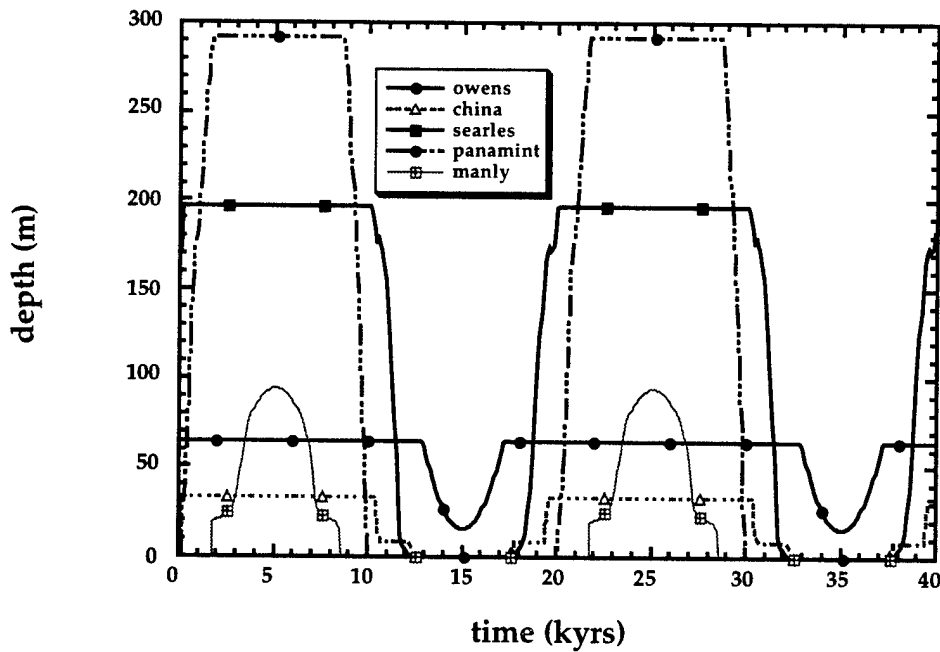


Fig. 3.12a: Climatic forcing functions for oscillating climate with a 20 kyr period. All lakes are initially empty and lakes down-chain from Owens receive water solely by overspill from one basin to the next. Runoff varies between modern and 10x modern values. Evaporation varies between modern and 0.7x modern values and is shown only for Owens Lake.

Fig. 3.12b: Lake depth versus time for oscillating climate with 20 kyr period. Runoff and evaporation go through modern values at 15 and 35 ka. At these times, Owens Lake reaches its historic lake level (14 m), and all other lakes in the chain dry out completely. Conversely, at 5 and 25 ka, runoff and evaporation are at assumed maximum pluvial values. All lakes upchain from Manly are at their spill points, and Manly Lake achieves a depth of ~95 m. The fact that the lakes reach their historic sizes with historic climate parameters indicates that the chain of lakes is at steady state, unlike the situation portrayed in Figure 3.8.



b) Lake level history for sinusoidally driven climate.
Period = 20 kyrs



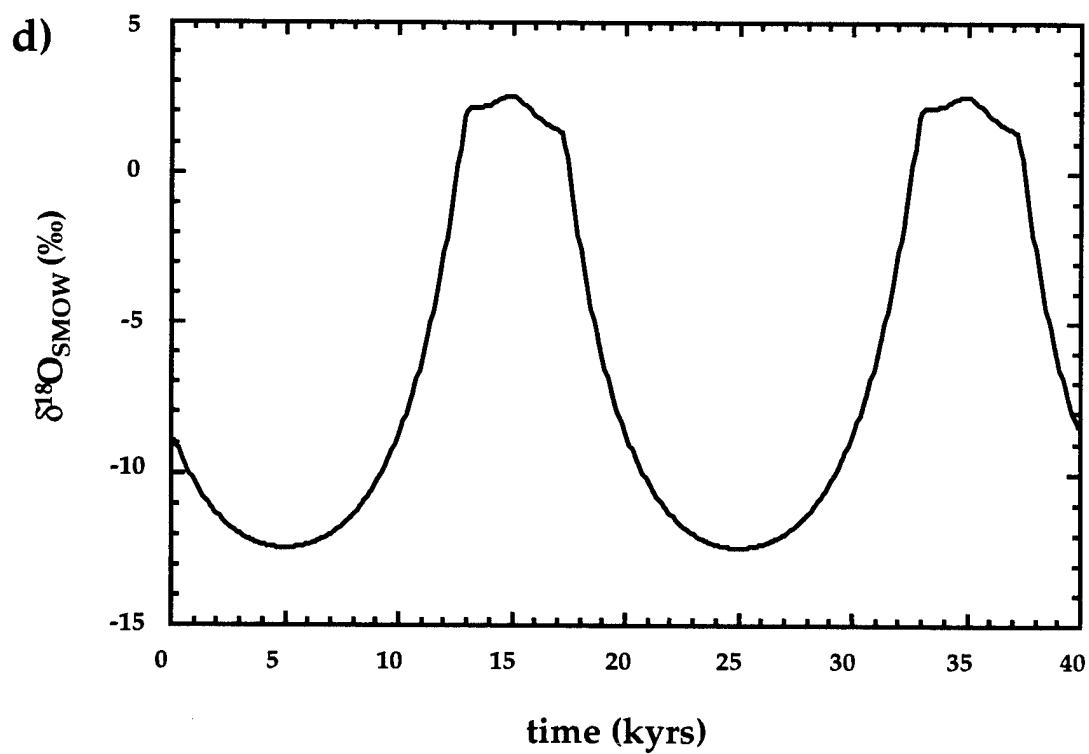
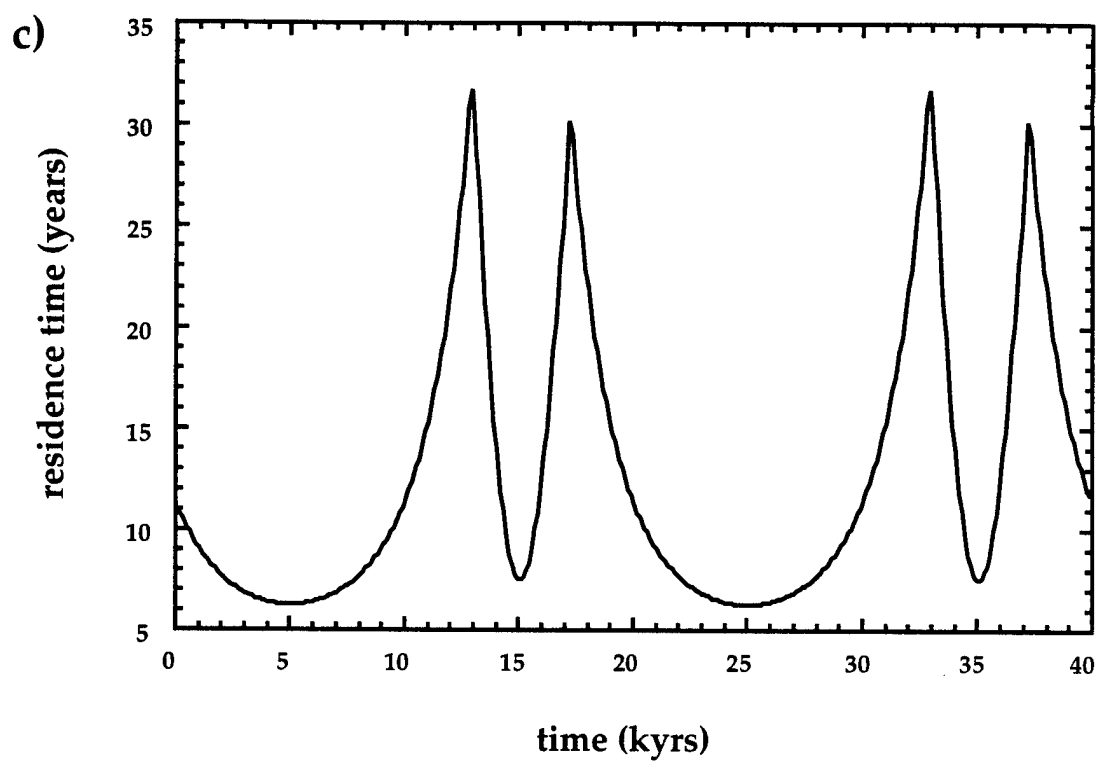
Panamint lakes also fill to overspilling, resulting in a 90 m deep Lake Manly in Death Valley every 20 kyrs. Owens Lake achieves a steady state modern lake level of 14 m at 15 and 35 ka when runoff and evaporation reflect modern values. Comparison of the lake level graph (Fig. 3.12b) to a plot of residence time for water in Owens Lake (Fig. 3.12c) shows that residence time is influenced by two competing processes. Between 0 and 10 ka, and then again between 20 and 30 ka, residence time for Owens Lake water is very short due to high runoff pushing water rapidly through the system. From 10-12 ka, and 30-32 ka, runoff declines while evaporation rises, causing increasing residence times. At 15 and 35 ka, residence time has again become very short. At these times, however, the calculated residence time is dominated by the small volume of Owens Lake and the relatively large evaporation rate. The inflection points at 12, 17, 32 and 37 years, then, represent changeover from residence times dominated by the runoff signal to residence times dominated by evaporation. Figure 3.12d shows the oxygen isotopic composition of Owens Lake water reflecting this residence time behavior. Isotopic composition is nearest that of the input Owens River water (-16‰) when residence times are short and dominated by runoff (0-10 and 20-30 ka). $\delta^{18}\text{O}$ increases as runoff declines and evaporation increases (10-12 and 30-32 ka) and becomes most enriched at 15 and 35 ka, when residence time is dominated by evaporation.

Runoff and Evaporation Driven by the Marine Oxygen Isotopic Record

We now examine a more complicated climatic forcing function. Antevs (1955), Kutzbach (1987), and Spaulding and Graumlich (1986) suggested that the growth of the Laurentide ice sheet might have deflected the jet stream from its

Fig. 3.12c: Residence time for water in Owens Lake for oscillating climate with 20 kyr period (calculated by dividing lake volume by inflow rate). Residence time is influenced by two competing processes. Between 0 and 10 ka, and then again between 20 and 30 ka, residence time for Owens Lake water is very short due to the large amounts of runoff pushing through the system. From 10-12 ka, and 30-32 ka, runoff declines while evaporation rises causing increasing residence times. At 15 and 35 ka, residence time has again become very short. At these times, however, residence time reflects the small volume of Owens Lake and the relatively large evaporation rate. The inflection points at 12, 17, 32 and 37 years, then, represent changeover from residence times dominated by the runoff signal to residence times dominated by evaporation.

Fig. 3.12d: Oxygen isotopic value of Owens Lake water through time for oscillating climate with 20 kyr period (here reported SMOW units). Lake water becomes most enriched at 15 and 35 kyrs when climate goes through modern values of runoff and evaporation (i.e. minimum runoff and maximum evaporation). Comparison of isotopic composition of lake water to residence time (Fig. 3.9c) shows that Owens Lake water becomes most enriched during the short residence time periods dominated by evaporation.



present mean location at $\sim 45^\circ\text{N}$ latitude to a more southerly location. Southerly latitudes with an arid modern climate would then have received more precipitation during glacial periods as storm tracks moved southward. Lao and Benson (1988) supported this hypothesis by showing that Lake Lahonton reached highstands either directly during or slightly after ice sheets reached their maximum sizes, and that moderate size lakes formed when ice sheets were 80% of their maximum sizes. Likewise, Oviatt and others (1990) called on a migrating jet stream to produce the Stansbury oscillation in lake level in the Lake Bonneville basin. We have incorporated the effects of a migrating jet stream in the following way: we modulate between the assumed maximum paleo-runoff and modern runoff using a temporal pattern derived from the deep sea oxygen isotope record (Imbrie and others, 1984). Because $\delta^{18}\text{O}$ reflects global ice volume (Bradley, 1985, p. 180), in fact, primarily the Laurentide ice sheet, and the position of the jet stream is influenced by that volume (Antevs, 1955; Kutzbach, 1987), we suggest that the $\delta^{18}\text{O}$ record may be used to scale a proxy for jet stream position, and, therefore, precipitation falling over our study area. We also use the marine $\delta^{18}\text{O}$ record to drive evaporation rates between modern and assumed glacial values. Phillips and others (1992, p. 101) used a similar approach, allowing temperature, and therefore evaporation rate, to scale between assumed maximum and minimum values with the marine $\delta^{18}\text{O}$ record.

For both evaporation and runoff, we normalize the marine isotopic curve so that its values fall between 0 and 1, with maximum runoff and evaporation given a value of one, and minimum values of these parameters given a value of zero. We also specify that maximum evaporation rates occur when runoff values are at a minimum, and vice versa. As in the sinusoidally driven climate

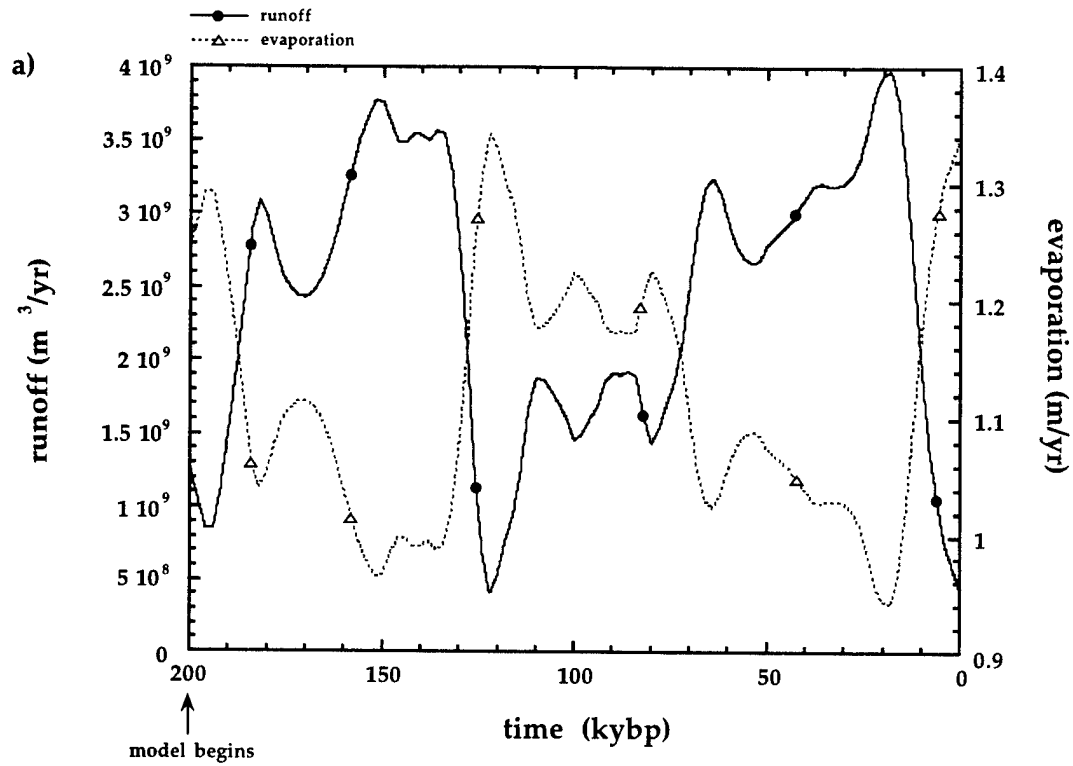
experiments above, maximum runoff is specified to occur during periods of minimum evaporation, maximum runoff is set to 10x modern runoff, and minimum evaporation taken to be 0.7 x modern. Figure 3.13a shows the runoff and evaporation forcing histories at Owens Lake through time, and Figure 3.13b the depth histories of the 5 lakes. Comparison of this lake level history to those reported by Phillips and others (1991) and Jannik and others (1991) does not show very good agreement. Overflow from Searles Lake to Panamint Lake occurs over much too long a period, and Lake Manly receives overspilled water at many times in this model run. It appears that the maximum glacial estimate of runoff of 10 times the modern value may be too large, or that the estimated evaporation rate is too small. Figure 3.13c shows the modeled oxygen isotopic composition (converted to calcium carbonate equivalent) along with the measured OL-92 oxygen isotopic composition of carbonate from Benson and Bischoff (1993). The modeled $\delta^{18}\text{O}$ values are generally much more depleted than the measured isotopic values, again reflecting that too much runoff is coursing through the system during glacial periods. Finally, the magnitude of the predicted isotopic enrichment at ~195 ka and at ~125 ka is not borne out in the measured data.

SENSITIVITY ANALYSES

Because our most robust test of the modeled lake level history is the measured $\delta^{18}\text{O}$ of Owens Lake carbonates (Benson and Bischoff, 1993), we must determine the sensitivity of the modeled $\delta^{18}\text{O}$ to variations in the parameters that control $\delta^{18}\text{O}$. These include runoff, evaporation rate, input Owens River $\delta^{18}\text{O}$, relative humidity, atmospheric $\delta^{18}\text{O}$, and calcification temperature. Variations in

Fig. 3.13a: Climatic forcing functions for potentially more realistic climate variations. All lakes are initially empty and lakes down-chain from Owens receive water solely by overspill from one basin to the next. Runoff varies between modern and 10x modern values. Evaporation varies between modern and 0.7x modern values and is shown only for Owens Lake. Both runoff and evaporation are driven with the marine oxygen isotope curve of Imbrie and others (1984). Maximum precipitation and minimum evaporation occur at the last glacial maximum (18 ka).

Fig. 3.13b: Lake level history derived from the climatic forcing functions shown in Figure 3.10a. Owens Lake is nearly continuously overflowing except at ~125 ka and at present. Likewise, China and Searles Lakes are overflowing for about 75% of the model run time. Large lakes grow in Panamint Valley, and overspill into Death Valley occurs at roughly 180 ka, from 130-160 ka, from 60-68 ka, and again from 12-43 ka. The data of Bischoff and others (in press) and Jannik and others (1993) do not support the frequent overflows into Death Valley, or the duration of overspill from Searles Lake to Panamint Lake.



Modeled lake level history

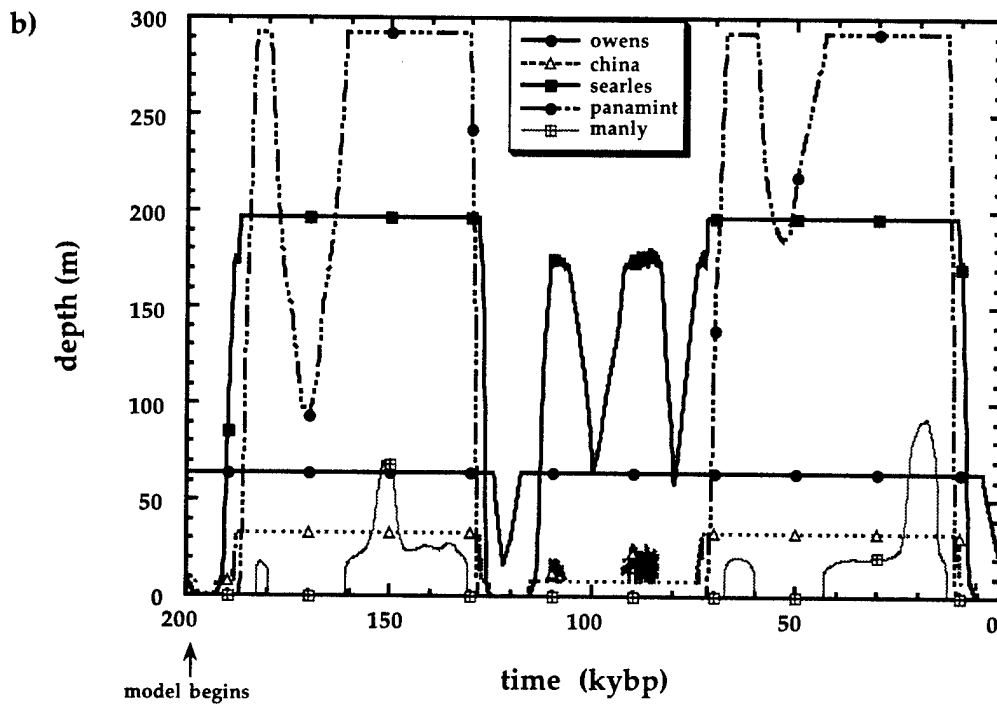
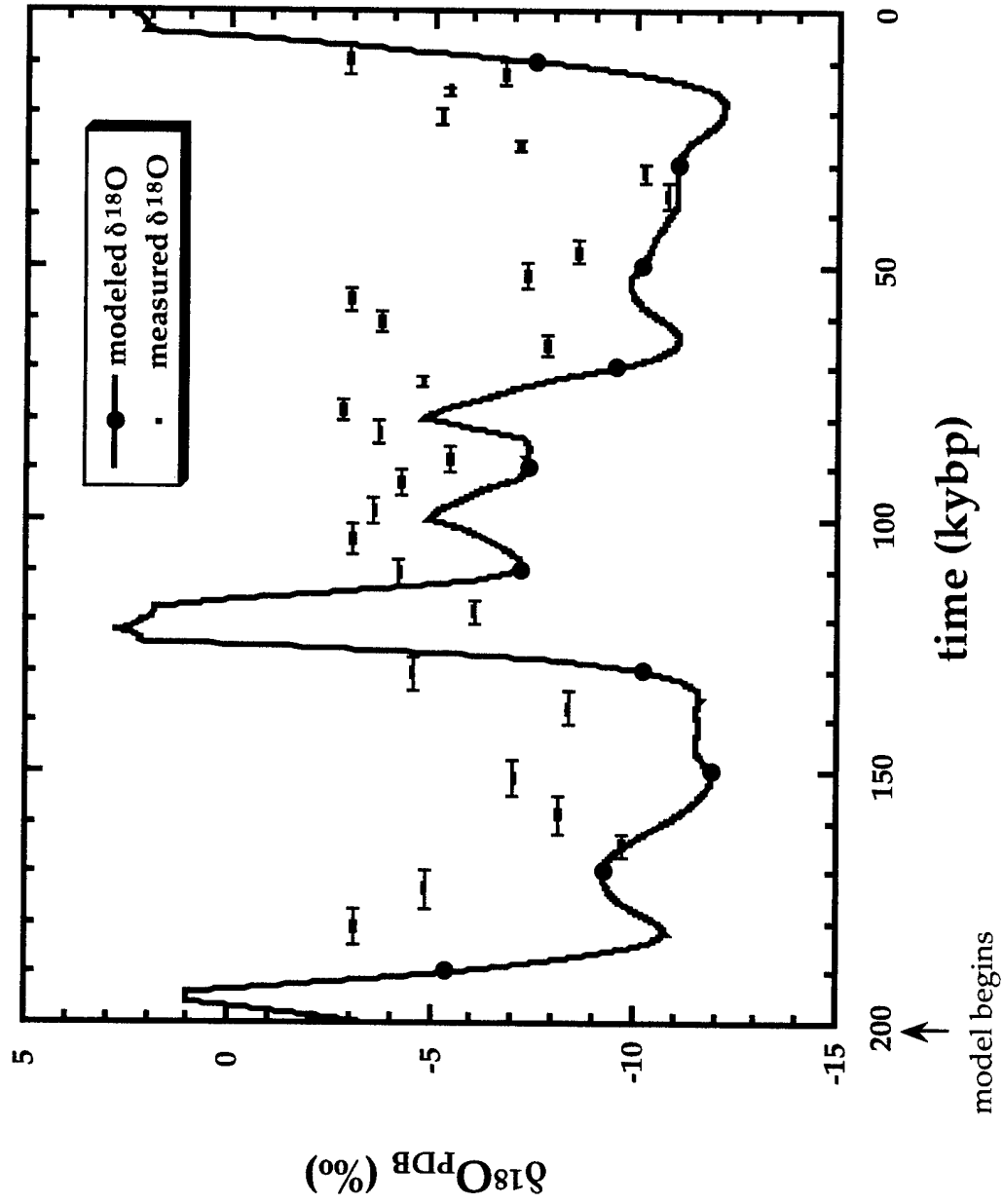


Fig. 3.13c: Comparison of measured carbonate $\delta^{18}\text{O}$ values (Benson and Bischoff, 1993) of Owens Lake carbonates to modeled isotopic composition of carbonates forming in a modeled Owens Lake (shown in PDB units) given the climatic forcing functions found in Figure 3.10a. Input Owens River d^{18}O is specified at -16‰, carbonates are assumed to be precipitating at 15 °C, relative humidity is set at 35%, and an atmospheric $\delta^{18}\text{O}$ value of -21‰ is assumed. In general, the modeled isotopic values tend to be more depleted than the measured values. Only at 195 and 125 ka do the modeled isotopic values become more enriched than the measured values.

Modeled and measured carbonate $\delta^{18}\text{O}$ values

relative humidity exercise no control on isotopic composition because the fraction of water evaporating from Owens Lake during any particular timestep is very small relative to the total volume of the lake (the fraction of remaining liquid is ~ 0.95). Were Owens Lake ever to desiccate completely, however, the relative humidity would play an important role in the isotopic evolution of the brine and resulting carbonate precipitates as shown by Gonfiantini (1986).

While relative humidity plays no role in setting the isotopic composition of Owens Lake water, variations in the oxygen isotopic composition of the atmosphere over the lake could play a small role (Fig. 3.14). A range of atmospheric $\delta^{18}\text{O}$ values from -11‰ to -25‰ results in a lake isotopic range of $\sim 2\text{--}3\text{‰}$, with highly depleted atmospheric values giving rise to most depleted lake values. In our model, we have used an atmospheric isotopic value of -21‰ , which Hostetler and Benson (1994) reported for the air over Pyramid Lake, ~ 350 km north of Owens Lake. This value would presumably have been lower during glacial periods as colder air should have carried more isotopically depleted water vapor. In any case, the effect of atmospheric $\delta^{18}\text{O}$ on lake carbonate $\delta^{18}\text{O}$ is very small.

Calcification temperature exerts a similarly small effect on isotopic composition (Fig. 3.15). We have assumed that calcium carbonate is precipitating inorganically within Owens Lake at temperatures equivalent to the mean annual temperature at Owens Lake (15°C for the modern case, and inferred to be 10°C for the glacial periods). This is undoubtedly an oversimplification inasmuch as carbonates are sometimes precipitated in saline lakes in "whiting" events (Benson, 1994) when temperatures in the lake's epilimnion exceed 20°C (i.e., during the summer). Because Owens Lake is currently dry, we have no way of

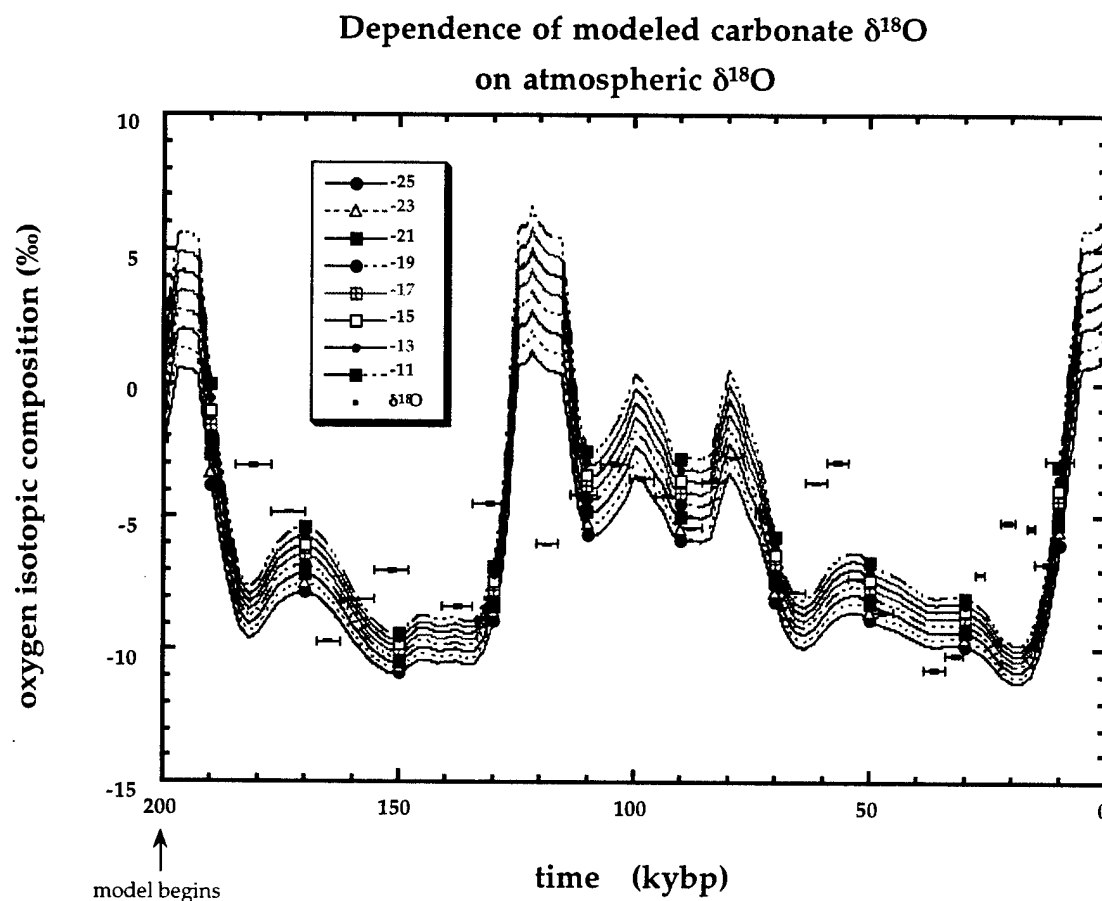


Fig. 3.14: Dependence of modeled oxygen isotopic value of carbonates on atmospheric $\delta^{18}\text{O}$ value. Eight different isotopic values are shown, ranging from -11‰ to -25‰. As we have no knowledge of the atmospheric $\delta^{18}\text{O}$ over Owens Lake, we give a range that allows both a more enriched value than at Pyramid Lake due to Owens Lake's more southerly location and lower altitude, and a more depleted value possibly reflecting glacial periods. Runoff is modulated between modern and 7x modern values with the marine $\delta^{18}\text{O}$ record. Evaporation varies between modern and 0.7x modern again with the marine $\delta^{18}\text{O}$ record. Input Owens River water has a $\delta^{18}\text{O}$ value of -16‰. Relative humidity is specified as 35%. Finally, carbonates are assumed to be forming at 15°C. Measured carbonate $\delta^{18}\text{O}$ values (Benson and Bischoff, 1993) are also shown with the age ranges for each sample plotted as error bars parallel to the time axis, and with precision plotted as error bars parallel to the oxygen isotopic composition axis.

Dependence of modeled carbonate $\delta^{18}\text{O}$ value on calcification temperature

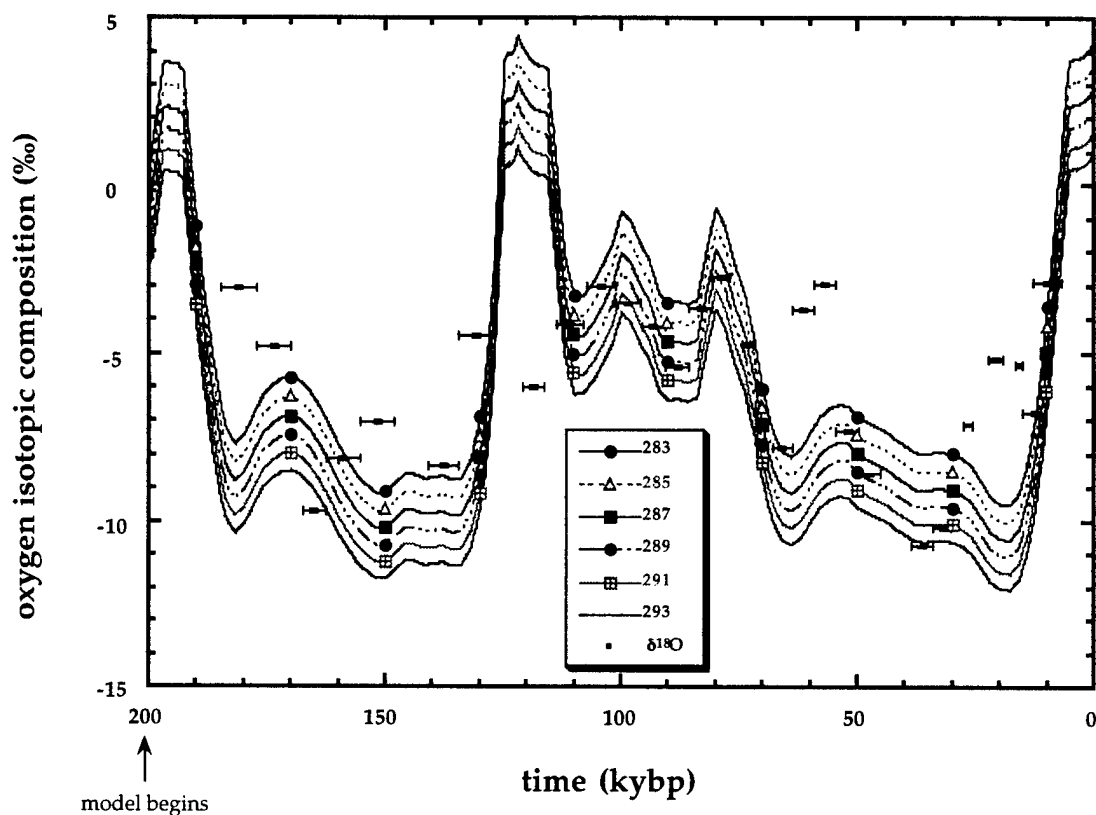


Fig. 3.15: Dependence of modeled oxygen isotopic value of carbonates on calcification temperature. Six different temperatures are shown, ranging from 283 K (10°C) to 293 K (20°C). Runoff is modulated between modern and 7x modern values with the marine $\delta^{18}\text{O}$ record. Evaporation varies between modern and 0.7x modern again with the marine $\delta^{18}\text{O}$ record. Input Owens River water has a $\delta^{18}\text{O}$ value of -16‰. The atmosphere over the lake is assumed to have a $\delta^{18}\text{O}$ value of -21‰. Finally, relative humidity is specified to be 35%. Measured carbonate $\delta^{18}\text{O}$ values (Benson and Bischoff, 1993) are also shown with the age ranges for each sample plotted as error bars parallel to the time axis, and with precision plotted as error bars parallel to the oxygen isotopic composition axis.

assessing the importance of this process. Nor do we have any information about what the lake's thermal structure would have been for different lake levels. We can, however, model the isotopic evolution of lake carbonates for temperatures between 10 and 20°C (shown as 283 to 293 K on the plot). This 10°C range in calcification temperature results in an ~2‰ range in isotopic composition, with the highest temperatures giving rise to the most depleted, least fractionated, carbonate isotopic values. Glacial period evaporation rate also exerts a small effect on $\delta^{18}\text{O}$ (Fig. 3.16) since variations in runoff are large enough to swamp the much smaller expected changes in evaporation rate. In general, however, the lower the evaporation rate during maximum glacial periods, the less enriched the carbonates precipitating in Owens Lake. The amplitude of isotopic variation in the measured carbonate samples is ~10‰. Relative to this amplitude, the ~2‰ variations associated with the calcification temperature, the isotopic composition of the atmosphere, and the glacial period evaporation rate are small, though not negligible. In model runs to follow we will explore the results of allowing all parameters to vary within reasonable ranges.

The two most important controllers of modeled oxygen isotopic composition are the amount of runoff (Fig. 3.17) and the isotopic composition of the runoff (Fig. 3.18). We first address changes in runoff quantity. For maximum glacial runoffs only 2x greater than modern (this value does not allow overspill from Owens Lake to China Lake), structure in the isotopic curve between 130 and 80 ka is lost completely due to the fact that the steady-state isotopic composition of a lake receiving 2x modern runoff is nearly identical to that of a lake receiving modern runoff (Fig. 3.10). Furthermore, isotopic values are much more enriched than those observed in the Owens Lake carbonates. In contrast,

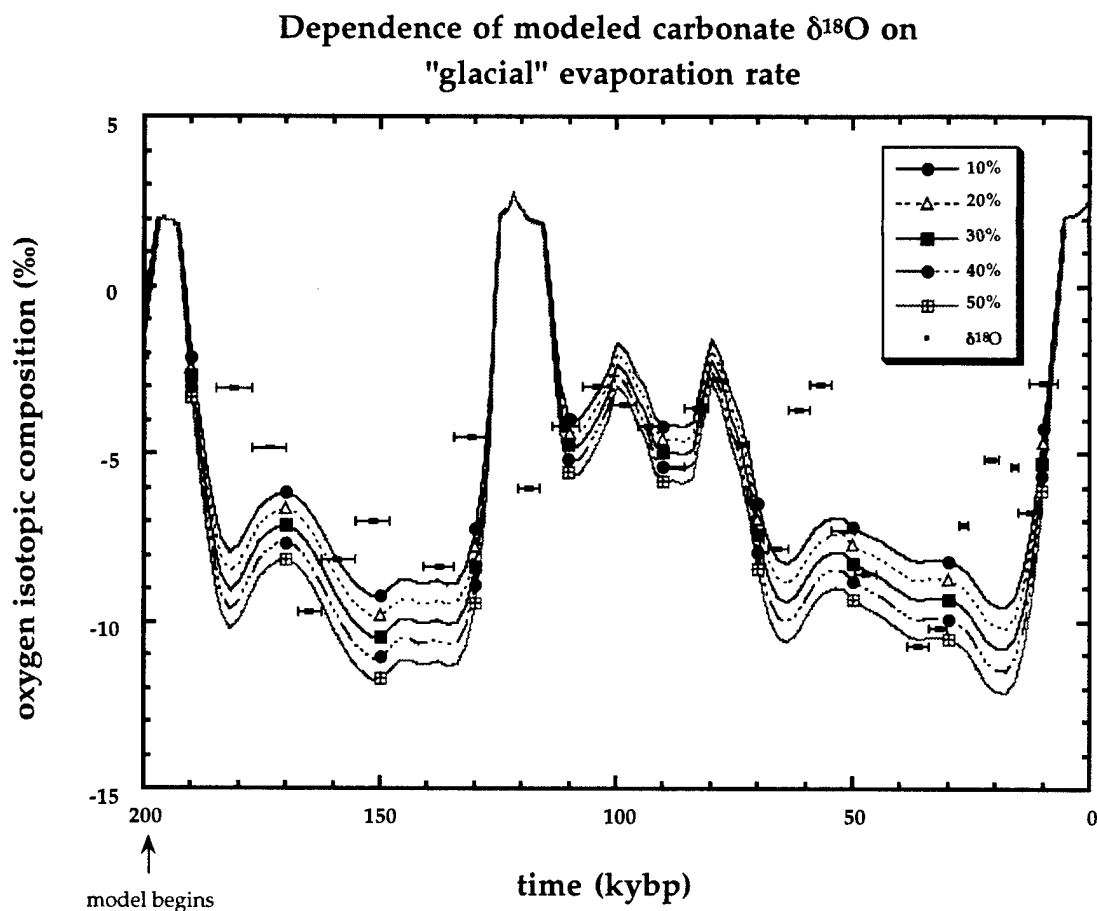


Fig. 3.16: Dependence of modeled oxygen isotopic value of carbonates on evaporation rate. Five different glacial evaporation rates are shown, ranging from 10% lower than modern to 50% lower than modern values. Runoff is modulated between modern and 7x modern values with the marine $\delta^{18}\text{O}$ record. Evaporation is again modulated with the marine $\delta^{18}\text{O}$ record. Input Owens River water has a $\delta^{18}\text{O}$ value of -16‰ . The atmosphere over the lake is assumed to have a $\delta^{18}\text{O}$ value of -21‰ and a relative humidity of 35%. Carbonates are assumed to be forming at 15°C . Measured carbonate $\delta^{18}\text{O}$ values (Benson and Bischoff, 1993) are also shown with the age ranges for each sample plotted as error bars parallel to the time axis, and with precision plotted as error bars parallel to the oxygen isotopic composition axis.

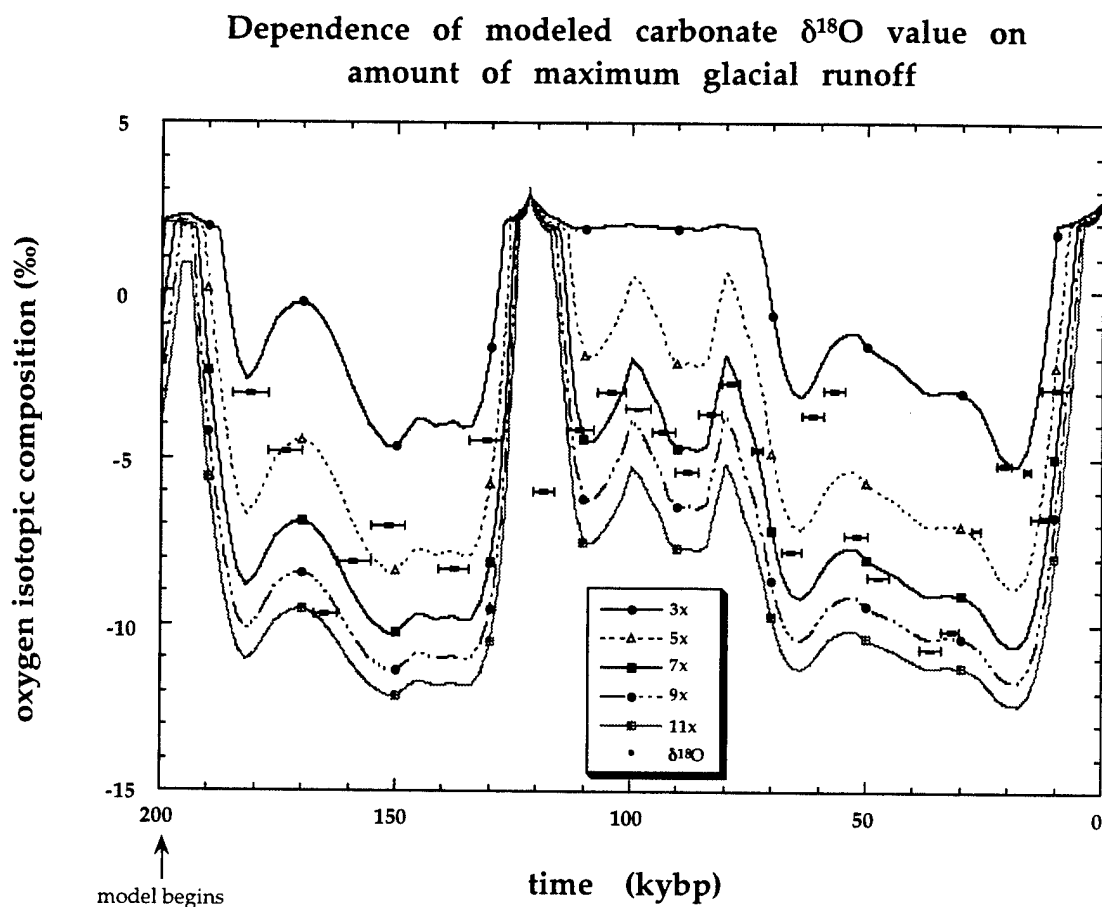


Fig. 3.17: Dependence of modeled oxygen isotopic value of carbonates on amount of runoff. Five different maximum glacial runoff values are shown, ranging from 2x modern runoff to 10x modern runoff. Runoff is again modulated between modern and assumed glacial values with the marine $\delta^{18}\text{O}$ record. Evaporation varies between modern and 0.7x modern also with the marine $\delta^{18}\text{O}$ record. Input Owens River water has a $\delta^{18}\text{O}$ value of -16‰. The atmosphere over the lake is assumed to have a $\delta^{18}\text{O}$ value of -21‰ and a relative humidity of 35%. Finally, carbonates are assumed to be forming at 15°C. Measured carbonate $\delta^{18}\text{O}$ values (Benson and Bischoff, 1993) are also shown with the age ranges for each sample plotted as error bars parallel to the time axis, and with precision plotted as error bars parallel to the oxygen isotopic composition axis.

Dependence of modeled carbonate $\delta^{18}\text{O}$ on input Owens River isotopic composition

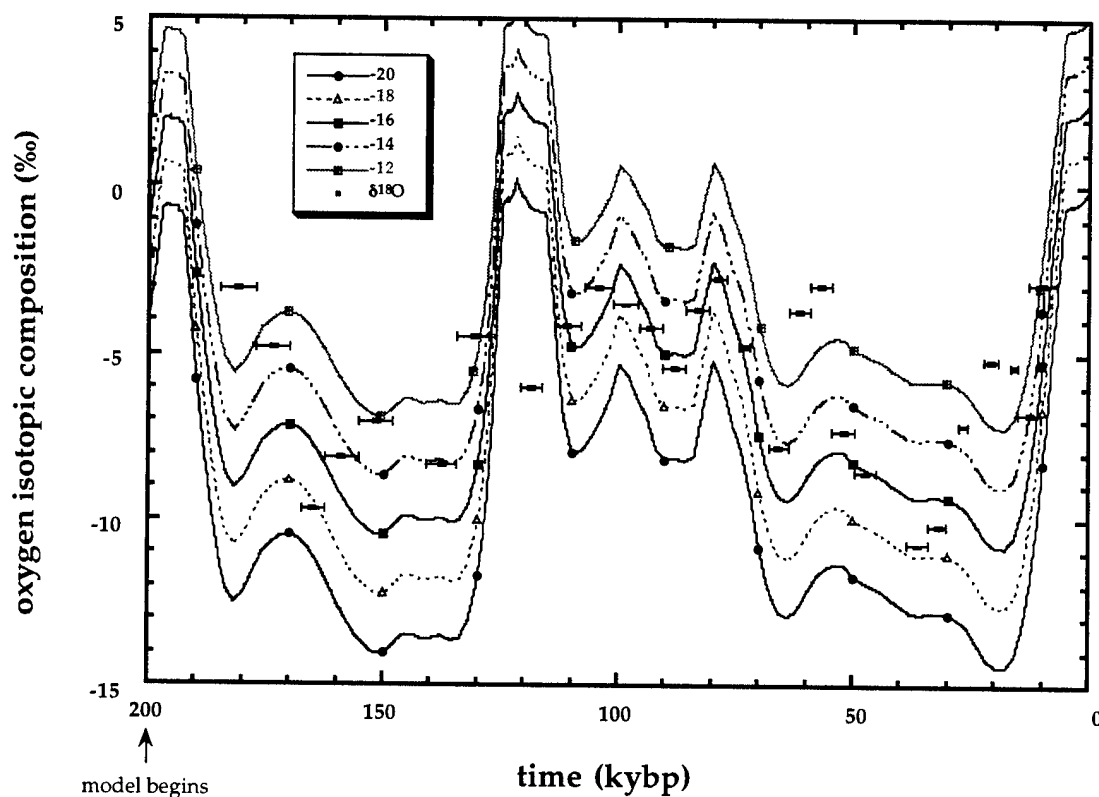


Fig. 3.18: Dependence of modeled oxygen isotopic value of carbonates on input Owens River isotopic value. Five different input isotopic values are shown, ranging from -12‰ to -20‰ . These values have been chosen to reflect both more depleted, glacial values, and more enriched, "super-interglacial" values, or values that might be expected if the Sierra Nevada were at a lower elevation resulting in less orographically-induced fractionation. Runoff is modulated between modern and $7\times$ modern values with the marine $\delta^{18}\text{O}$ record. Evaporation varies between modern and $0.7\times$ modern again with the marine $\delta^{18}\text{O}$ record. Input Owens River water has a $\delta^{18}\text{O}$ value of -16‰ . The atmosphere over the lake is assumed to have a $\delta^{18}\text{O}$ value of -21‰ and a relative humidity of 35%. Carbonates are assumed to be forming at 15°C . Measured carbonate $\delta^{18}\text{O}$ values (Benson and Bischoff, 1993) are also shown with the age ranges for each sample plotted as error bars parallel to the time axis, and with precision plotted as error bars parallel to the oxygen isotopic composition axis.

maximum glacial runoff of 10x modern results in modeled lake isotopic values that are more depleted than those measured, and an isotopic curve with a much higher amplitude or range of values than that found in the data. The runoff value that appears to match the measured data best has a 7x modern precipitation during glacial maxima.

Benson (1994) showed that the isotopic composition of precipitation falling in the Lake Tahoe drainage basin varied seasonally by 20‰ or more, with a mean value of -14.7‰. Precipitation falling in winter was typically more depleted than that falling in summer, which he ascribed to the lower winter air temperatures. Given the relationship between the isotopic value of precipitation and air temperature, we might expect that the $\geq 5^{\circ}\text{C}$ decline in air temperature associated with glaciation would result in a depletion of isotopic values of precipitation falling in the Owens Lake drainage basin during glacials relative to modern mean annual values. We must therefore explore the sensitivity of modeled carbonate $\delta^{18}\text{O}$ values to changes in input water $\delta^{18}\text{O}$ values. In Figure 3.18 we show the modeled isotopic composition for 5 different input runoff $\delta^{18}\text{O}$ values, ranging from -12‰ to -20‰. It is readily apparent that the value chosen for the input runoff is crucial in determining the absolute isotopic value of the modeled carbonates, although the amplitude of isotopic variation between glacial and interglacial periods would remain the same for any particular input isotopic value. If, however, input runoff isotopic value were allowed to change with time, amplitude of isotopic variation would also change.

A close examination of Figures 3.14 through 3.18 shows that changes in some parameters simply shift the pattern of modeled carbonate isotopic composition toward more depleted or more enriched values, while other

parameters change the amplitude of the modeled isotopic pattern. Those parameters that do not influence the residence time of water in the lake, such as the isotopic compositions of the atmosphere and input Owens River water, and the calcification temperature, have no effect on the amplitude of the isotopic pattern. Rather, they modulate the isotopic "starting point" of the model run, and thus also control the absolute isotopic values attainable in the model run. Runoff rate and evaporation rate *do* influence the residence time of water in the lake, and therefore, strongly influence the amplitude of the isotopic curve. As we showed in the sinusoidally fluctuating climate scenarios, residence time of water in a lake is influenced by two competing effects. Residence time is short both when the volume of runoff is large so that water spends a short time in the lake prior to being spilled into the next lake in the chain, and when the lake is small such that evaporation removes a large fraction of the lake water volume in each timestep. Between these two short residence time periods lies a period of much longer residence time, which reflects the changeover from residence time dominated by runoff to residence time dominated by evaporation. In Figure 3.19 we show the residence time for the five different runoff values leading to Figure 3.17. It is clear that glacial period runoff values of 10x modern show much shorter residence times (~5 years) than runoff values of 2x modern (~10 years). Likewise, at present and at ~125 ka, residence time is again very short, but this time it reflects the small volume of Owens Lake and the comparatively large evaporative flux out of the lake at each timestep. Comparison of Figures 3.19 and 3.17 shows that lake waters become most isotopically enriched during periods of long residence time or short residence time dominated by evaporation.

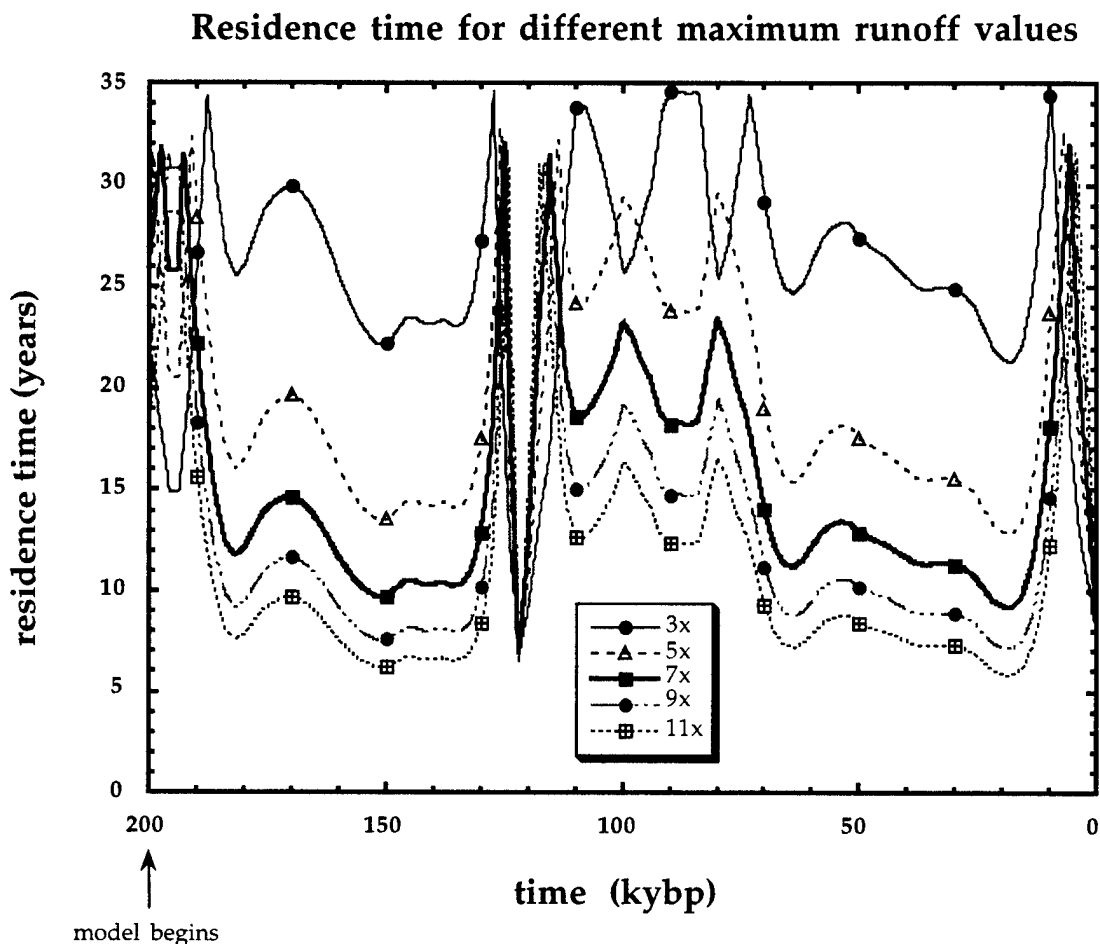


Fig. 3.19: Residence time for water in Owens Lake for 5 different values of glacial maximum runoff ranging from 2x modern to 10x modern runoff. Increasing runoff leads to decreasing residence time as water is pushed rapidly through the lake chain. Short residence times at ~123 ka and at present reflect the small volume of Owens Lake and comparatively large evaporative flux out of the lake at each timestep.

DISCUSSION AND CONCLUSIONS

Now that the sensitivity of the modeled $\delta^{18}\text{O}$ values to various climatic parameters is known, we may attempt to create a best-fitting scenario to constrain further lake-level fluctuations. Glacial period precipitation and atmospheric water vapor may have been very much more depleted than modern values due to the 5-7°C cooler air temperatures that prevailed at those times (Porter, 1983; Dohrenwend, 1984; Spaulding and Graumlich, 1986; Stamm, 1991). The isotopic composition of precipitation changes with temperature at a rate of 0.7‰/°C (Benson, 1994). Therefore, a 5°C cooling may have led to a glacial Owens River isotopic value of -19.5‰ and an atmospheric isotopic value of -24.5‰. In Figure 3.20, we explore the effects of modulating temperature and isotopic composition of atmosphere and runoff between assumed glacial and modern values. Three pairs of model output are shown, each pair differing by the amount of glacial runoff prescribed. For each pair, one curve allows runoff and evaporation to vary between modern and assumed glacial values while the other parameters--atmospheric and runoff $\delta^{18}\text{O}$ and temperature--are held fixed at modern values. The other curve depicts models in which all parameters are allowed to vary between modern and assumed glacial values. We find that modulating runoff between modern and 7x modern values, modulating evaporation between modern and 0.7x modern values, setting the isotopic composition of the input Owens River water and atmosphere to -16‰ and -21‰ respectively, and setting the calcification temperature to 15°C yields a good visual match between modeled and measured $\delta^{18}\text{O}$ values (Fig. 3.21a). Between 70 and 110 ka, the model matches the measured isotopic data well. Furthermore,

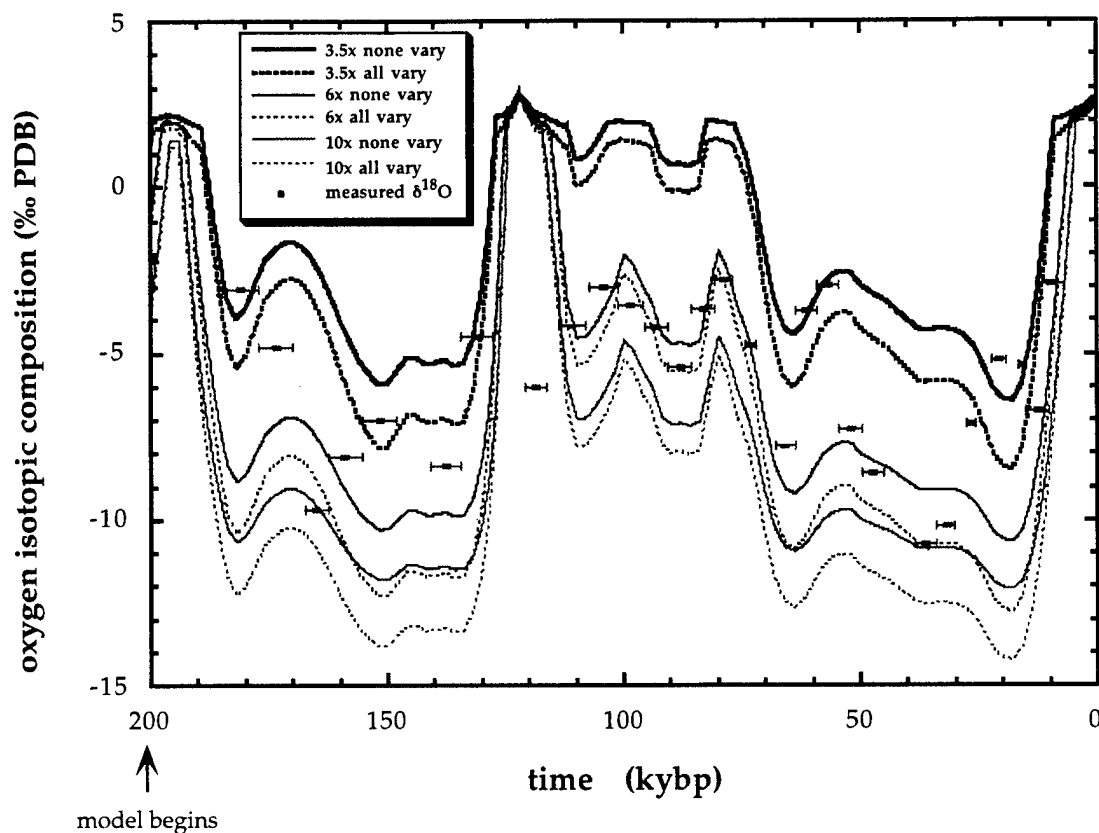


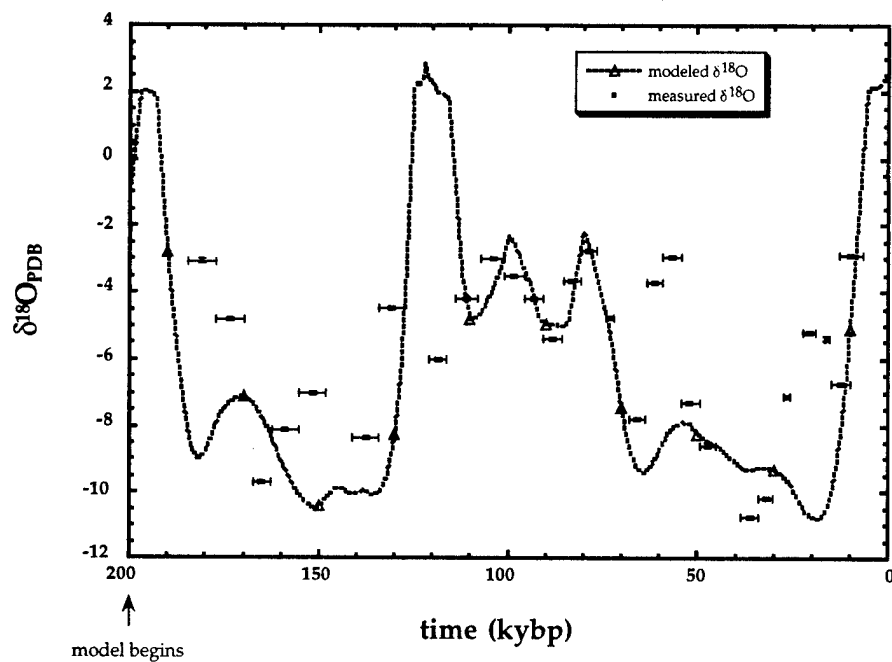
Fig. 3.20: Three pairs of model runs which differ in from each other in amount of glacial runoff prescribed. 3.5x refers to 3.5 x modern runoff during glacial maxima, likewise for 7x and 10x. For all model runs, glacial evaporation rate is specified as 70% of modern. None vary refers to model runs in which temperature and isotopic composition of input runoff and atmosphere are held fixed at modern values. All vary refers to runs in which these parameters are allowed to vary between modern and assumed glacial values (5 °C cooler).

Fig. 3.21a: Measured and modeled oxygen isotopic composition of carbonates in Owens Lake. Measured values come from Benson and Bischoff (1993). Modeled values result from the following parameters: runoff varies between modern and 7x modern values with the marine $\delta^{18}\text{O}$ curve, evaporation varies between modern and 0.7x modern also with the marine $\delta^{18}\text{O}$ curve, input Owens River water and the atmosphere have $\delta^{18}\text{O}$ values of -16‰ and -21‰ respectively, relative humidity of the atmosphere over the lake is 35%, and carbonates are forming at 15°C.

Fig. 3.21b: Comparison of modeled oxygen isotopic composition of carbonates in Owens Lake to measured carbonate content in the Owens Lake core sediments. Note that while the two curves appear to be chronologically offset from one another, their shapes are very similar. The model predicts that isotopic values of Owens Lake carbonates should be very enriched at 125 ka (>2‰), and somewhat less enriched at 80 and 100 ka (-2‰). These are periods of very low runoff and high evaporation rates. The measured isotopic data shown in Fig. 3.17a do not bear out the model predictions for the enrichment at 125 ka, with the modeled isotopic peak nearly the same amplitude as those at 100 and 80 ka. The carbonate content measurements, however, do show that the lake was more saline, and presumably more evaporatively concentrated.

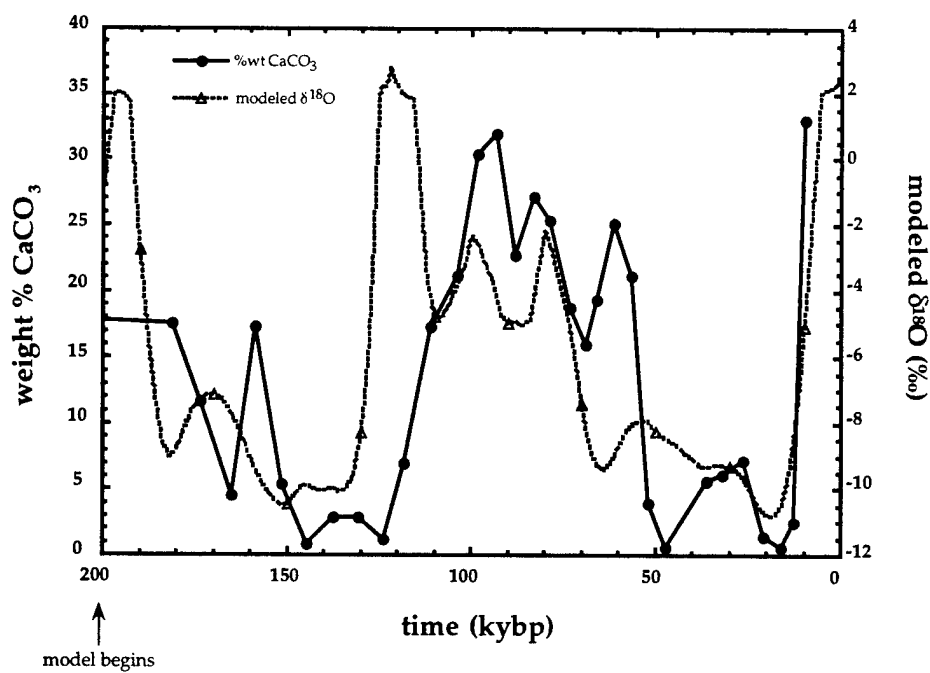
a)

Model that best fits measured isotopic data



b)

Measured carbonate content and modeled isotopic composition



the degree of isotopic depletion centered about 38 ka in the measured data is generally matched by the low modeled isotopic values between 70 and 20 ka. The model predicts much more enriched isotopic values at 120 and 195 ka than are found in the data. However, as the measured isotopic data are sparse between 120 and 128 ka and again between 185 and 198 ka, we cannot confidently say that enrichments of magnitude similar to those in the modeled data did not occur.

Interestingly, in some ways the carbonate content data determined by Bischoff and others (in press (a)) more closely mimic the modeled isotopic fluctuations than they do the measured isotopic values (Fig. 3.21b). While there is clearly a chronological offset between the measured and modeled records, the carbonate content data show the same pattern of two small peaks (at 60 and 85 ka) preceded by a larger peak (at 100 ka) as do the modeled isotopic data (peaks at 80, 100 and 120 ka). This chronological offset may be due to error in the age/depth model constructed for the Owens Lake core, or to an actual lag in the response of the carbonate content proxy relative to the marine isotopic proxy. Whatever the cause for the offset, the similarities in the two curves are striking.

Figure 3.21c depicts the lake-level history devised for the best-fitting scenario. The history captures 4 periods of overflow from Searles Lake to Panamint Valley, two of which nicely correlate to episodes described by Jannik and others (1991). A small overflow from Panamint Lake to Death Valley (Lake Manly) is modeled at ~20 ka. This event is not seen in the chloride accumulation data of Jannik and others (1991), although a shallow saline lake has been identified in Death Valley that existed from 10-30 ka (Lowenstein and others, 1994; Ku and others, 1994; Li and others, 1994; Robert and others, 1994). We

c)

Modeled lake level history

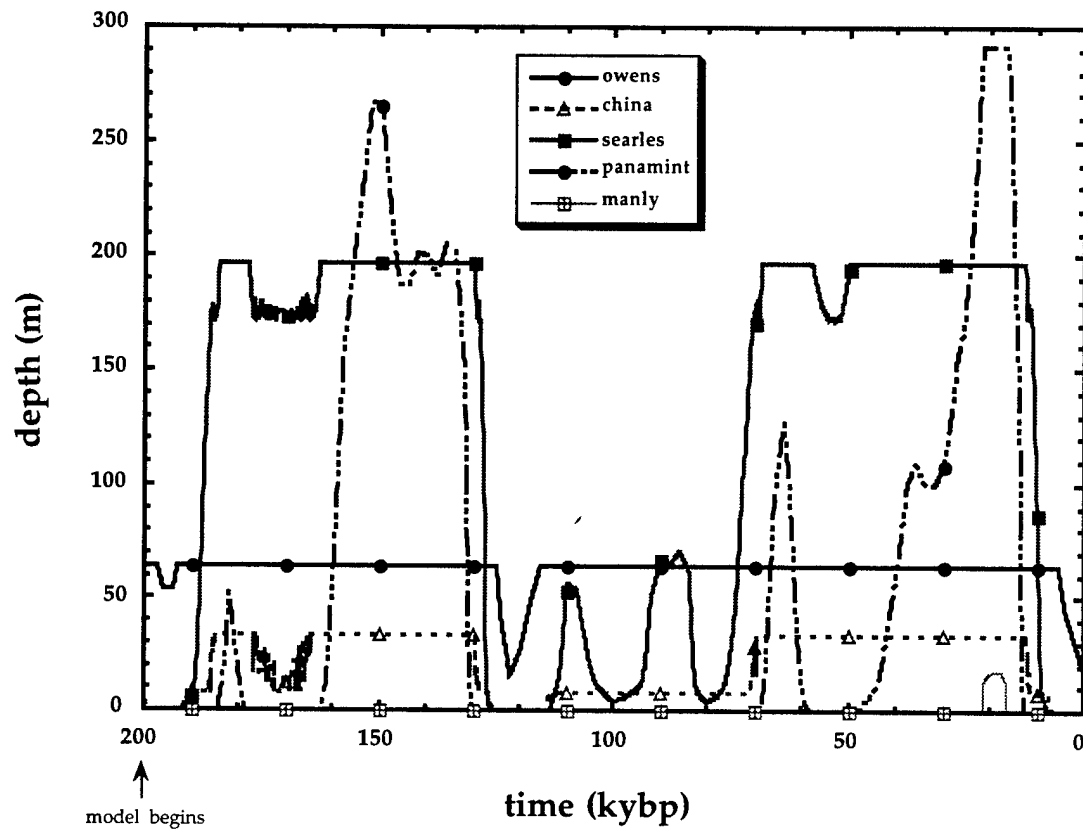


Fig. 3.21c: Lake level history associated with the model run that visually best fits the measured isotopic data. Modeled depths result from the following parameters: runoff varies between modern and 7x modern values with the marine $\delta^{18}\text{O}$ curve, and evaporation varies between modern and 0.7x modern also with the marine $\delta^{18}\text{O}$ curve.

caution that the source of water responsible for creating the 10-30 ka Lake Manly is not presently known (Lowenstein, personal communication), however, (it could have come from the Amargosa river or from overspill from the Tecopa lake system) and therefore, this correspondence cannot be used as a test of the model.

We draw the following conclusions from the modeling exercise:

- The response time of Owens Lake to changes in climatic forcing is on the order of one century. The response time for the entire lake chain is about 300 years. Therefore, the lake chain should be at steady state with respect to long time-scale climatic fluctuations such as those induced by orbital forcing, and lake response should be lagged behind climate forcing by about one century. Thus, long-period forcings should be fully recorded in the sediments of Owens Lake.
- It takes only about 50 years to desiccate Owens Lake with modern evaporation values (smaller evaporation rates, as might have prevailed during glacial periods, require slightly longer periods) (Fig. 3.9). Given this result and the response time data, droughts of durations longer than 1 century (such as those reported by Stine, 1994) should be recorded in the sediments of Owens Lake in the form of evaporite layers. That these layers have not been identified indicates either that droughts did not occur in this area in the last 786 ka, or that the deposits dissolved upon reintroduction of water into the lake. As already noted, there exists no evidence for dissolution features in core OL-92, which favors the absence of >100 yr droughts.

- A maximum glacial runoff value of 10x modern, inferred from the empirical curves of Langbein and others (1949) and from estimates for paleo-temperature and -precipitation, is not supported. This value leads to modeled isotopic compositions that are much less enriched than the measured values (Benson and Bischoff, 1993), and to lakes that are too large. On the other hand, maximum glacial runoff of 3.5x modern, as suggested by Orndorff (personal communication), leads to modeled interglacial isotopic values that are too enriched.
- We capture fairly well the amplitude of oxygen isotope variation between glacial and interglacial periods when we assume a 7-fold increase in runoff and a 30% decrease in evaporation rates during glaciations relative to modern values (Fig. 3.21a); this corresponds to about a 2.7-fold increase in runoff during isotope stages 5a (~80 ka) and 5c (~100 ka). The details of the measured isotopic curve are not as well accounted for, however. These details may be related to shorter-term climatic fluctuations than the Milankovitch time-scale variations we use to drive runoff. Such shorter-term fluctuations have been found in ice- and oceanic sediment-core studies around the North Atlantic region (Johnsen and others, 1992; Alley and others, 1993; Greenland Ice-core Project (GRIP) Members, 1993; Ruddiman and others, 1977; Broecker and others, 1990; Bond and others, 1993), and are associated with temperature variations of 7-13 °C acting over a few hundred to ~2000 years. These events motivate the higher-resolution study of Owens Lake core sediments described in Chapter 4, which addresses whether short-term fluctuations in water balance are observed in the eastern Sierra Nevada region.

- Comparison of Jannik and others' (1991) chronology to our modeled chronology in Figure 3.21c shows general agreement; our model shows overflow from Searles Lake to Panamint Valley between 130 and 160 ka and between 12 and 30 ka. Jannik and others reported overflow from 120-150 ka, and from 10-24 ka. However, we model two overflows into Panamint (from 60-70 ka, and from 180-185 ka) that are not reported by Jannik and others. Our model is successful in capturing the Holocene aridification noted by these authors and by Smith (1984) inasmuch as lake levels decline dramatically beginning at roughly 10 ka.
- The chronology shown in Figure 3.21c has Owens Lake spilling into Searles Lake for most of the last 200 kyrs. This conflicts with Bischoff and others' (in press (a)) estimates of the overflow using CaCO_3 content; that proxy leads to the conclusion that Owens Lake was closed for up to 50 kyrs at a time. However, studies conducted on cores of Searles Lake suggest that Owens Lake overflowed throughout much of the last 200 kyrs (Smith, 1984; Phillips and others, 1992) supporting the lake-level history reported here. The chronology indicates that any oxygen isotopic value more depleted than $\sim 0\text{‰}$ is associated with an overflowing Owens Lake.

ACKNOWLEDGMENTS

This research was funded by a National Defense Science and Engineering Graduate Fellowship awarded to KMM. Discussions with Greg Dick and Eric Small proved enormously helpful. Thanks to Wes Danskin, Tim Lowenstein, and Rick Orndorff for sharing their ideas and data, and to Jim Bischoff and Bob Garrison for comments on the manuscript.

CHAPTER 4

Sub-Milankovitch Climatic Variations Recorded in Core OL-92, Owens Lake, Southeastern California

KIRSTEN M. MENKING¹ and JAMES L. BISCHOFF²

*¹Department of Earth Sciences and Institute of Tectonics,
University of California, Santa Cruz, CA 95064*

*²Branch of Volcanic and Geothermal Processes,
U.S. Geological Survey, Menlo Park, CA 94025*

ABSTRACT

Grain size analyses, carbonate content measurements, and stable isotope determinations on 70-cm-long (~1500 years) channel samples from Owens Lake core OL-92 indicate many high-frequency water-balance oscillations in the eastern Sierra Nevada region during both the last glacial maximum and the last interglacial. Fluctuations in grain size are thought to reflect variations in lake level, while changes in carbonate content and $\delta^{18}\text{O}$ of carbonates probably indicate the degree of evaporative concentration of Owens Lake water. In addition, $\delta^{13}\text{C}$ may be an indicator of biological productivity within the lake. To first order, the detailed records match well the marine $\delta^{18}\text{O}$ record; we focus on the exceptions to this. The last interglacial (in OL-92, the last interglacial appears

to have occurred from 50 to 120 ka; in the marine record, it occurred from 70 to 128 ka) appears to have been punctuated by short periods of wetter conditions in the midst of an otherwise dry climate. Isotopic fluctuations within samples deposited during the last glacial (~13 to 30 ka) are enigmatic, possibly indicating overspill of enriched Mono Lake water into the Owens Lake system or reflecting incorporation of detrital carbonates from the Owens Valley drainage basin into the lake sediments. Spectral analysis of subsets of the record shows dominant periodicities at 24, 11, 5.1, and 4.2 ka in several of the records.

INTRODUCTION

Variations in Earth's orbital parameters have been called upon to produce the major 20, 40, and 100 ka glacial-interglacial climate cycles prevalent during the Pleistocene (Imbrie and others, 1984; and many others). $\delta^{18}\text{O}$ in deep sea sediments (Imbrie and others, 1984), magnetic susceptibility changes in loess deposits in China (Kukla and others, 1988), and carbonate content, $\delta^{18}\text{O}$ of carbonate, grain size, and clay mineralogical variations in sediments from Owens Lake, eastern California (Menking, in press, Chapter 2; Bischoff and others, in press (a); Benson and Bischoff, 1993), among other records, appear to be coincident over the timescales with which these orbital variations occur. These long-term variations in climate have been recognized for several decades. Recently, however, much more rapid, sub-orbital-forcing-period climate changes have been recognized in the last ~150 ka of Earth history in such proxies as ice cores (Johnsen and others, 1992; Alley and others, 1993; Greenland Ice-core Project (GRIP) Members, 1993), beetle remains from England (Atkinson and others, 1986), $\delta^{18}\text{O}$ in deep sea sediments (Ruddiman and others, 1977; Broecker

and others, 1990; Bond and others, 1993), and the relative abundance of polar versus sub-polar planktonic foraminifera in North Atlantic sediment cores (Ruddiman and others, 1977; Broecker and others, 1990).

Johnsen and others (1992), working on the Greenland Ice-core Project (GRIP) core, interpreted changes in ice $\delta^{18}\text{O}$ values as evidence for major climatic fluctuations with durations of 500 to 2000 years and temperature variations of 12-13 °C between maximum stadial and interstadial periods from 11.5 to ~37 ka. Atkinson and others (1986) used the remains of beetles found in various sites in Great Britain to show that air temperatures over that island nation vacillated over a 7 to 8 °C range between 15 and 9.5 ka. Similarly, Ruddiman and others (1977) and Broecker and others (1990) reported foraminiferal and continentally-derived detrital sediment data to portray rapid and large temperature changes during the last deglaciation. In all of these records, which are derived from localities either in or adjacent to the North Atlantic, the last glaciation (35 to 11.5 ka) shows evidence of rapid warming events with gradual resumption of colder conditions. Likewise, the Eemian interglacial (~115-125 ka) (Greenland Ice-core Project (GRIP) Members, 1993) and the return to the present interglacial climate since 11.5 ka appear to have been marked by several brief cold snaps, the best known of which is the Younger Dryas [variously placed at 11-10 ka (Atkinson and others, 1986; Bard and others, 1994), and 13-11.6 ka (Alley and others, 1993; Fairbanks, 1990)]. In the case of both the warming and cooling events, temperatures are interpreted to have changed on average 7 °C but may have changed by as much as 12-13 °C. Events lasted between 500 and 2000 years and occurred at seemingly random intervals. The mechanisms for these rapid variations are not readily apparent, though several suggestions have been made.

For example, Broecker and others (1988 and 1990) called on oscillations in oceanic thermohaline circulation to produce observed fluctuations in ocean sediment cores, but while Johnsen and others (1992) interpreted variations in $\delta^{18}\text{O}$ of ice in terms of temperature changes over Greenland, Charles and others (1994) offered a different explanation: shifting source areas for precipitation falling on the Greenland ice sheet, rather than temperature changes, can explain much of the ice isotopic variability. Regardless of the causative mechanisms, the existence of short-term climatic events is now recognized.

In this paper, we report evidence for similar "sub-Milankovitch" climatic phenomena in eastern California. Rather than reflecting variations in temperature, however, the data described here mark changes in water balance over the last ~155 ka in the Owens Lake chain of lakes. We use grain size, carbonate content, and stable isotopic measurements to document at high resolution the variations in water balance. The first order agreement of the Owens Lake record with the marine isotopic record, reported in our earlier studies (Bischoff and others, in press (a); Menking, in press) in which the core was sampled more coarsely, is supported here. In this paper, the higher sampling rates allow us to address mismatches in the behavior of different climate proxies, the periodicity of higher frequency water-balance variations, and the timing of Termination II (the transition from glacial stage 6 to interglacial stage 5). We find that dry interglacials exhibit several excursions to wetter climates. We also explore several hypotheses to explain the apparent incongruity of different water-balance proxies during the last glacial (~13 to 30 ka), which show low carbonate contents and mean grain sizes indicative of an overflowing Owens Lake, but also occasionally show enriched isotopic values which would

suggest a shallower, closed body of water. Before discussing the completed work and interpretations, we turn first to a description of the study area and previous work conducted on Owens Lake core OL-92.

LOCATION AND GEOLOGIC SETTING

Owens Lake heads a chain of Pleistocene pluvial lakes separated by bedrock sills found to the east and south of the Sierra Nevada (Fig. 4.1). The lake lies at the southern end of the topographically-closed Owens Valley, which is bounded on the west by the Mesozoic plutons of the Sierra Nevada, on the east by the Paleozoic and Mesozoic metasediments and Mesozoic plutons of the White and Inyo Mountains, and on the south by the Cenozoic volcanic and sedimentary rocks of the Coso Range. Owens Valley is the westernmost expression of Basin and Range extension, and as such consists of a downdropped fault-block valley bounded by northwest-southeast trending ranges. Prior to the construction of the Los Angeles aqueduct, Owens Lake received runoff from the Sierra Nevada via the Owens River and its tributaries, making it an ideal location for the continuous recording of global climatic fluctuations as they have been manifested in the Sierra Nevada. During glacial periods, Owens Lake exceeded the confines of the southern Owens Valley and spilled over a sill into the China Lake basin (Smith and Street-Perrott, 1983; Smith, 1984; Benson and Thompson, 1987a). That lake quickly filled and overflowed into the Searles Lake basin. During exceptionally wet periods, Sierra Nevada runoff flowed from Owens Valley all the way to Death Valley to help create Lake Manly. During interglacials, Owens Lake remained at a level lower than the spillway, precluding the formation of large lakes in the downstream basins (Smith, 1976).

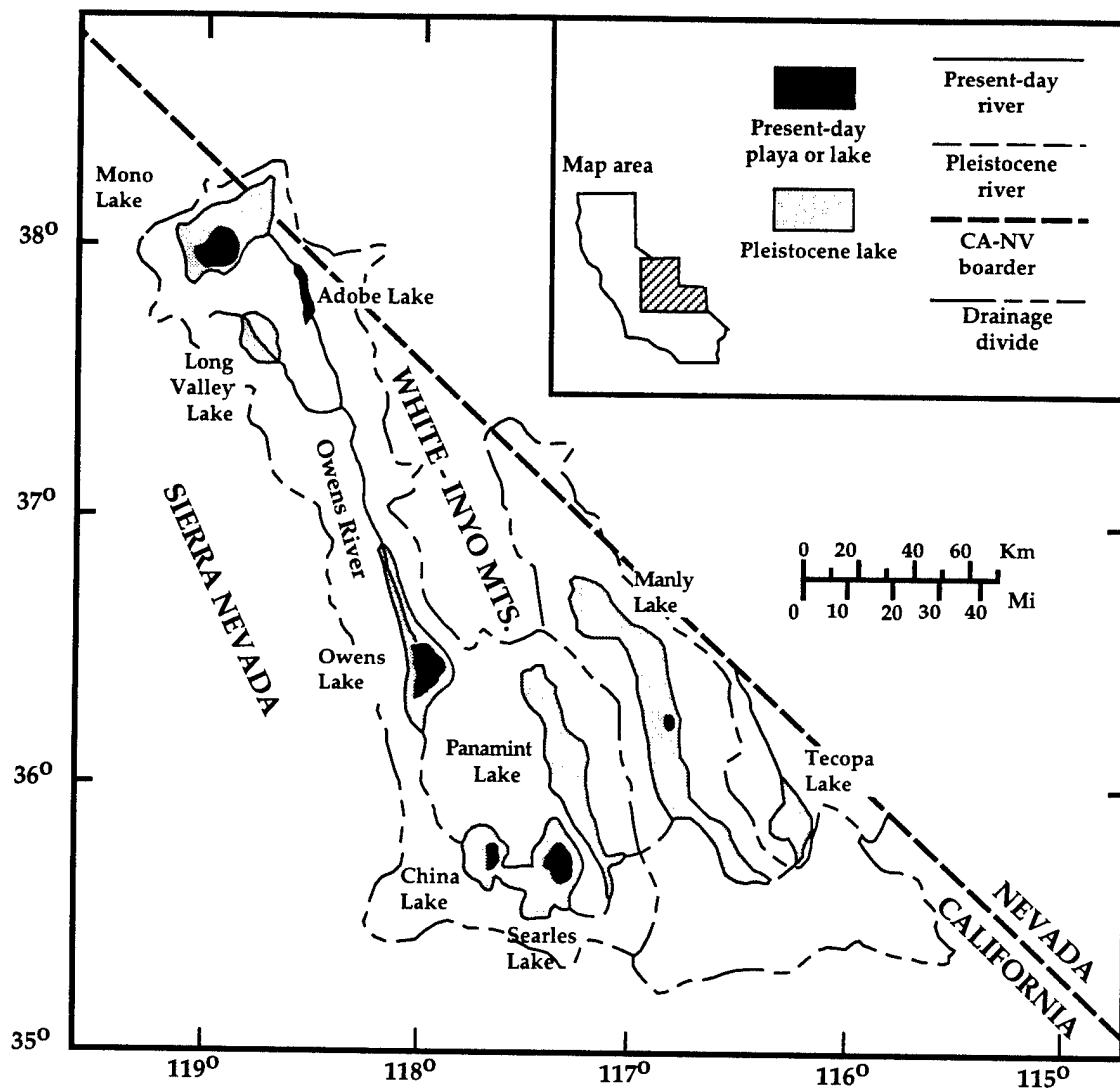


Fig. 4.1: Map of eastern California and western Nevada showing the location of the Owens Lake chain of lakes, Mono Lake, and Adobe Lake. The black pattern marks the extent of modern lakes and playas. Grey stippling corresponds to maximum pluvial lake extents. Also shown are the overflow routes between the different lake basins.

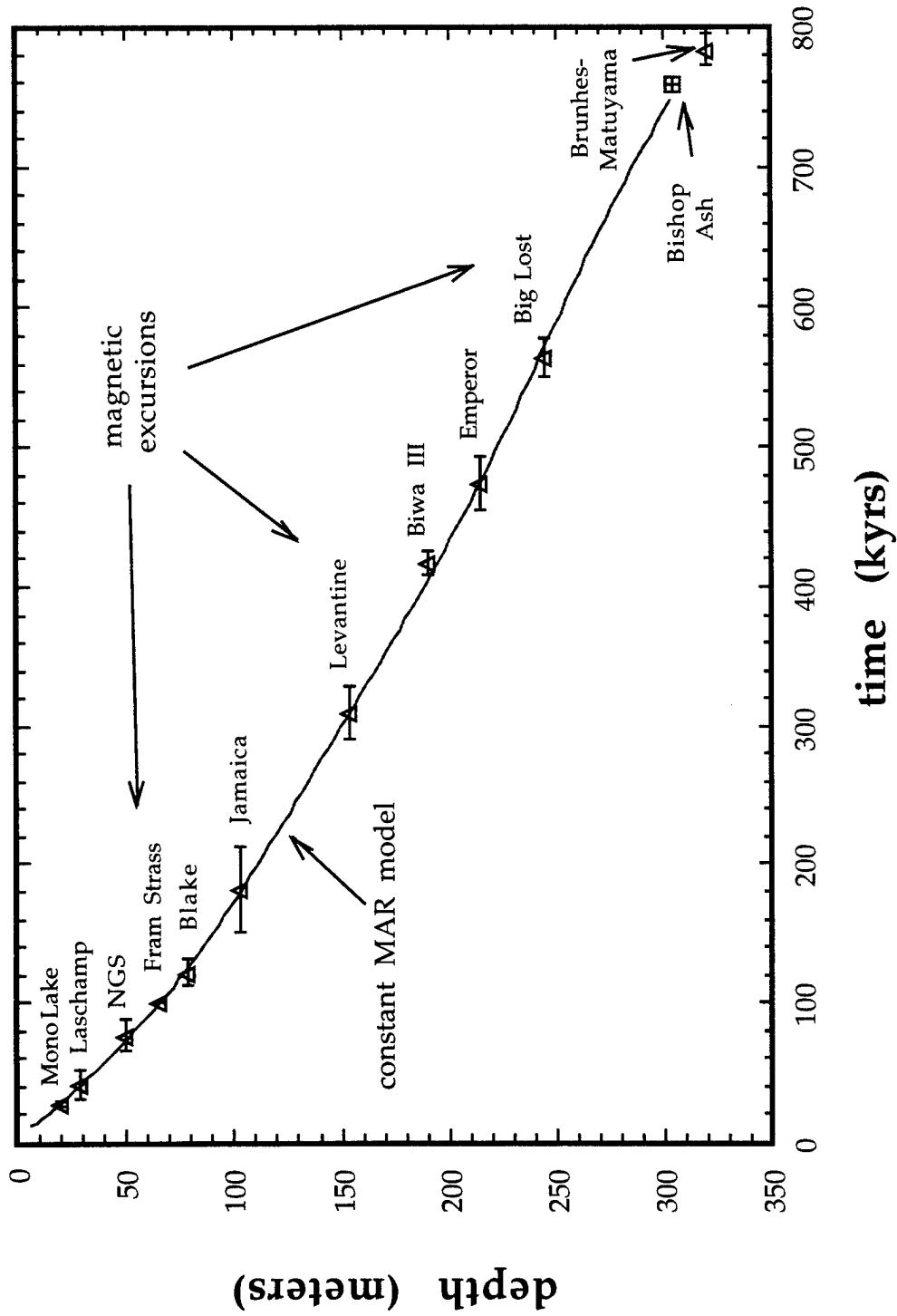
At present, Owens Lake is largely a playa due to diversion of Owens Valley runoff into the Los Angeles aqueduct. The historic desiccation of the lake produced a 1- to 2-m-thick layer of sodium carbonate minerals which coat the valley floor.

THE OWENS LAKE CORE, SOUTHEASTERN CALIFORNIA

In the spring of 1992, the U.S. Geological Survey drilled a 323-m-deep core into Owens Lake to obtain a continuous record of terrestrial paleoclimate for the Sierra Nevada region (Smith and Bischoff, in press). The core spans 786 ka giving an average sedimentation rate of ~40 cm/kyr. Age control consists of ^{14}C dates for the last 30 ka (Bischoff and others, in press (b)), tephrochronology (Sarna-Wojcicki and others, in press), and magnetostratigraphy (Glen and Coe, in press) (Fig. 4.2). Sediments range from an evaporite package at the top of the core to lacustrine clay-, silt-, sand-, and granule-sized clastic materials plus carbonate muds. The dominant clastic sediment size at the top of the core is clay- to silt-sized material, changing to interbedded silts and sands below about 200 m depth. The core has been sampled for grain size, organic carbon and carbonate contents, $\delta^{18}\text{O}$ of inorganically-precipitated carbonate, clay mineralogy, pollen, pore-water chemistry, microfossil analyses, and bulk chemistry (Smith and Bischoff, in press). Work conducted to date on 3-m-long channel samples and point samples (see definitions in next section) has revealed strong similarities between carbonate content, mean grain size, $\delta^{18}\text{O}$, and clay mineralogy proxy records (Menking, in press, Chapter 2; and Menking and Anderson, in prep., Chapter 3). In addition, all of these records bear strong similarities to the marine $\delta^{18}\text{O}$ record from deep-sea sediments, although they appear to be somewhat (~8

Fig. 4.2: Age-depth model constructed for the Owens Lake core based on the assumption of constant mass accumulation rate from the top of the core to the Bishop Ash at 758 ka (Bischoff and others, in press (b)). Also shown are the magnetic excursions of Glen and others (in press), and the identified tephra of Sarna-Wojcicki and others (in press). The close agreement between the three independently-derived chronologies lends faith to the age-depth assignment.

Chronology for the Owens Lake core

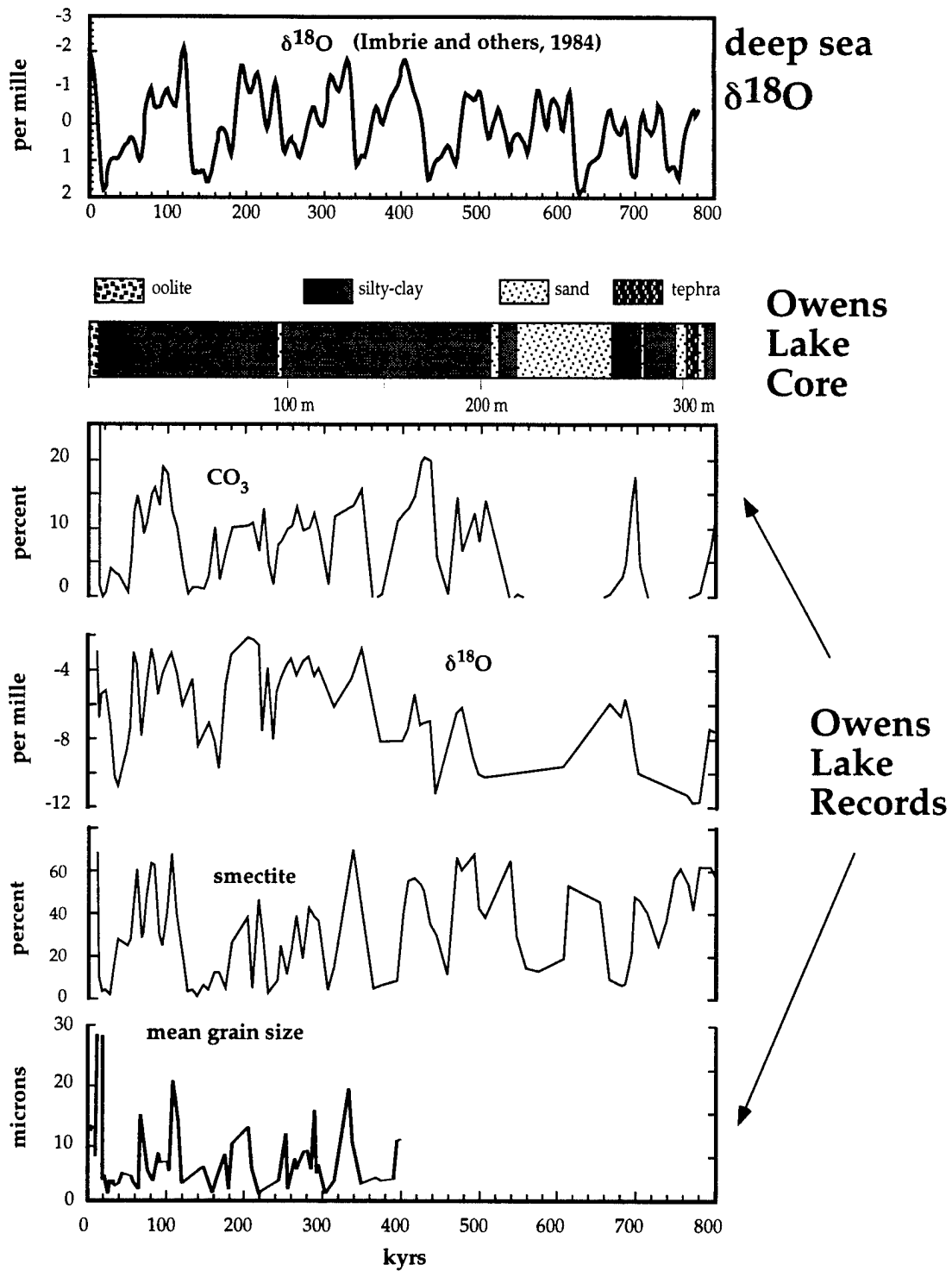


kyrs) chronologically offset from that record (Fig. 4.3); the Owens Lake CaCO_3 content shows Termination II at 120 ka (Bischoff and others, in press (a)), while the marine record places this event at 128 ka (Imbrie and others, 1984).

In the Owens Lake core, low carbonate contents and depleted $\delta^{18}\text{O}$ values have been interpreted as evidence of overspilling, fresh-lake conditions, while high carbonate contents and enriched $\delta^{18}\text{O}$ values are taken as evidence of saline-lake conditions, and an Owens Lake below its sill level (Bischoff and others, in press (a)). Likewise, fine grain sizes are thought to indicate a large lake whose shores were at a great distance from the core site while coarse grain sizes probably indicate that the lake was smaller and the shores closer to the core site. Clay mineralogy has been used to identify periods when the Sierra Nevada were glaciated (Menking, in press, Chapter 2). Close correspondence between smectite and illite fluctuations and variations in carbonate content, $\delta^{18}\text{O}$, and mean grain size suggests that Owens Lake was large and overflowing during glacial periods, and shallower and closed during interglacials.

In spite of the difference in timing between the paleoclimatic proxies in the Owens Lake core and the marine $\delta^{18}\text{O}$ record, it appears that the core is a good recorder of global climatic fluctuations. We therefore decided to conduct a detailed study of the last ~155 ka of core sediments to determine whether evidence for the high frequency and rapid climatic changes such as are found in regions surrounding the North Atlantic exists in the western United States, or if such evidence is lacking. Sampling resolution precludes direct comparison of our records to those from the North Atlantic region [sampling resolution of Owens Lake records is roughly 1500 years per sample while resolution of North Atlantic records range from annual in the case of ice-core studies (Johnsen and

Fig. 4.3: Comparison of Owens Lake core OL-92 carbonate content (Bischoff and others, in press (a)), mean grain size (from point samples), smectite content (Menking and others, in press), and isotopic values (Benson and Bischoff, 1993) (all records but mean grain size from 3.5-m-long channel samples) to the deep-sea oxygen isotopic record (Imbrie and others, 1984). Though some chronologic mismatch exists between the records, the similarity between the marine and Owens Lake records is striking, and suggests that Owens Lake responds to the same general climatic forcing recorded by the deep-sea $\delta^{18}\text{O}$ value.



others, 1992; GRIP Members, 1993), to 300-500 years (Bond and others, 1993) or 200-1000 years (Ruddiman and McIntyre, 1977) in the case of sediment cores], but does allow us to address whether similar short-term events might exist. In addition to looking for higher frequency climatic variations, we make use of the more detailed records to better resolve the timing of Ice Age Terminations, and we address whether the chronologic offset between the marine and Owens Lake datasets observed by Bischoff and others (in press (a)) might simply be an artifact of their 3-m sampling resolution. We also discuss the fact that the timing of Terminations appears to be proxy-dependent, with carbonate content and isotopic records leading to different estimates of the age of these events. In the following sections we report the methods used and the results of our investigation.

METHODS

Seventy-centimeter-long channel samples, each representing ~1500 years of sedimentation, were collected from the core by pushing a U-shaped spatula down the split face of the core (3-m long channel samples previously analyzed were taken in the same fashion; point samples are discrete samples taken at 2-3 m intervals, each having a length of ~5 cm). These samples were homogenized and washed with deionized water to remove any interstitial brine that may have percolated through lake sediments during the historic desiccation of Owens Lake. Aliquots were removed and ground to silt- and clay-sized material for carbonate content and oxygen isotopic analyses. Carbonate content was measured with a UIC Inc. Coulometrics Model 5010 CO₂ coulometer. Replicate measurements indicate an analytical precision of 0.01% carbon. Samples for

stable isotope measurement were roasted for one hour at 380 °C in a vacuum to oxidize and remove organic carbon. Carbonates were reacted for 7 minutes with 106% phosphoric acid at 75 °C in a Kiel carbonate extraction device in-line with a Finnigan MAT 251 mass spectrometer. Analytical precision, determined from repeat standards (NBS-18, -19, and -20), is 0.08‰ for $\delta^{18}\text{O}$ and 0.06‰ for $\delta^{13}\text{C}$ (Burdett, personal communication).

A separate aliquot was taken from each channel sample for grain size analysis. These aliquots were not ground, and were treated with dilute acetic acid and hydrogen peroxide to remove organic material and calcium carbonate. Sieving separated the sand and gravel component of each sample from the silt and clay fraction. Silt and clay grain-sizes were determined with a Micromeritics Sedigraph 5100. Sands constitute <10% of each sample [except for four samples that are noticeably coarser (sample #s 2, 42, 44, and 79)], and usually constitute <4%, and were therefore ignored. Since we are interested in trends in grain size, rather than in precise values, this action is justified; in general, incorporation of the sands into the mean grain size would change the mean by only a few tenths of microns. Replicate measurements indicate an analytical precision of ± 0.09 microns for the silt and clay values.

RESULTS

The results of all analyses are given in Table 4.1. Where replicate measurements were made, the mean of the various measurements is reported.

TABLE 4.1: Analysis results on 70-cm-long channel samples.

<u>Sample number</u>	<u>Age</u>	<u>Wt. % Carbonate</u>	<u>Mean grain size</u>	<u>$\delta^{13}\text{C}$</u>	<u>$\delta^{18}\text{O}$</u>
1	7.79	8.16	3.57	5.1	-2.00
2	9.17	53.45	12.51	4.93	-2.70
3	10.60	51.68	7.62	3.00	-2.00
4	12.28	26.30	-	1.27	-6.70
5	12.60	16.25	3.69	1.50	-7.65
6	13.31	14.71	3.77	1.70	-4.00
7	14.57	10.18	2.46	1.90	-2.50
8	17.08	1.92	1.24	0.48	-10.50
9	17.94	2.65	0.70	0.70	-3.99
10	19.30	1.96	1.28	1.34	-9.75
11	20.47	3.64	1.16	1.09	-9.30
12	21.40	3.28	0.82	1.20	-8.61
13	22.28	1.24	1.22	1.83	-6.77
14	23.11	1.63	1.56	1.35	-9.60
15	23.95	4.76	1.36	1.25	-10.88
16	24.69	5.60	1.84	1.23	-10.30
17	25.44	3.19	0.63	4.25	-6.90
18	26.44	1.93	0.76	2.03	-9.10
19	27.16	5.83	2.85	2.31	-10.05
20	28.76	12.34	2.92	2.25	-8.84
21	29.35	13.77	4.03	2.10	-9.28
22	30.51	8.74	3.31	1.69	-9.90
23	31.26	4.45	1.60	1.87	-10.22
24	32.01	5.57	3.39	2.23	-10.34
25	32.76	3.94	3.49	1.17	-10.22
26	33.65	4.09	2.43	1.53	-10.82
27	34.64	3.90	1.52	1.91	-10.80
28	35.69	4.19	2.83	1.73	-10.58
29	36.75	6.28	3.19	1.37	-10.74
30	37.98	6.17	1.70	1.68	-10.72
31	44.48	4.64	2.26	1.83	-9.40

<u>Sample number</u>	<u>Age</u>	<u>Wt. % Carbonate</u>	<u>Mean grain size</u>	<u>$\delta^{13}\text{C}$</u>	<u>$\delta^{18}\text{O}$</u>
32	45.85	1.33	2.98	0.74	-9.36
33	47.20	5.07	2.99	1.42	-10.38
34	48.68	1.36	1.96	1.24	-9.98
35	50.11	2.01	0.89	2.49	-9.63
36	51.29	1.94	1.78	2.80	-7.66
37	52.40	2.73	1.82	2.14	-9.53
38	53.44	12.95	1.55	3.03	-8.23
39	54.38	16.22	1.81	2.86	-5.49
40	56.37	16.06	3.99	4.05	-3.63
41	57.50	13.52	1.38	4.13	-3.48
42	58.59	31.90	2.96	6.49	-3.33
43	59.74	16.27	2.79	3.90	-2.50
44	60.87	23.18	10.73	7.05	-2.37
45	61.95	30.07	5.10	4.70	-2.88
46	62.97	26.77	6.55	5.43	-3.58
47	64.13	26.98	4.81	5.40	-5.11
48	65.20	18.68	3.43	3.51	-9.21
49	66.28	16.11	3.97	3.04	-10.40
50	67.34	16.07	6.32	3.10	-9.64
51	68.62	15.95	5.51	3.14	-9.55
52	69.50	15.56	3.60	2.90	-9.74
53	72.71	20.55	5.20	8.28	-2.70
54	73.72	12.50	9.17	4.69	-3.86
55	77.40	17.55	4.56	7.59	-2.55
56	78.48	22.45	7.25	7.85	-2.55
57	79.42	27.09	-	7.03	-2.84
58	80.37	27.58	7.17	6.55	-2.80
59	81.51	28.77	6.18	6.51	-3.59
60	82.62	27.36	6.13	4.76	-3.80
61	83.73	23.11	3.69	8.29	-2.66
62	84.90	30.39	7.00	8.07	-2.95
63	86.22	25.90	6.48	9.13	-2.79
64	87.47	28.58	4.24	9.58	-2.71

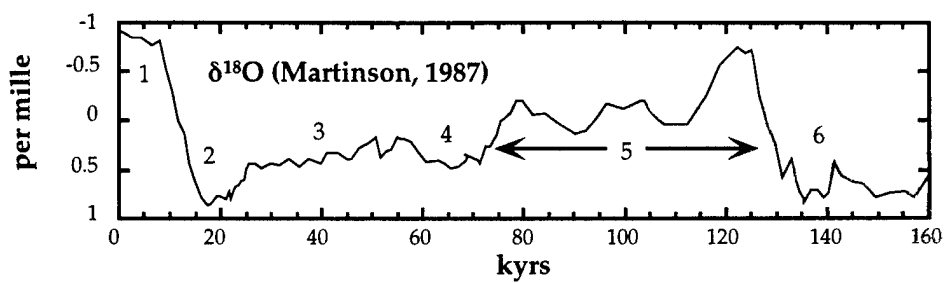
<u>Sample number</u>	<u>Age</u>	<u>Wt. % Carbonate</u>	<u>Mean grain size</u>	<u>$\delta^{13}\text{C}$</u>	<u>$\delta^{18}\text{O}$</u>
65	88.73	17.65	3.85	3.19	-8.27
66	90.03	20.14	4.18	3.01	-6.88
67	91.15	18.71	6.71	3.43	-6.03
68	92.25	16.37	5.79	3.89	-5.87
69	93.35	35.61	5.72	9.49	-2.56
70	94.52	30.99	4.06	3.85	-5.82
71	95.78	23.06	4.69	2.97	-8.25
72	97.04	19.70	3.72	3.03	-9.58
73	98.26	17.79	4.43	3.31	-6.99
74	99.47	14.94	6.17	4.00	-4.34
75	100.58	38.21	4.17	7.44	-1.97
76	101.63	34.24	5.93	9.91	-1.46
77	102.76	19.61	7.10	3.14	-4.19
78	104.01	16.52	14.63	2.74	-3.53
79	105.53	17.45	16.31	4.09	-3.35
80	107.23	20.06	3.94	4.49	-3.58
81	108.72	19.38	4.01	5.00	-3.61
82	110.05	17.39	3.61	5.05	-3.94
83	111.48	17.73	4.25	4.15	-4.01
84	113.05	17.59	3.81	4.04	-4.43
85	115.30	21.88	4.13	6.42	-2.86
86	117.04	19.49	-	2.87	-5.47
87	118.53	0.12	0.98	-	-
88	120.03	0.36	1.34	6.16	-3.25
89	121.70	2.30	0.83	5.37	-4.10
90	123.35	1.14	0.64	4.56	-4.81
91	125.02	1.54	0.64	4.22	-4.50
92	126.68	1.33	0.69	3.32	-5.34
93	128.34	3.29	0.70	3.91	-6.01
94	130.02	0.81	0.67	3.74	-5.59
95	131.70	2.28	0.91	2.02	-8.05
96	133.42	2.03	0.54	2.46	-7.33
97	135.13	1.84	0.69	2.17	-8.40

<u>Sample number</u>	<u>Age</u>	<u>Wt. % Carbonate</u>	<u>Mean grain size</u>	<u>$\delta^{13}\text{C}$</u>	<u>$\delta^{18}\text{O}$</u>
98	136.84	3.44	0.67	2.58	-7.13
99	138.56	3.49	0.79	2.70	-7.77
100	140.24	2.43	1.03	1.38	-8.52
101	142.17	4.89	1.50	2.00	-9.22
102	143.89	2.87	1.92	1.41	-9.84
103	145.63	0.79	2.86	1.44	-9.08
104	147.37	4.61	0.63	1.32	-8.35
105	149.10	4.78	0.59	1.98	-7.02
106	150.87	4.60	0.60	1.32	-8.44
107	152.65	8.29	0.55	1.99	-6.44
108	154.43	6.62	0.61	2.36	-6.78

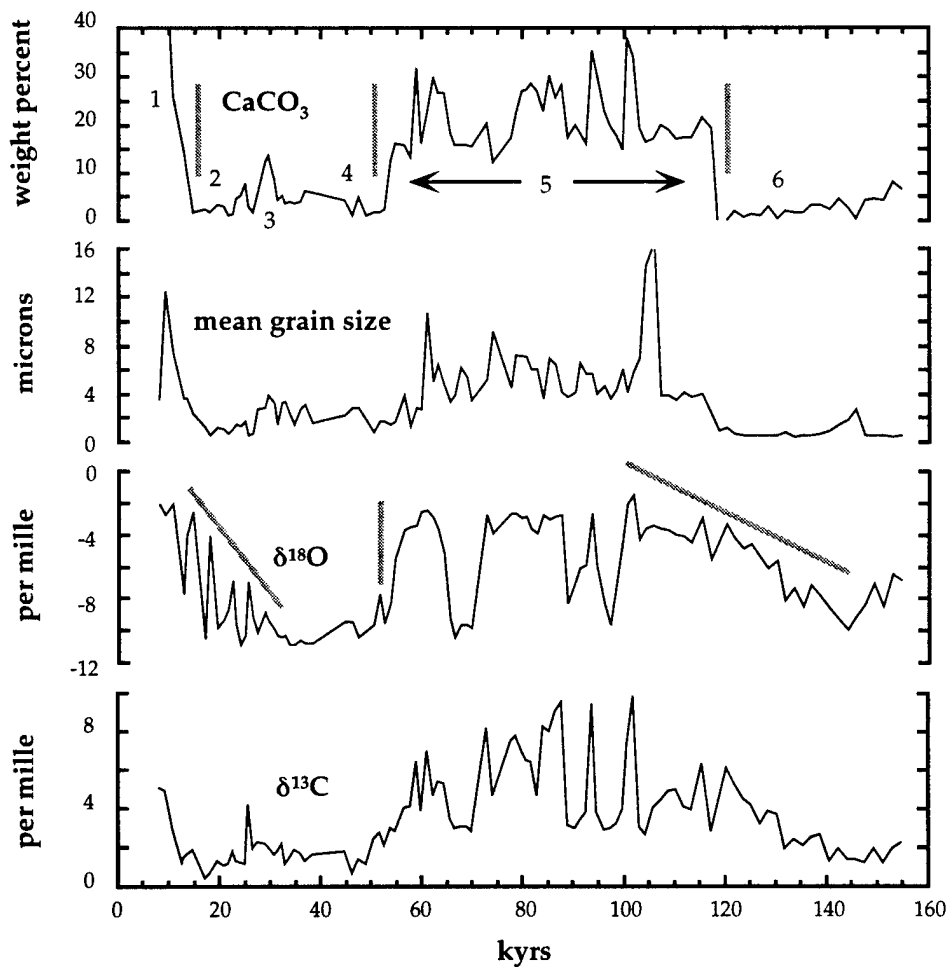
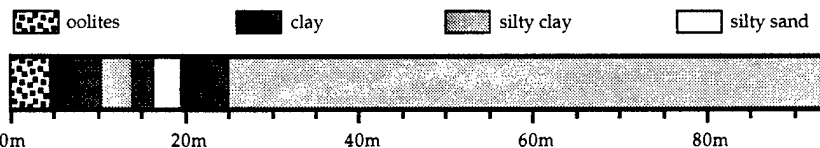
Carbonate Content

Carbonate content is highly variable down the core but generally shows high values from 5-10 ka (15-54%), and from 56-117 ka (12-38%), and very low values during the last glacial maximum (~15-22 ka), from 45-52 ka, and prior to 120 ka (Fig. 4.4). The 70-cm-long channel samples show the same broad trends displayed by the 3-m-long channel samples (Fig. 4.3), but show many shorter-duration oscillations superimposed upon the longer trends. The time period 56-117 ka shows particularly large-amplitude (>15 wt. %) fluctuations in carbonate content which last on order 5-10 kyrs (i.e., much longer than our 1.5 ka sampling resolution).

Fig. 4.4: Comparison of Owens Lake core OL-92 carbonate content, mean grain size, and stable isotopic values from 70-cm-long channel samples to the deep-sea oxygen isotopic record (Martinson and others, 1987). Isotopic stages are shown in the deep sea record, and their inferred equivalents are shown in the Owens Lake carbonate record. Heavy grey lines in the Owens Lake diagrams show the different responses of the carbonate content and $\delta^{18}\text{O}$ proxies to climate changes associated with the stage 6/5, stage 5/4, and stage 2/1 boundaries. $\delta^{18}\text{O}$ values increase gradually from 145-120 ka while carbonate content abruptly increases at 120 ka. Likewise, from 30-13 ka, $\delta^{18}\text{O}$ again gradually increase (with oscillations) while carbonate content shows a much more abrupt increase at ~15 ka. Both records show abrupt transitions from stage 5 to stage 4.



deep
sea
 $\delta^{18}\text{O}$



Oxygen and Carbon Isotopic Values

The oxygen isotopic composition of carbonates varies between values of -2 and -11‰ (PDB) (Fig. 4.4). Again, as in the case of the carbonate content, the $\delta^{18}\text{O}$ values in the 70-cm-long channel samples display the same overall trends exhibited by the 3-m-long samples (Fig. 4.3). In general, $\delta^{18}\text{O}$ is depleted in the same samples showing low carbonate contents and is enriched in high carbonate samples, with the exception of the interval ~13 to 30 ka in which carbonate values are very low but oxygen isotopic values fluctuate widely (4-8‰ range), and the interval 120-154 ka in which oxygen isotopic value gradually rises while carbonate content remains low. Furthermore, the $\delta^{18}\text{O}$ value is very depleted from 65-70 ka, at 87 ka, and at 96 ka. Carbon isotopic measurements generally mirror the trends in oxygen isotopic composition down the core (Fig. 4.4), and range in value from ~0.5 to a little less than 10‰ (PDB).

Grain Size Analyses

Mean grain size of clastic grains in 70-cm-long channel samples exhibits similar trends to those of previously measured point-samples (Figs. 4.3 and 4.4). However, the point samples tend to show coarser mean grain sizes. This is likely due in part to our neglect of the sand-size fraction in the 70-cm-long channel samples, and in part to the different instrumentation used to measure grain size on these two sample suites. The point samples were analyzed with settling tubes for the sand and gravel fraction, and with a hydrophotometer for the silt and clay fraction (Menking, in press, Chapter 2), while the 70-cm-long channel samples were analyzed by Sedigraph. Mean grain size of 70-cm-channels is very fine (<1 to 3 μm) from ~15-56 ka and again from 120-154 ka, and much coarser (3-16 μm)

from 56-117 ka. This latter interval is marked by frequent fluctuations in grain size, typically with an amplitude of 2-3 μm .

CORRELATIONS AND TIME-SERIES ANALYSIS

In general, the carbonate content, isotopic, and mean grain size measurements closely parallel one another down the core (Fig. 4.4). Formal correlation (Marsal, 1987) shows that all of the proxies are positively correlated at the 99% confidence level for the full suite of samples; Table 4.2 lists the correlation coefficients calculated for the full suite. However, if the data are subsampled, the degree of correlation changes, in some instances becoming negative, and in others showing no correlation. Based on major base-line variations in carbonate content and mean grain size, we divide the dataset into three sections, 7-56 ka, 56-117 ka, and 117-154 ka. Correlation coefficients for these sections are given in Table 4.3. For the depth interval 7-56 ka, carbonate content and mean grain size are strongly correlated in a positive sense with $r = 0.74$. Between 56 and 117 ka, however, the good correlation vanishes ($r = 0.02$), and from 117-154 ka becomes negative. Carbonate content and $\delta^{18}\text{O}$ value are positively correlated from 7-117 ka, before which they show essentially no correlation. $\delta^{18}\text{O}$ and $\delta^{13}\text{C}$ show a strong positive correlation throughout the sample suite, with highest correlation ($r = 0.91$) from 117-154 ka.

Time-series analyses were conducted on the different core subsections using the Arand software package provided by Phillip Howell of Brown University. The data were interpolated and resampled to yield a uniform sampling interval of 300 years between data points; this spacing does not alter the primary data signals. The data were then linearly detrended before time-

TABLE 4.2: Correlation coefficients calculated for the entire suite of 70-cm-long channel samples.

Data sets	r
CaCO ₃ -grain size	0.64
CaCO ₃ - $\delta^{18}\text{O}$	0.63
CaCO ₃ - $\delta^{13}\text{C}$	0.68
$\delta^{18}\text{O}$ -grain size	0.47
$\delta^{13}\text{C}$ -grain size	0.43
$\delta^{18}\text{O}$ - $\delta^{13}\text{C}$	0.77

TABLE 4.3: Computed correlation coefficients for different age ranges in the 70-cm-long channel samples.

Data sets	8-56 ka	56-117 ka	117-154 ka
CaCO ₃ -grain size	0.74	0.02	-0.29
CaCO ₃ - $\delta^{18}\text{O}$	0.63	0.44	+0.01
CaCO ₃ - $\delta^{13}\text{C}$	0.73	0.66	-0.22
$\delta^{18}\text{O}$ -grain size	0.46	0.22	-0.39
$\delta^{13}\text{C}$ -grain size	0.48	0.04	-0.19
$\delta^{18}\text{O}$ - $\delta^{13}\text{C}$	0.55	0.7	+0.91

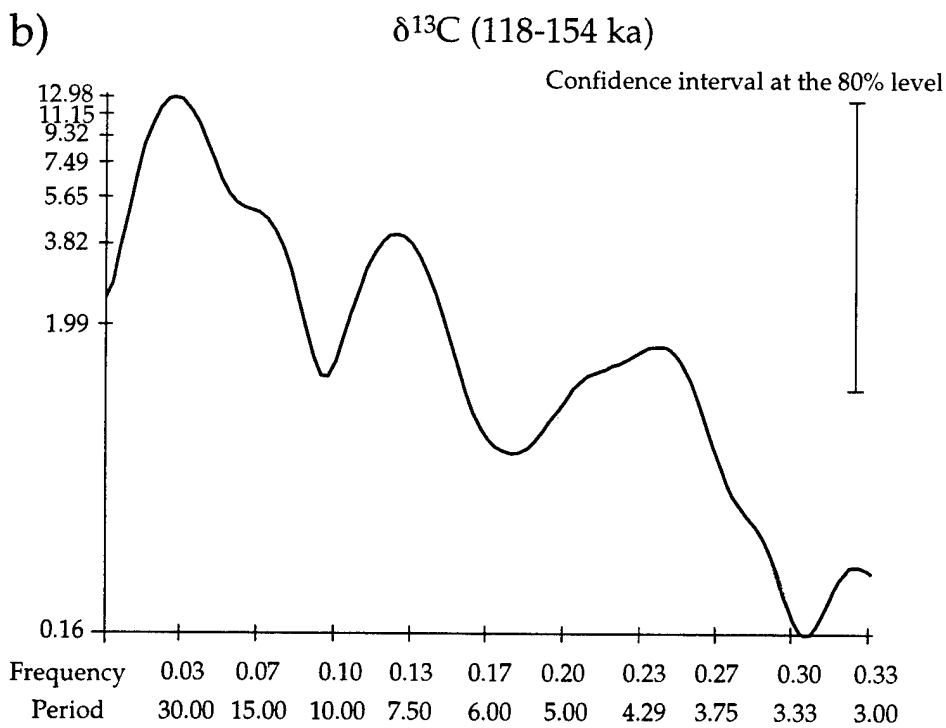
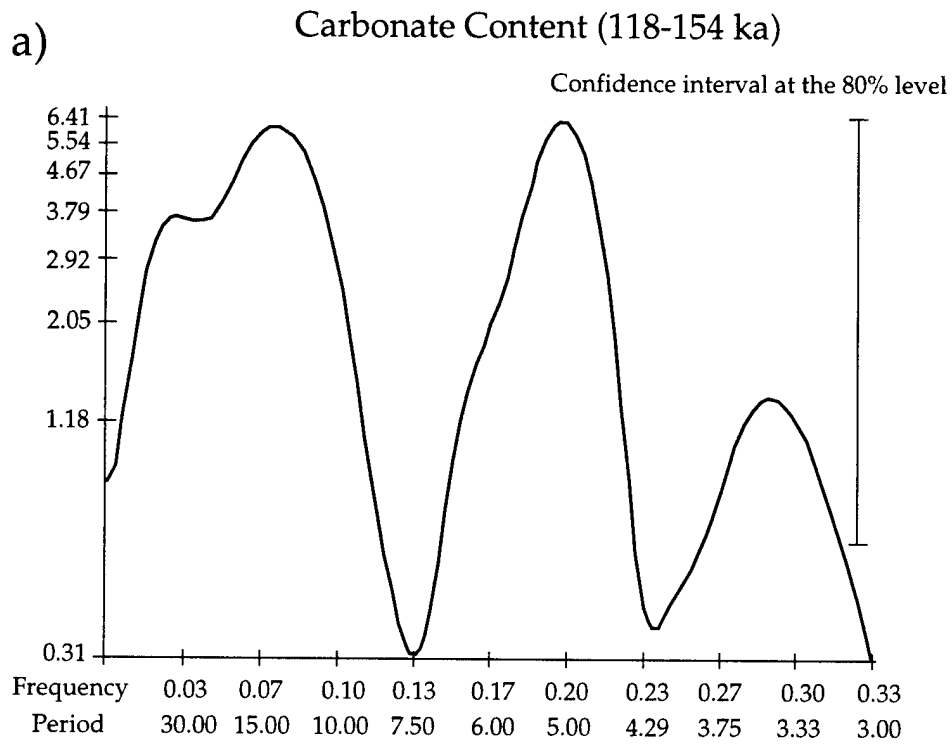
series analysis. Several spectral peaks present above the 80% confidence level recur in the different proxies and time intervals (Fig. 4.5). These include peaks at 24, 11, 5.1, and 4.2 ka; other peaks are also present but do not occur in multiple records. Because we have performed spectral analyses on core subsections with durations of 49-, 61-, and 34 ka, spectral peaks associated with climate cycles longer than approximately half of these lengths are precluded, making the 24 ka spectral peak suspect.

DISCUSSION

The co-variation over the full sample suite of Owens Lake oxygen and carbon isotopes with mean grain size and carbonate content indicates that these proxies are genetically related to one another. However, the computed correlation coefficients for the different core subsections (Table 4.3) also strongly suggest that the mechanisms by which these proxies are related change throughout the core. We turn now to an exploration of the possible relationships between the proxies.

Bischoff and others (in press (a)) have suggested that variations in carbonate accumulation rates in Owens Lake sediments may constrain periods of closed- and open-lake conditions. These authors propose that low carbonate contents (i.e., < 11%) reflect an Owens Lake that is overflowing into the China Lake basin, the water in Owens Lake never becoming sufficiently concentrated to cause significant precipitation of carbonate salts. High carbonate contents (>11%), on the other hand, most likely indicate a lake that is below its sill level and which becomes progressively concentrated in dissolved salts as water is

Fig. 4.5: Example spectral analyses for two different proxy records in the interval 118-154 ka. a) carbonate content, b) $\delta^{13}\text{C}$. The spectral peaks at 5.1 in the carbonate and 4.2 in the carbon isotopic record recur in some other sections of the core and in other proxies.



removed from the lake through evaporation. Implicit in Bischoff and others' (in press (a)) calculations is the assumption that the bulk of the carbonate is precipitated authigenically within Owens Lake rather than being detrital material derived from the White and Inyo Mts. These authors used the carbonate abundance to argue that Owens Lake remained closed for periods lasting up to 50 kyrs, separated by shorter (20-30 kyr) durations of overflow. Given this interpretation of the carbonate content data, it appears as though Owens Lake spilled into the China Lake basin from 13-50 ka, with a possible short interval of closed-lake conditions at 28 ka (Fig. 4.4), and that Owens Lake was closed from 56-117 ka.

Carbonate content and mean grain size show very similar large-scale trends. In general, when carbonate content is low, mean grain size is very fine ($\sim 1 \mu\text{m}$), and high carbonate contents are mirrored by grain sizes that are 4-15 μm coarser. Since low carbonate contents indicate an overspilling Owens Lake, fine mean grain sizes must also indicate a lake at or very near its sill level. Likewise, coarse grain sizes suggest a shallower lake. A close examination of the interval 50-120 ka, however, shows that while both proxies undergo rapid fluctuations (3-5 kyrs), they do not covary. Nor does there appear to be a simple lag between the two records. This may result from the fact that there are other factors contributing to the grain size record besides the position of the shoreline relative to the core site. Aeolian input, ice rafting of material, changes in input material grain size, and turbidity currents, among other factors, may act to obscure the simple relationship between lake stage and grain size of material deposited at the core site (Menking, in press, Chapter 2; Smith, in press).

The relationship between carbonate content and $\delta^{13}\text{C}$ can be understood in terms of salinity fluctuations in Owens Lake. Biological productivity is strongly related to the amount of nutrients, i.e., total dissolved solids, present in lake water. This is readily apparent in the low productivity typical of oligotrophic alpine lakes and the much higher productivity in lakes impacted by farm and urban runoff or evaporation (McKenzie, 1985; Laws, 1993). For Owens Lake, carbonate content is a measure of the salinity (which itself reflects the size of the lake, Bischoff and others, in press (a)); those time periods represented by high carbonate contents reflect more saline and, therefore, more biologically productive episodes in the lake's history than those periods marked by very low contents (Bischoff and others, in press (a)). In addition, carbon isotopic values in water-bodies frequently indicate the extent of primary production in the water column (Stuiver, 1970; Johnson and others, 1991). Aquatic plants prefer ^{12}C , thus leaving the water enriched in ^{13}C . McKenzie (1985) has stated that biological drawdown of CO_2 dissolved in lake waters through primary production can cause supersaturation with respect to calcite, and calcium carbonate precipitation. Because primary production removes ^{12}C and enriches the water column in ^{13}C , carbon isotopic values for the carbonate precipitates tend to become enriched when primary production is active (McKenzie, 1985; O'Shea and others, 1988). In Owens Lake then, periods of high salinity led to great nutrient availability, active biologic productivity, and a consequent enrichment of inorganically-precipitated carbonates in ^{13}C . Low salinity times experienced the converse.

Talbot (1990) compiled stable isotopic data from modern and ancient, and closed and open lakes throughout the world. He found that closed-basin lakes

typically showed high variation in both carbon and oxygen isotopic values through time and that these proxies covaried with a correlation coefficient >0.7 ; the covariation is most likely due to the fact that evaporation causes both an enrichment in oxygen isotopic composition of lake water, and a concentration of nutrients available for primary production (McKenzie, 1985). Open lakes were marked by very little fluctuation in $\delta^{18}\text{O}$ value with changing $\delta^{13}\text{C}$, and with a lower correlation between the two isotopes of <0.7 . Examination of the stable isotopic records from the 70-cm-long channel samples shows a wide variation in isotopic values ($\sim 10\%$ range for each isotope) and a computed correlation coefficient of 0.77 (Fig. 4.6). By Talbot's criteria then, it would appear as though Owens Lake remained closed throughout its lifetime. We know this not to be the case for a variety of reasons. First, lacustrine sequences in China, Searles, and Panamint Lakes require overspill from Owens Lake (Smith, 1984; Droste, 1961b; Bischoff and others, 1985). Secondly, Bischoff and others (in press (a)) showed that the lack of gaylussite and gypsum in the Owens Lake sediments required flushing of salts accumulated in lake water at least every 10-50 kyrs. Menking and Anderson (in prep., Chapter 3) have shown that oxygen isotopic composition of carbonate forming in Owens Lake is sensitive to the amount of runoff flowing into Owens Lake, as well as the evaporation rate. Their results suggest that the $\delta^{18}\text{O}$ value of the carbonates should be depleted during periods of strong overflow, and enriched during episodes of shallow, closed-lake conditions. We therefore apply Talbot's test for open and closed-lake conditions to two subsets of the isotopic data: 1) highly enriched ($>-4\%$) $\delta^{18}\text{O}$ value carbonates (shallow, closed lake-evaporatively concentrated), and 2) highly depleted ($<-7.5\%$) $\delta^{18}\text{O}$ value carbonates (large, overflowing lake). In Figure 4.7

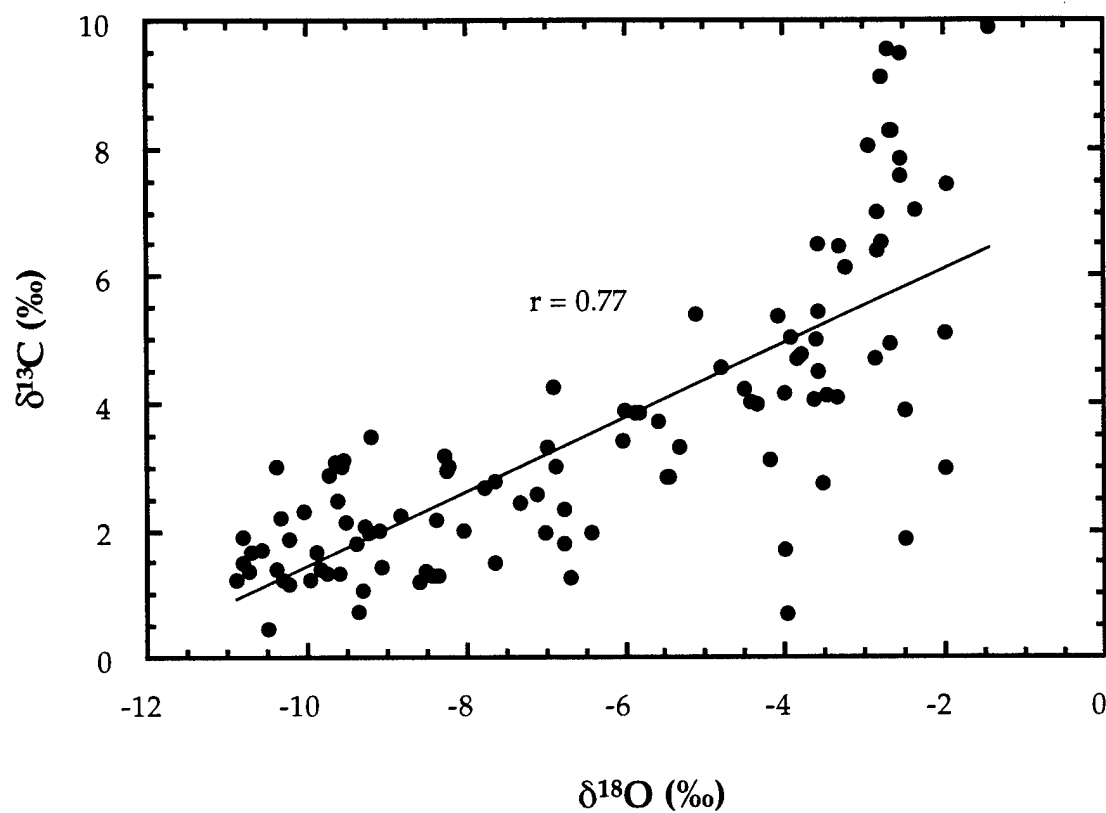


Fig. 4.6: Plot of Owens Lake carbonate $\delta^{18}\text{O}$ versus $\delta^{13}\text{C}$. All samples are shown. The data define a linear trend with a regression coefficient of 0.77. According to the criteria of Talbot (1990), Owens Lake appears to have been closed throughout its lifetime. This is known not to have been the case.

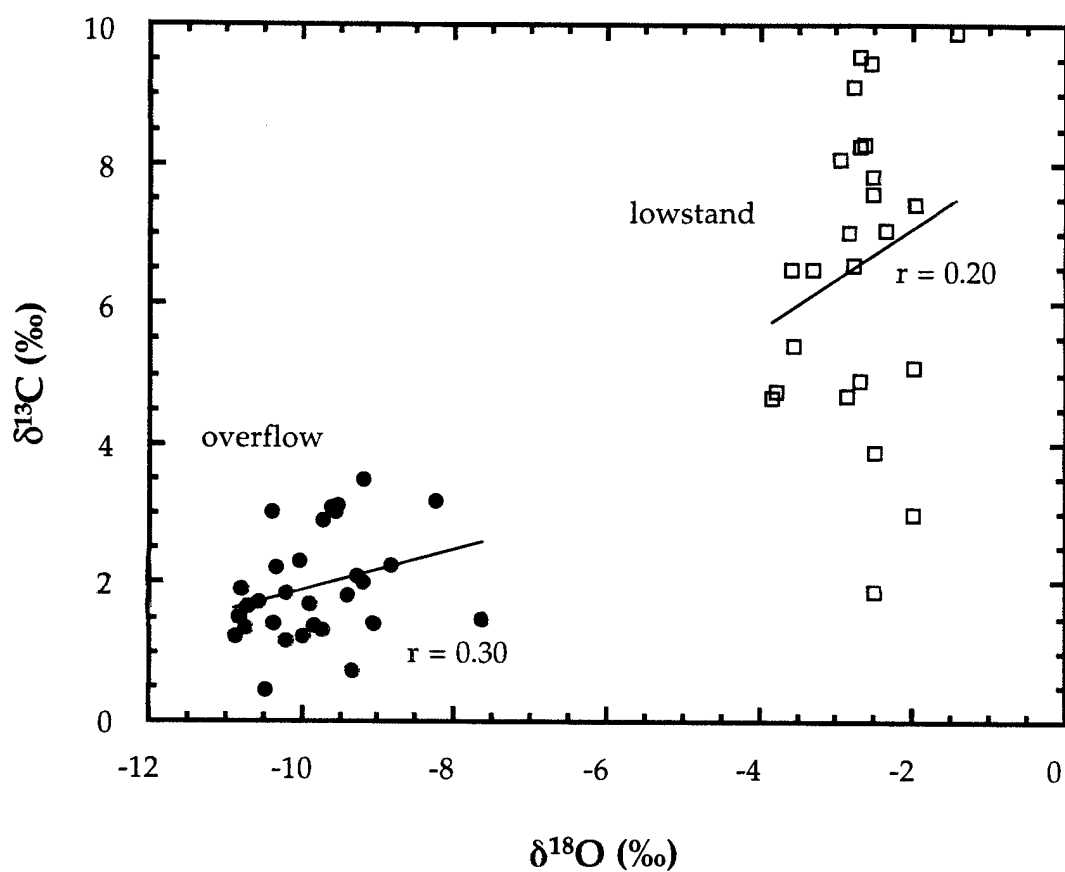


Fig. 4.7: $\delta^{18}\text{O}$ versus $\delta^{13}\text{C}$ for two subsets of data, 1) highly enriched ($>-4\text{‰}$) carbonates probably formed during lake low-stands, and 2) highly depleted ($<-7.5\text{‰}$) carbonates probably formed during episodes of Owens Lake overspill. Also shown are the regression coefficients calculated for the lines that best fit the data.

we show the results of this analysis. The two data subsets plot in different regions on the $\delta^{18}\text{O}$ - $\delta^{13}\text{C}$ graph, but neither has a high correlation coefficient. Indeed, the overflowing-lake data show a higher correlation coefficient than do the closed-lake data, opposite of Talbot's findings. Unfortunately, it appears as though Talbot's test for overflow is not applicable in Owens Lake.

It has been suggested that (Menking and Anderson, in prep., Chapter 3) the $\delta^{18}\text{O}$ value of Owens Lake carbonates should be depleted during periods of strong overflow, and enriched during episodes of shallow, closed-lake conditions. Thus, if CaCO_3 content is also an indicator of overflow (Bischoff and others, in press (a)), variations in $\delta^{18}\text{O}$ should mirror variations in carbonate content. Close examination of the carbonate content and $\delta^{18}\text{O}$ records from the 70-cm-long channel samples (Fig. 4.4) shows that in general, this relationship holds. However, in the interval ~13-30 ka, oxygen isotopic values vary widely while carbonate contents maintain low values. Furthermore, from 120-154 ka, carbonate content again maintains a low value (<5%), rising rapidly to >20% between 118 and 120 ka, a trend which is mirrored in the grain size record. In this same time interval, however, oxygen and carbon isotopes rise gradually. Several possibilities exist to explain the discrepancy between the carbonate content and stable isotope values in these periods. These include: 1) the small percentage of carbonate in glacial-period sediments led to error in measurement of the isotopic values, 2) overspill of isotopically-enriched water from Mono Lake during glacial periods allowed precipitation of very small amounts of isotopically-enriched carbonate in Owens Lake, and 3) isotopically-enriched detrital carbonates from the White and Inyo Mts. washed into Owens Lake and

were not diluted as much by inorganically-precipitated carbonates during glacial periods as during interglacials. We explore these possibilities next.

Measurement error

All samples for stable isotopic analysis were reacted in a Kiel carbonate extraction device in-line with a Finnigan MAT 251 mass spectrometer. This method of isotopic analysis allows samples as small as 10 micrograms CO_2 to be run which corresponds to a CaCO_3 content of 0.1% (Burdett, personal communication). Furthermore, isotopic measurements on low-carbonate samples from Owens Lake core OL-92 were successfully replicated, indicating that the fluctuations in $\delta^{18}\text{O}$ observed in the interval 13-30 ka are in fact real, and not an artifact of small sample sizes giving spurious results.

Overspill from Mono Lake

Lajoie (1968) used core and shoreline evidence to show that Mono Lake went through a pluvial cycle between 34.9 and 12.8 ka and that it may have flowed over its sill into Adobe Valley (Fig. 4.1) at 22 ka. A small lake then formed in Adobe Valley, which drained into an Owens River tributary when it overtopped its sill (Batchelder, 1970). To assess the importance of spillover from Mono and Adobe Lakes to Owens Lake in setting the isotopic composition of Owens Lake, we make use of the water-balance model developed by Menking and Anderson (in prep., Chapter 3). The model incorporates an oxygen isotope subroutine which determines the isotopic composition of Owens Lake water in response to changes in runoff amount and isotopic value, evaporation rate, relative humidity, and isotopic composition of atmospheric water vapor. The

isotopic value of the water is then converted to the isotopic value of inorganically-precipitated carbonate in order to facilitate comparison to measured carbonate $\delta^{18}\text{O}$ values. This calculation assumes equilibrium fractionation between calcite and water at a specified temperature (taken to be mean annual temperature at Owens Lake). We have modified this model to include Mono and Adobe Lakes, and to calculate the evolving isotopic composition of lake water in these lakes in addition to that in Owens Lake. The model uses hypsometric information derived from USGS 3-arc-second digital elevation models to relate the volume of lake water to the surface area, and depth of the lakes in each timestep. For Owens Lake, modern runoff was specified by Los Angeles Department of Water and Power data ($3.98 \times 10^8 \text{ m}^3/\text{yr}$), and modern evaporation rate (1.34 m/yr) calculated by assuming that the historic Owens Lake (14 m depth, and $\sim 290 \text{ km}^2$ surface area prior to diversion of Owens River flow into the Los Angeles aqueduct (Smith and Street-Perrott, 1983)) was in steady-state (Menking and Anderson, in prep., Chapter 3).

Vorster (1985, p. 72) reported the mean annual runoff on gauged streams tributary to Mono Lake as $1.85 \times 10^8 \text{ m}^3/\text{yr}$ (149,696 acre-ft/yr) and estimated the amount flowing in ungauged streams as $4.6 \times 10^7 \text{ m}^3/\text{yr}$ (37,319 acre-ft/yr), for a total of $2.31 \times 10^8 \text{ m}^3/\text{yr}$. He further reported the mean annual evaporation rate at the lake surface as 1.14 m/yr (45 inches/yr, p. 96). We make use of this evaporation rate for both Mono and Adobe Lakes, and assume that Adobe Lake receives water only through overspill from Mono Lake. The modeled Owens Lake is allowed to receive water both from its own drainage basin and through overspill from Adobe Lake. Previous modeling experiments (Menking and Anderson, in prep., Chapter 3), which ignored contributions from Mono and

Adobe Lakes, showed that the measured oxygen isotopic values of carbonate in the 3-m-long channel samples (Benson and Bischoff, 1993) could be best explained by varying runoff between modern and 7x modern values, and evaporation between modern and 70% of modern values using the marine $\delta^{18}\text{O}$ record to scale the fluctuations. In these experiments, runoff was assumed to have increased during glacial periods, while evaporation decreased. The modeling exercise also showed that the amount of and isotopic composition of runoff are of primary importance in setting the isotopic composition of the lake water. Values of calcification temperature and $\delta^{18}\text{O}$ value of atmospheric water vapor, while not negligible, are minor contributors to the carbonate isotopic composition.

In the present modeling experiments, we seek to determine whether addition of Mono-Adobe Lake water to Owens Lake can cause an increase in Owens Lake oxygen isotopic composition of the magnitude called for between 13 and 30 ka (Fig. 4.4). The present experiments show that runoff must be increased by 5.5-fold relative to modern values in order to fill Mono and Adobe Lakes to overflowing if evaporation rate is held at the modern value. If, on the other hand, evaporation rate is decreased by 30%, as is thought to have occurred for the Owens chain of lakes during glacial periods (Smith and Street-Perrott, 1983), a minimum of a 3.6-fold increase in runoff is necessary to cause spill of Mono Lake water into Owens Lake; see Menking and Anderson (in prep., Chapter 3) for the other necessary parameters in the modeling exercise. These values of runoff and evaporation lead to steady-state isotopic values in Mono and Adobe Lakes of slightly greater than 1.5 and 2‰ respectively. The steady-state isotopic

value of Owens Lake depends on the relative proportions of inflow from Adobe Lake and from the Owens Valley drainage basin.

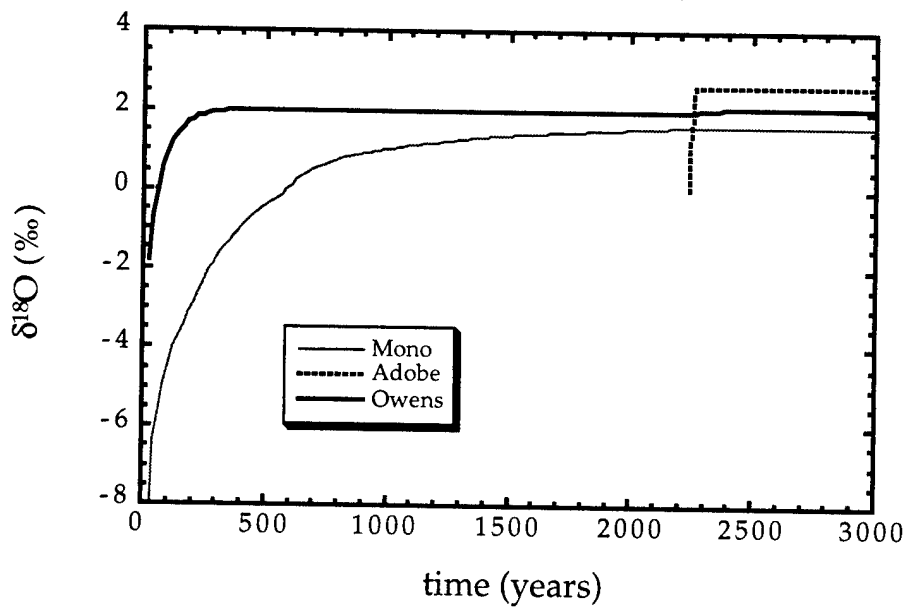
Five different runoff scenarios for the lake chain, and the resulting isotopic composition of lake water are depicted in Figure 4.8. In two of the cases, runoff into Mono Lake is specified as 3.6x modern, and evaporation rates for Mono, Adobe, and Owens lakes are at their assumed glacial values. In the first scenario, Owens Lake receives its modern runoff from the Owens Valley drainage basin, and achieves a steady-state isotopic value of $\sim 2\text{‰}$ in <2500 years. After about 2200 years, Mono Lake has filled to overflowing, a small lake is formed in Adobe Valley, and runoff from that lake feeds into Owens Lake. At this point, enriched Mono-Adobe overspill combines with Owens Valley runoff, but no large change in Owens Lake isotopic composition ensues. The second scenario allows Owens Lake to receive 3.6x modern runoff from its own drainage basin which results in a steady-state isotopic value of -7‰ . Again, after 2200 years, Mono-Adobe overspill flows into Owens Lake, but, as in the case of the 1x modern runoff experiment, the quantity of overspill is so small that no marked change occurs in the Owens Lake water composition.

A second set of experiments allows Mono Lake to receive 7x modern runoff and to experience an 0.7x modern evaporation rate. Owens Lake receives either 7-, 4-, or 1x modern runoff. In all three situations, Mono and Adobe Lakes achieve a steady-state isotopic composition of -5‰ , and overflow from Adobe to Owens Lake begins at about 180 years. In the case in which Owens Lake receives only 1x modern runoff from its own drainage basin, the lake would have achieved a steady-state isotopic value of $\sim 2\text{‰}$. However, overflow from the Mono-Adobe system causes a decline to slightly over 0‰ . The 4x modern runoff

Fig. 4.8: Five modeled scenarios of oxygen isotopic value of Owens Lake water resulting from different combinations of overflowing Mono and Adobe Lake water and Owens Valley drainage basin runoff. First two scenarios allow 3.6x modern flow in Mono and Adobe Lakes, and 70% of modern evaporation rate (assumed glacial evaporation rate). Owens Lake receives either 1x (a) or 3.6x (b) modern runoff from its own drainage basin, and experiences a "glacial" evaporation rate. The contribution of Mono-Adobe runoff to the lake is small compared to the Owens Valley runoff resulting in only a very small enrichment of Owens Lake water when overflow occurs at ~2200 years. The other three scenarios allow 7x modern runoff in Mono and Adobe Lakes, and either 1x (c), 4x (d), or 7x (e) modern flow in Owens Lake. Small enrichments occur in the 4x and 1x modern cases, and a small depletion occurs in the 7x modern case.

a)

Mono 3.6x modern runoff
Owens 1x modern runoff



b)

Mono 3.6x modern runoff
Owens 3.6x modern runoff

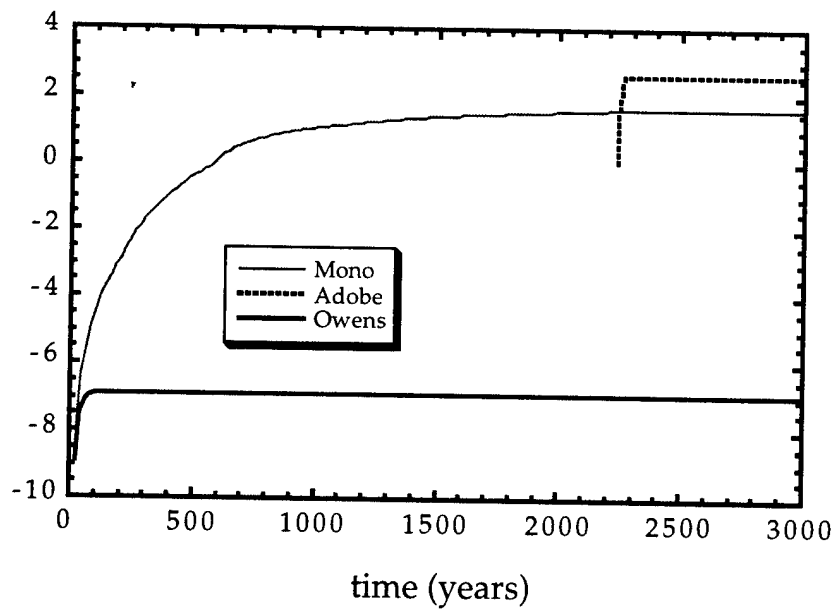


Fig. 4.8 continued:

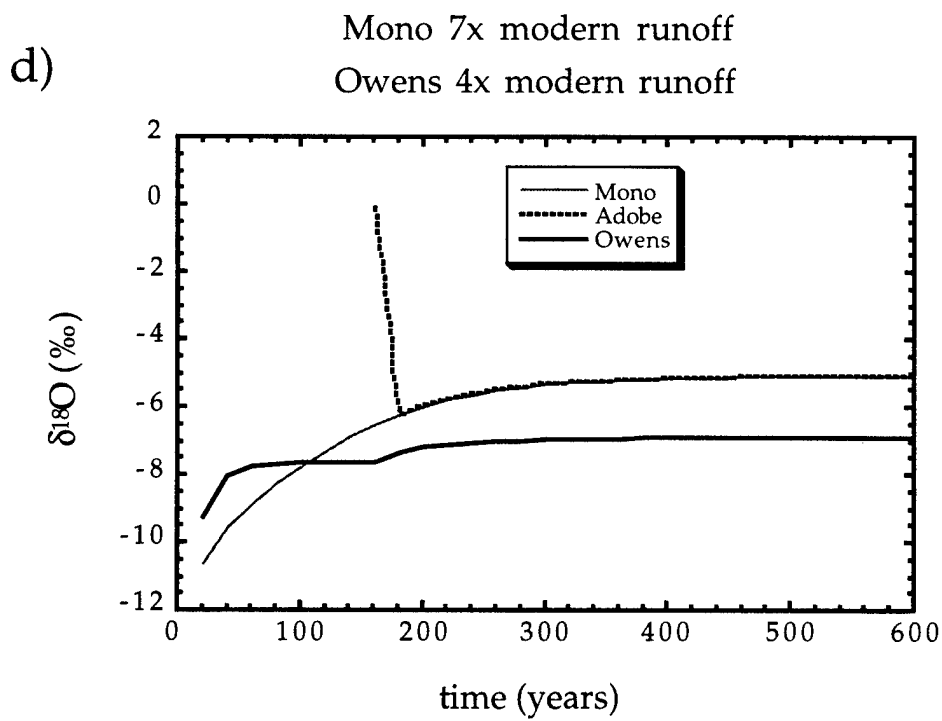
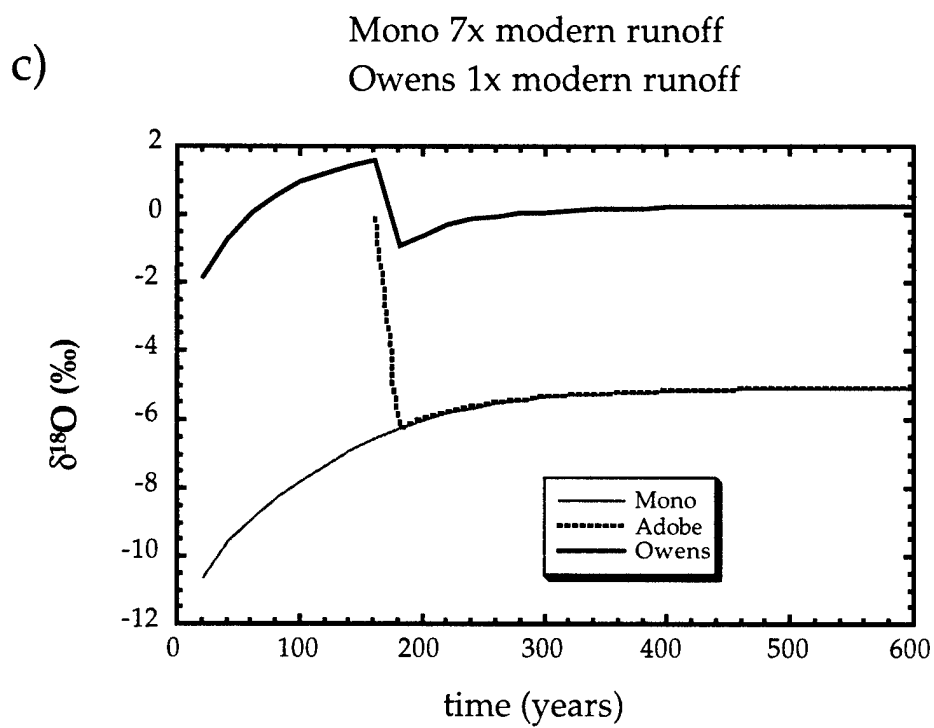
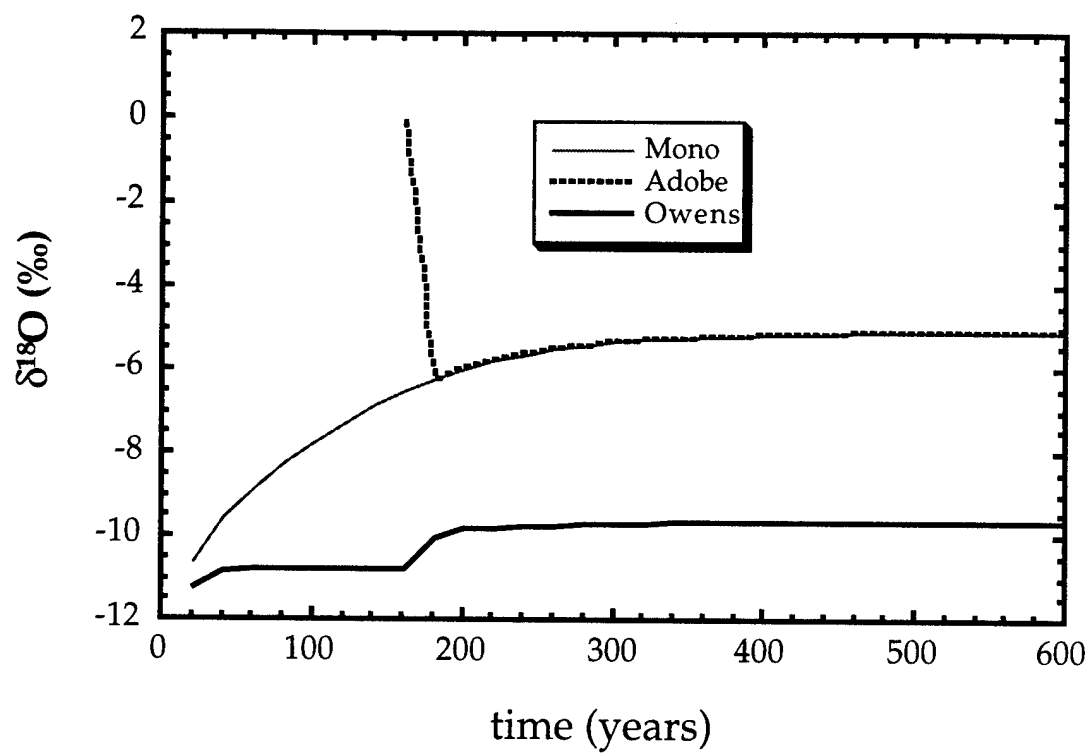


Figure 4.8 continued:

e)

Mono 7x modern runoff
Owens 7x modern runoff



case shows that Owens Lake would achieve a $\delta^{18}\text{O}$ of -7.6‰ in the absence of Mono-Adobe overflow, and a value of -6.9‰ in the presence of such overflow. In the 7x modern runoff case, Owens Lake achieves an initial isotopic composition of ~-11‰, but jumps to -9.5‰ upon the addition of Mono-Adobe overflow.

In all of the above scenarios, addition of Mono-Adobe overflow to Owens Lake changes the $\delta^{18}\text{O}$ value by only 1-2‰ at most, far less than the 4-8‰ fluctuation called upon by the data. Indeed the largest change in Owens Lake isotopic composition occurs in the case in which Mono Lake receives 7x modern runoff while Owens Lake receives 1x modern runoff. It is difficult to imagine a climatic scenario which would allow such a large spatial gradient in runoff response to climate change. Furthermore, this case also shows addition of Mono-Adobe overspill leading to depletion of Owens Lake carbonates, rather than the expected enrichment. Finally, the only scenario which allows Owens Lake to have the proper isotopic value prior to overspill from the Mono-Adobe system is the one in which both Mono and Owens Lakes receive 7x their modern runoff during glacial periods. The overspill from Mono-Adobe leads to a mere 1.5 ‰ enrichment of Owens Lake in this case. For these reasons we doubt the importance of Mono-Adobe overspill in generating the variations in the carbonate $\delta^{18}\text{O}$ value of Owens Lake.

Incorporation of detrital carbonate from the White and Inyo Mts.

The White and Inyo Mountains, which bound Owens Valley on the east side, consist of Proterozoic, Paleozoic, and Mesozoic sedimentary and metasedimentary rocks intruded by Jurassic plutons (McKee and others, 1982;

Conrad and McKee, 1985). Marine limestones and dolomites of various ages outcrop at the surface. Corsetti and Kaufman (1994), Roselle and others (1994), and Bergfeld and others (1992) have measured oxygen and carbon isotopic ratios on rocks from some of the stratigraphic section exposed in these and surrounding mountains [the Cambrian Poleta formation appears to be a major contributor of carbonate rocks, and Corsetti (personal communication) has found oxygen isotopic values of -10 to -15‰, and carbon isotopic values of ~0‰ for this formation; these results are unpublished and are not shown here]. Their results are shown in Figure 4.9 along with isotopic measurements on the carbonates in the Owens Lake core. In general, Proterozoic and Paleozoic marine carbonates appear to be much more depleted in ^{18}O than are late Cenozoic carbonates, reflecting either ongoing equilibration with meteoric waters (Veizer and Hoefs, 1976), burial diagenesis and metamorphism (Corsetti and Kaufman, 1994), or an ancient ocean composition quite different from today's (Veizer and Hoefs, 1976). Comparison of $\delta^{18}\text{O}$ and $\delta^{13}\text{C}$ values for White-Inyo carbonates to Owens Lake core carbonates suggests that the latter are not largely composed of detrital minerals washed into Owens Lake. However, no published isotopic values exist for middle- to upper-Paleozoic and lower-Mesozoic carbonate rocks in the White-Inyo region; caution is therefore warranted in ruling out a detrital source for some of the Owens Lake carbonates.

Veizer and Hoefs (1976) compiled marine limestone and dolomite oxygen- and carbon-isotopic measurements from many different countries, spanning time since the Archean. They found evidence for progressive enrichment of ocean waters over the last 3 Ga with respect to oxygen, but documented large scatter in the data for individual time periods. Carbon isotopes also showed enrichment

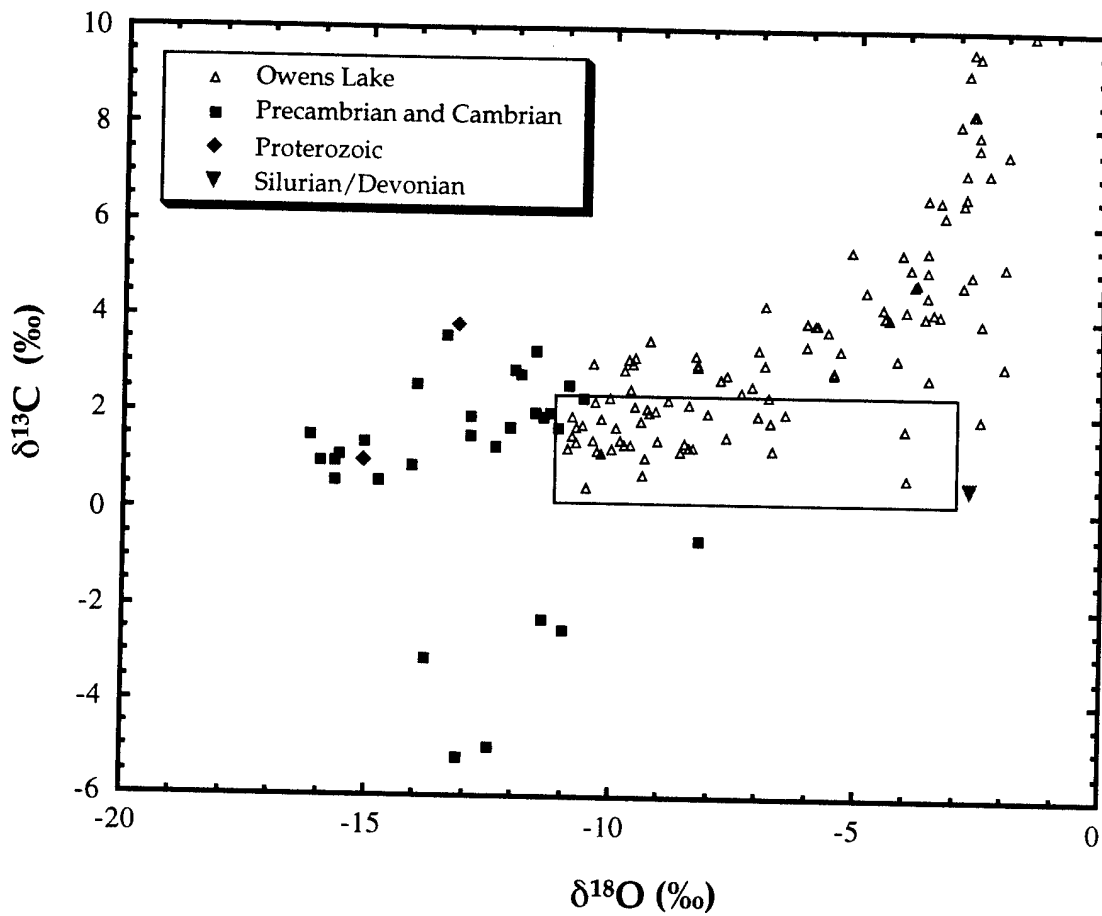


Fig. 4.9: Carbon versus oxygen isotopic composition for White and Inyo Mtn. limestones and dolomites, and for carbonates from the Owens Lake core. The box marks the position where upper Paleozoic and lower Mesozoic carbonates might plot.

toward the present, but by a much smaller degree. This progressive enrichment could lead to upper Paleozoic and lower Mesozoic isotopic values in the White-Inyo Mts. that fall within the boxed area on Figure 4.9, making it possible that some of the Owens Lake carbonates could in fact be detrital in origin. In addition, some of the Owens Lake carbonates may be mixtures of both detrital and authigenically-precipitated carbonates. Measurements of late Paleozoic and early Mesozoic carbonate isotopic values, as well as a study to delineate which White-Inyo formations are likely to provide the most detrital carbonate, are needed to resolve this problem.

In the absence of isotopic data, we can at least assess the contribution of detrital carbonate to Owens Lake from the White-Inyo Mts that would be necessary to generate the magnitude of the variations in $\delta^{18}\text{O}$ within the intervals 10-30 ka and 150-120 ka. We therefore conduct the following exercise. We assume that all of the carbonate in the Owens Lake core is detritally derived. Multiplication of the mass accumulation rate for the core, m , ($\sim 50 \text{ g/cm}^2\text{kyr}$, Bischoff and others, in press (b)) by the carbonate content, cc , constrains the mean accumulation rate of carbonate sediment in the lake. Multiplication by the area of an average Owens Lake, A_L , [here taken to be the average of the historic and highstand lake levels (450 km^2)], yields an estimate of the delivery rate of carbonate to the lakebed through time, f :

$$f = m * cc * A_L \quad (1)$$

Assuming the hypothetical end-member case in which all of the carbonate in the Owens Lake core is detritally derived. division of this value by the total area of

exposed carbonate rocks in the White and Inyo Mts., A_E , constrains the mean mass loss rate per unit basin area from these mountains. Dividing by the density of the carbonate rocks, ρ_c , (here taken to be that of calcite, 2.71 g/cm³) yields the denudation rate, d , necessary to provide Owens Lake with detrital carbonate:

$$d = \frac{f}{A_E * \rho_c} \quad (2)$$

We have used geologic maps (geology mapped onto USGS 15 min. quadrangles including Benton, White Mtn. Peak, Mt. Barcroft, Bishop, Blanco Mtn., Waucoba Mtn., Independence, Waucoba Wash, Keeler, and Darwin) to delineate carbonate units and have measured their areas; a total of ~250 km² of exposed carbonate rock in outcrop appear in the maps. We multiply this value by 2 to account for talus (mapped as Quaternary alluvium) and for the lack of geologic maps for two quadrangles. We find that the average denudation rate over the last 154 ka would have to be in excess of 20 mm/kyr in order for the carbonate in the Owens Lake core to have been derived solely from the White and Inyo Mts. However, in the interval 13-30 ka, the denudation rate would have to fluctuate greatly, between 2 and 13 mm/kyr, and in the interval 120-154 ka, between 1 and 14 mm/kyr.

Consideration of the isotopic record further constrains the calculation. The low carbonate values in these intervals could not have originated from Cambrian and Precambrian rocks in the White-Inyo ranges because the isotopic values, for those carbonates are isotopically too light. Therefore, we must recast the previous analysis in terms of younger and presumably more isotopically-enriched rocks. Examination of geologic maps for the area shows that the

Ordovician, Silurian, Devonian, and Mississippian sections are largely missing from the Owens Valley. About 50 km² of Permian, Triassic and Jurassic limestones, dolomites, and marbles are exposed, however. The five-fold lower area results in an estimate of five-fold higher denudation rates: the denudation rate within the late Paleozoic and Mesozoic White-Inyo carbonate terrain would have to have fluctuated between 9 and 108 mm/kyr, with an average of 42 mm/kyr, in the 13-30 ka interval, and between 3 and 65 mm/kyr, with an average of 24 mm/kyr, in the 120-154 ka section.

Denudation rates in fluvial catchments throughout the world have been compiled by Summerfield and Hulton (1994); these range from 4 to 688 mm/kyr. Granger and Kirchner (1994) have measured denudation rates in a small arid catchment in the Mojave Desert, eastern California. They find values between 35 ± 9 mm/kyr and 99 ± 25 mm/kyr. Likewise, Marchand (1971) determined denudation rates of 10-30 mm/kyr for the White Mountains by observing the amount of material eroded below a marker of known age, and Bierman and others (1993) used cosmogenic radionuclides to determine a bedrock weathering rate of 8 mm/kyr for granites exposed in the central Owens Valley.

Given these values, we cannot exclude the hypothesis that some of the Owens Lake carbonates are detritally derived. The rapid fluctuations in OL-92 isotopic composition from 13-30 ka, however, would require rapid (2-4 ka period) 10- to 20-fold fluctuations or pulses in the denudation rate of the White-Inyos through time. Although no independent data exist to constrain the magnitudes of temporal variations in erosion rates in this area, these variations do seem large. The necessary fluctuations would be even larger if a significant component of the carbonate in the lake is indeed precipitated.

CLIMATIC IMPLICATIONS AND CONCLUSIONS

Results from 70-cm-channels indicate that Owens Lake fluctuated between overflowing fresh, low-productivity water to China Lake, and being a shallow, saline, and highly productive lake. Carbonate content and mean grain size variations show that Owens Lake went through many short-duration (<6 kyr) wetting and drying cycles during the Owens Lake interglacial stage 5 equivalent (50-120 ka). As already mentioned, sample resolution (~1.5 kyr) precludes comparison of these records to the high-resolution ice core and North Atlantic sediment cores. However, as in the case of these latter records, it does appear that Owens Lake has recorded many climatic oscillations with periods below those generally attributed to orbital forcing (20, 40, and 100 ka). The 4.2, 5.1, and 11 ka periods evident in these proxies do not, to our knowledge, correspond to known climatic cycles. Molino and others (1984) found similar short-period fluctuations in pollen records in France and attributed these oscillations to harmonics in the precessional parameter of Earth's orbit. As the timings of the fluctuations in the OL-92 record do not match those documented by Molino and others (1984), it is unlikely that the same mechanisms drive the fluctuations at the two sites.

The transitions from Owens Lake stage 6 equivalent to stage 5 and from stage 5 to stage 4 in the carbonate and mean grain size records are remarkably abrupt, occurring over a mere 2-3000 years. The abrupt transition from stage 6 to stage 5 (Termination II) has been observed in the marine record (Broecker and van Donk, 1970; Imbrie and Imbrie, 1980; Winograd and others, 1992) and is in keeping with the pattern of slow accumulation of ice followed by rapid

deglaciation seen many times over the last 800 ka. The abrupt transition from stage 5 to stage 4 (~4 kyrs), however, is interesting in that it implies that the onset of glacial conditions occurs as rapidly as does the onset of interglacial climates in the Owens Valley drainage basin. None of the OL-92 70-cm-channel sample records show the characteristic "saw-tooth" shape of the marine oxygen isotopic record which has been interpreted (Broecker and van Donk, 1970; Imbrie and Imbrie, 1980; Ruddiman and Wright, 1987; Winograd and others, 1992) as evidence for slow buildup of continental ice followed by rapid retreat. This may be due simply to the fact that we have captured fewer than two full glacial cycles in the data; we do not know if earlier cycles show the "saw-tooth" pattern. An alternative possibility is that different proxy records have different response times to climatic change. The marine oxygen isotopic record, which reflects global ice sheet volume, changes slowly due to the long time constants associated with ice sheet growth and decay (Imbrie and Imbrie, 1980). The Owens Lake records, on the other hand, reflect changing water balance in eastern California, and may change much more rapidly since 1) the smaller mass of the Sierran glacial system should allow it to respond more rapidly to changing temperature and precipitation; and 2) the response time of the Owens Lake is only a few decades (Menking and Anderson, in prep., Chapter 3).

Bischoff and others (in press (a)) pointed out that the transition from glacial stage 6 to interglacial stage 5 (Termination II) occurs ~8 kyrs later in the Owens Lake 3-m-long channel sample records (120 ka) than in the marine oxygen isotope record (128 ka), and ~20 kyrs later than in the Devils Hole chronology (140 ka; Winograd and others, 1992). Because the resolution of the 3-m-long channel samples is approximately 7 kyrs, it was suggested that the chronologic

offset between the datasets might simply be an artifact of the sampling interval or might be due to uncertainty in the OL-92 age-depth model. In the 70-cm-long channel samples (Fig. 4.4), Termination II is markedly abrupt in the grain size and carbonate content records and occurs at 120 ka. These data negate the hypothesis that the offset is due to sampling resolution, and instead require that the offset is either real or due to uncertainty in the age-depth model. However, the oxygen and carbon isotopic records show a much more gradual approach to interglacial conditions lasting from 145 to 120 ka. Indeed, if the isotopic records were used to define the timing of Termination II, that event would be placed at roughly 130 ka, concordant with the marine record. Thus the choice of age for Terminations is proxy-dependent in the Owens Lake records, and may suggest that the carbonate content and grain size parameters are in some way thresholded. In other words, carbonate content and grain size might have continued to exhibit glacial values beyond the time that the climate began changing toward interglacial conditions. In the grain size record, this behavior may be explained by the fact that Owens Lake has a bathtub morphology (Menking, in press), such that the shorelines remain equidistant from the core site regardless of lake surface altitude until lake levels fall below a threshold altitude. From this point onward, small changes in lake altitude may result in large changes in lake surface area, thereby driving the shorelines close to the core site and allowing coarser material to be deposited there. In the case of the carbonate content, Bischoff and others (in press (a)) have reported that CaCO_3 should begin precipitating within Owens Lake within 38 years of cessation of spillover to China Lake, and that within 8-50 kyrs (depending on lake level) the lake should become concentrated enough to precipitate gaylussite. Perhaps,

then, the rapid change in carbonate content at 120 ka reflects the precise moment of transition from an open to a closed Owens Lake (± 38 yrs). The gradual change in oxygen isotopic composition over this same interval may simply be due to the increasing residence time of water in the lake as the amount of runoff from the Sierra Nevada declined (see Menking and Anderson, in prep., Chapter 3, for an explanation of how lake residence time and isotopic composition are affected by runoff quantity).

We have addressed several possibilities to explain the discrepancy between carbonate content and stable isotopic records in the intervals 13-30 ka, and 120-154 ka. The variable response of different proxies to climate change may explain the mismatch in the isotopic and carbonate/grain size records in the interval 120-154 ka. However, the rapid fluctuations in oxygen isotopic values in the interval 13-30 ka during a period of low carbonate content are harder to explain. Oxygen isotopic analyses should be conducted on carbonate rocks from the upper Paleozoic and Mesozoic sections exposed in the White and Inyo Mts. to assess the potential importance of a detrital source for carbonates in these intervals.

ACKNOWLEDGMENTS

The authors wish to thank the following people for assistance in data collection: Jeff Fitts for conducting the sampling and carbonate content analyses, Kathy Vencill for assisting with the grain size analyses, John Fitzpatrick for preparing samples for isotopic analysis, and Jim Burdett for running the isotopic analyses. Many thanks also to Robert S. Anderson for helpful comments on the manuscript.

REFERENCES

- Alley, R.B. and others, 1993, Abrupt increase in Greenland snow accumulation at the end of the Younger Dryas event: *Nature*, v. 362, p. 527-529.
- Antevs, E., 1955, Geologic-climatic dating in the west: *American Antiquity*, v. 20, p. 317-335.
- Atkinson, T.C., Briffa, K.R., Coope, G.R., Joachim, M.J., and Perzy, D.W., 1986, Climatic calibration of coleopteran data, *in* Berglund, B.E., ed., *Handbook of Holocene Palaeoecology and Palaeohydrology*: Chichester, GBR, John Wiley and Sons, p. 851-858.
- Banfield, J.F., Jones, B.F., and Veblen, D.R., 1991, An AEM-TEM study of weathering and diagenesis, Abert Lake, Oregon: II. Diagenetic modification of the sedimentary assemblage: *Geochimica et Cosmochimica Acta*, v. 55, p. 2795-2810.
- Bard., E., Arnold, M., Mangerud, J., Paterne, M., Labeyrie, L., Duprat, J., Melieres, M.-A., Sonstegaard, E., and Duplessy, J.-C., 1994, The North Atlantic atmosphere-sea surface ^{14}C gradient during the Younger Dryas climatic event: *Earth and Planetary Science Letters*, v. 126, p. 275-287.
- Batchelder, G.L., 1970, Post-glacial fluctuations of lake level in Adobe Valley, Mono County, California: *American Quaternary Association Abstracts*, v. 1, p. 7.
- Benson, L.V., 1994, Stable isotopes of oxygen and hydrogen in the Truckee River-Pyramid Lake surface-water system. 1. Data analysis and extraction

of paleoclimatic information: *Limnology and Oceanography*, v. 39, p. 344-355.

Benson, L.V., and Bischoff, J.L., 1993, Isotope Geochemistry of Owens Lake Drill Hole OL-92: U.S. Geological Survey Open-File Report 93-683, p. 106-109.

Benson, L.V., Currey, D.R., Dorn, R.I., Lajoie, K.R., Oviatt, C.G., Robinson, S.W., Smith, G.I., and Stine, S., 1990, Chronology of expansion and contraction of four Great Basin lake systems during the past 35,000 years: *Palaeogeography, Palaeoclimatology, Palaeoecology*, v. 78, p. 241-286.

Benson, L.V., and Paillet, F.L., 1989, The use of total lake-surface area as an indicator of climatic change: examples from the Lahontan Basin: *Quaternary Research*, v. 32, p. 262-275.

Benson, L.V., and Thompson, R.S., 1987a, The physical record of lakes in the Great Basin, *in* Ruddiman, W.F., and Wright, H.E., Jr., eds., *North America and adjacent oceans during the last deglaciation*: Boulder, Colorado, Geological Society of America, *The geology of North America*, v. K-3, p. 241-260.

Benson, L.V., and Thompson, R.S., 1987b, Lake-level variation in the Lahontan Basin for the past 50,000 years: *Quaternary Research*, v. 28, p. 69-85.

Bergfeld, D., Nabelek, P.I., and Labotka, T.C., 1992, Stable isotope evidence for hydrologic conditions during regional metamorphism in the Panamint Mountains, California: *Geological Society of America Abstracts with Programs*, v. 24, p. 249-250.

- Bierman, P., Gillespie, A., Whipple, K., and Clark, D., 1991, Quaternary geomorphology and geochronology of Owens Valley, California: Geological Society of America field trip: Geological Society of America, 1991 Annual Meeting, Guidebook, p. 199-223.
- Bierman, P.R., Massey, C.A., Gillespie, A.R., Elmore, D., Caffee, M., 1993, Erosion rate and exposure age of granite landforms estimated with cosmogenic ^{36}Cl : Geological Society of America Abstracts with Programs, v. 25, p. 141.
- Birman, J.H., 1964, Glacial geology across the crest of the Sierra Nevada, California: Geological Society of America, Special Paper 75, 80 p.
- Biscaye, P., 1965, Mineralogy and sedimentation of recent deep-sea clay in the Atlantic Ocean and adjacent seas and oceans: Geological Society of America Bulletin, v. 76, p. 803-832.
- Bischoff, J.L., Fitts, J.P., and Fitzpatrick, J.A., in press (a), Responses of sediment geochemistry to paleoclimate in Owens Lake, California: an 800 ky record of saline/fresh cycles: submitted to Geological Society of America, Special Paper.
- Bischoff, J.L., Rosenbauer, R.J., and Smith, G.I., 1985, Uranium-series dating of sediments from Searles Lake: Differences between continental and marine climate records: Science, v. 227, p. 1222-1224.
- Bischoff, J.L., Stafford, T.W., Jr., and Rubin, M., in press (b), A time-depth scale for Owens Lake lake sediments of core OL-92: Radiocarbon dates and constant mass-accumulation rate: submitted to Geological Society of America Special Paper.

- Blackwelder, E., 1931, Pleistocene glaciation in the Sierra Nevada and basin ranges: Geological Society of America Bulletin, v. 42, p. 865-922.
- Blackwelder, E., 1933, Lake Manly, an extinct lake of Death Valley: Geographical Review, v. 23, p. 464-471.
- Blackwelder, E., 1954, Pleistocene lakes and drainage in the Mojave region, southern California, *in* Jahns, R.H., ed., Geology of southern California: California Department of Natural Resources, Division of Mines Bulletin 170, p. 35-40.
- Boggs, S., Jr., 1987, Principles of sedimentology and stratigraphy: New York, Macmillan Publishing Company, 784 p.
- Bond, G., Broecker, W., Johnsen, S., McManus, J., Labeyrie, L., Jouzel, J., and Bonani, G., 1993, Correlations between climate records from North Atlantic sediments and Greenland ice: Nature, v. 365, p. 143-147.
- Bradbury, J.P., in press, A diatom-based paleohydrologic record of Owens Lake sediments from core OL-92: submitted to Geological Society of America Special Paper.
- Bradley, R.S., Quaternary Paleoclimatology: Boston, Allen and Unwin, 1985.
- Broecker, W.S., Andree, M., Wolfli, W., Oeschger, H., Bonani, G., Kennett, J.P., and Peteet, D., 1988, The chronology of the last deglaciation: implications to the cause of the Younger Dryas event: Paleoceanography, v. 3, p. 1-19.
- Broecker, W.S., Bond, G., and Klas, M., 1990, A salt oscillator in the glacial Atlantic? 1. the concept: Paleoceanography, v. 5, p. 469-477.

- Broecker, W.S., and van Donk, J., 1970, Insolation changes, ice volumes, and the O¹⁸ record in deep-sea cores: *Reviews of Geophysics and Space Physics*, v. 8, p. 169-197.
- Burbank, D., 1991, Late Quaternary snowline reconstructions for the southern and central Sierra Nevada, California and a reassessment of the "Recess Peak Glaciation": *Quaternary Research*, v. 36, p. 294-306.
- Carter, C., in press, Ostracodes in Owens Lake sediments of core OL-92: Alternation of saline and fresh water forms through time: submitted to *Geological Society of America Special Paper*.
- Chamley, H., 1989, *Clay sedimentology*: New York, Springer-Verlag, 623 p.
- Charles, C.D., Rind, D., Jouzel, J., Koster, R.D., and Fairbanks, R.G., 1994, Glacial-interglacial changes in moisture sources for Greenland; influences on the ice core record of climate: *Science*, v. 263, p. 508-511.
- Conrad, J.E., and McKee, E.H., 1985, Geologic map of the Inyo Mountains wilderness study area, Inyo County, California: U.S. Geological Survey Miscellaneous field studies map MF-1733-A.
- Corsetti, F.A., and Kaufman, A.J., 1994, Chemostratigraphy of Neoproterozoic-Cambrian units, White-Inyo Region, Eastern California and Western Nevada: Implications for global correlation and faunal distribution: *Palaios*, v. 9, p. 211-219.
- Currey, D.R., Oviatt, C.G., Czarnomski, J.E., 1984, Late Quaternary geology of Lake Bonneville and Lake Waring: Utah Geological Association publication 13: Geology of northwest Utah, southern Idaho and northeast Nevada, p. 227-237.

- Densmore, A.L., and Anderson, R.S., 1994, Recent tectonic geomorphology of Panamint Valley, California: *Eos*, v. 75, p. 296.
- Dohrenwend, J.C., 1984, Nivation landforms in the western Great Basin and their paleoclimatic significance: *Quaternary Research*, v. 22, p. 275-288.
- Droste, J.B., 1961a, Clay minerals in the playa sediments of the Mojave Desert, California: California Division of Mines and Geology Special Report 69, 21 p.
- Droste, J.B., 1961b, Clay minerals in sediments of Owens, China, Searles, Panamint, Bristol, Cadiz, and Danby Lake basins, California: *Geological Society of America Bulletin*, v. 72, p. 1713-1722.
- Fairbanks, R.G., 1990, The age and origin of the "Younger Dryas climate event" in Greenland ice cores: *Paleoceanography*, v. 5, p. 937-948.
- Feth, J.H., Roberson, C.E., and Polzer, W.L., 1964, Sources of mineral constituents in water from granitic rocks, Sierra Nevada, California and Nevada: U.S. Geological Survey Water-Supply Paper 1535-I, 70 p.
- Fitzpatrick, J.A., and Bischoff, J.L., 1993, Uranium-series dates on sediments of the high shoreline of Panamint Valley, California: U.S. Geological Survey Open-File Report 93-0232, 15 p.
- Friedman, I., Bischoff, J.L., Johnson, C.A., and Fitts, J.P., in press, Movement and diffusion of pore fluids from Owens Lake sediments in core OL-92: submitted to *Geological Society of America Special Paper*.
- Friedman, I., and O'Neil, J.R., 1977, Compilation of stable isotope fractionation factors of geochemical interest, in *Fleischer, M., Data of Geochemistry*, 6th edition, ch. kk.: U.S. Geological Survey Professional Paper 440, 49 p.

- Folk, R.L., 1968, Petrology of sedimentary rocks: Austin, Texas, Hemphill's, 170 p.
- Folk, R.L., and Ward, W.C., 1957, Brazos River bar (Texas)--a study in the significance of grain size parameters: *Journal of Sedimentary Petrology*, v. 27, n. 1, p. 3-26.
- Gale, H.S., 1914, Salines in the Owens, Searles, and Panamint Basins, Southeastern California: U.S. Geological Survey Bulletin 580, p. 251-323.
- Galehouse, J.S., 1971, Sedimentation analysis, *in* Carver, R.E., ed., Procedures in sedimentary petrology: New York, Wiley-Interscience, p. 69-94.
- Gillespie, A.R., 1982, Quaternary glaciation and tectonism in the southeastern Sierra Nevada, Inyo County, California [Ph.D. thesis]: California Institute of Technology, 695 p.
- Glen, J.M., and Coe, R.S., in press, Paleomagnetism and magnetic susceptibility of Owens Lake sediments in core OL-92: submitted to Geological Society of America Special Paper.
- Gonfiantini, R., Environmental isotopes in lake studies, *in* Fritz, P. and Fontes, J.-C., Handbook of environmental isotope geochemistry: The terrestrial environment, B, p. 113-168: Elsevier, Amsterdam, 1986.
- Granger, D.E., and Kirchner, J.W., 1994, Estimating catchment-wide denudation rates from cosmogenic isotope concentrations in alluvial sediment: For Sage Mountains, California: U.S. Geological Survey Circular 1107, p. 116.
- Greenland Ice-core Project (GRIP) Members, 1993, Climate instability during the last interglacial period recorded in the GRIP ice core: *Nature*, v. 364, p. 203-207.

- Hallberg, G.R., Lucas, J.R., and Goodman, C.M., 1978, Semi-quantitative analysis of clay mineralogy, *in* Hallberg, G.R., ed., Standard procedures for evaluation of Quaternary materials in Iowa: Iowa Geological Survey Technical Information Series No. 8, p. 5-21.
- Hay, R.L., 1966, Zeolites and zeolitic reactions in sedimentary rocks: Geological Society of America Special Paper 85, 130 p.
- Hay, R.L., Guldman, S.G., Matthews, J.C., Lander, R.H., Duffin, M.E., and Kyser, T.K., 1991, Clay mineral diagenesis in core KM-3 of Searles Lake, California: *Clays and Clay Minerals*, v. 39, n. 1, p. 84-96.
- Hay, R.L., and Moiola, R.J., 1963, Authigenic silicate minerals in Searles Lake, California: *Sedimentology*, v. 2, p. 312-332.
- Hodges, K.V., McKenna, L.W., Stock, J., Knapp, J., Page, L., Sternlof, K., Silverberg, D., Wüst, G., and Walker, J.D., 1989, Evolution of extensional basins and Basin and Range topography west of Death Valley, California: *Tectonics*, v. 8, p. 453-467.
- Hollett, K.J., Danskin, W.R., McCaffrey, W.F., and Walti, C.L., 1991, Geology and water resources of Owens Valley, California: U.S. Geological Survey Water-Supply Paper 2370, 77 p.
- Hooke, R.LeB., 1972, Geomorphic evidence for Late-Wisconsin and Holocene tectonic deformation, Death Valley, California: *Geological Society of America Bulletin*, v. 83, p. 2073-2097.
- Hostetler, S.W., and Benson, L.V., 1994, Stable isotopes of oxygen and hydrogen in the Truckee River-Pyramid Lake surface-water system. 2. A predictive model of $\delta^{18}\text{O}$ and $\delta^2\text{H}$ in Pyramid Lake: *Limnology and Oceanography*, v. 39, p. 356-364.

- Hunt, C.F., and Mabey, 1966, Stratigraphy and structure, Death Valley, California: U.S. Geological Survey Professional Paper 494-a, p. 1-162.
- Imbrie, J., Hays, J.D., Martinson, D.G., McIntyre, A., Mix, A.C., Morley, J.J., Pisias, N.G., Prell, W.L., and Shackleton, N.J., 1984, The orbital theory of Pleistocene climate: support from a revised chronology of the marine $\delta^{18}\text{O}$ record, *in* Berger, A.L., and others, eds., Milankovitch and Climate, Part 1: D. Riedel, Hingham, Mass., p. 269-305.
- Imbrie, J., and Imbrie, J.Z., 1980, Modeling the climatic response to orbital variations: *Science*, v. 207, p. 943-953.
- Jannik, N.O., Phillips, F.M., Smith, G.I., and Elmore, D., 1991, A ^{36}Cl chronology of lacustrine sedimentation in the Pleistocene Owens River system: *Geological Society of America Bulletin*, v. 103, p. 1146-1159.
- Johnsen, S.J. and others, 1992, Irregular glacial interstadials recorded in a new Greenland ice core: *Nature*, v. 359, p. 311-313.
- Johnson, T.C., Halfman, J.D., and Showers, W.J., 1991, Paleoclimate of the past 4000 years at Lake Turkana, Kenya, based on the isotopic composition of authigenic calcite: *Palaeogeography, Palaeoclimatology, Palaeoecology*, v. 85, p. 189-198.
- Kahrl, W.L., and others, 1978, The California Water Atlas: State of California, Sacramento, 118 p.
- Ku, T.L., Luo, S., Lowenstein, T.K., Li, J., and Spencer, R.J., 1994, U-series chronology for lacustrine deposits of Death Valley, California: implications for late Pleistocene climate changes: *Geological Society of America abstracts with programs*, v. 26, n. 7, p. A-169.

- Kukla, G. and others, 1988, Pleistocene climates in China date by magnetic susceptibility: *Geology*, v. 16, p. 811-814.
- Kutzbach, J.E., 1987, Model simulations of the climatic patterns during the deglaciation of North America, *in* Ruddiman, W.F., and Wright, H.E., Jr., eds., *North America and adjacent oceans during the last deglaciation*: Boulder, Colorado, Geological Society of America, *The Geology of North America*, v. K-3, p. 425-446.
- Lajoie, K.R., 1968, Late Quaternary stratigraphy and geologic history of Mono Basin, Eastern California, Ph.D. dissertation, University of California, Berkeley, 271p.
- Langbein, W., and others, 1949, Annual runoff in the United States: U.S. Geological Survey Circular 52, 14 p.
- Lao, Y., and Benson, L., 1988, Uranium-series age estimates and paleoclimatic significance of Pleistocene tufas from the Lahontan Basin, California and Nevada: *Quaternary Research*, v. 30, p. 165-176.
- Laws, E.A., 1993, *Aquatic Pollution*: New York, John Wiley and Sons, 611p.
- Li, J., Lowenstein, T.K., Brown, C.B., Ku, T.L., and Luo, S., 1994, Death Valley salt core: Holocene/Late Pleistocene (0-60,000 yr. b.p.) paleoenvironments and paleoclimates: *Geological Society of America abstracts with programs*, v. 26, n. 7, p. A-169.
- Litwin, R.J., Adam, D.P., Frederiksen, N.O., Woolfenden, W.B., *in press*, A palynomorph record of Owens Lake sediments of core OL-92: Preliminary analyses: submitted to *Geological Society of America Special Paper*.
- Loughnan, F.C., 1969, *Chemical weathering of the silicate minerals*: New York, American Elsevier Publishing Company, Inc., 154 p.

- Lowenstein, T.K., Li, J., Brown, C.B., Spencer, R.J., Roberts, S.M., Yang, W., Ku, T.L., and Luo, S., 1994, Death Valley salt core: 200,000 year record of closed-basin subenvironments and climates: Geological Society of America abstracts with programs, v. 26, n. 7, p. A-169.
- Marchand, D.E., 1971, Rates and modes of denudation, White Mountains, Eastern California: American Journal of Science, v. 270, p. 109-135.
- Marsal, D., 1987, Statistics for Geoscientists: New York, Pergamon Press, 176p.
- Martinson, D.G., Pisias, N.G., Hays, J.D., Imbrie, J., Moore, T.C., Jr., and Shackleton, N.J., 1987, Age dating and the orbital theory of the ice ages; development of a high-resolution 0 to 300,000-year chronostratigraphy: Quaternary Research, v. 27, n. 1, p. 1-29.
- McKee, E.H., Diggles, M.F., Donahoe, J.L., and Elliot, G.S., 1982, Geologic map of the White Mountains wilderness and roadless areas, California and Nevada: U.S. Geological Survey Miscellaneous field studies map MF-1361-A.
- McKenzie, J.A., 1985, Carbon isotopes and productivity in the lacustrine and marine environment, *in* Stumm, W., ed., Chemical Processes in Lakes: New York, John Wiley and Sons, p. 99-118.
- Menking, K.M., in press (Chapter 2), Climatic signals in clay mineralogy and grain-size variations in Owens Lake core OL-92, eastern California: submitted to Geological Society of America Special Paper.
- Menking, K.M., and Anderson, R.S., in prep. (Chapter 3), A Model of Runoff, Evaporation, and Overspill in the Owens River System of Lakes, Eastern California.

- Menking, K.M., Musler, H.M., Fitts, J.P., Bischoff, J.L., and Anderson, R.S., 1993a, Sediment size analyses of the Owens Lake core: U.S. Geological Survey Open File Report 93-683, p. 58-74.
- Menking, K.M., Musler, H.M., Fitts, J.P., Bischoff, J.L., and Anderson, R.S., 1993b, Clay mineralogical analyses of the Owens Lake core: U.S. Geological Survey Open File Report 93-683, p. 75-82.
- Meyers, 1962, Evaporation from the 17 western states: U.S. Geological Survey Professional Paper 272-D.
- Mifflin and Wheat, 1979, Pluvial lakes and estimated pluvial climates of Nevada: Nevada Bureau of Mines and Geology Bulletin, n. 94, 57 p.
- Molfino, B., Heusser, L.H., and Woillard, G.M., 1984, Frequency components of a Grande Pile pollen record: Evidence of precessional orbital forcing, *in* Berger, A.L., Imbrie, J., Hays, J., Kukla, G., and Saltzman, B., eds., *Milankovitch and Climate*: Dordrecht, Netherlands, D. Reidel, p. 391-404.
- Moore, D.M., and Reynolds, R.C., Jr., 1989, X-ray diffraction and the identification and analysis of clay minerals: New York, Oxford University Press, 332 p.
- Newton, M., 1991, Holocene stratigraphy and magnetostratigraphy of Owens and Mono Lakes, eastern California [Ph.D. thesis]: University of Southern California, 330 p.
- Orndorff, R.L., and Craig, R.G., 1994, Evaluating proxy-based paleoclimate estimates in the southwestern U.S.: a modeling approach: Geological Society of America abstracts with programs, v. 26, p. A-63.
- O'Shea, K.J., Miles, M.C., Fritz, P., Frap, S.K., and Lawson, D.E., 1988, Oxygen-18 and carbon-13 in the carbonates of the Salina formation of

- southwestern Ontario: *Canadian Journal of Earth Sciences*, v. 25, p. 182-194.
- Oviatt, C.G., McCoy, W.D., and Reider, R.G., 1987, Evidence for a shallow early or middle Wisconsin-age lake in the Bonneville Basin, Utah: *Quaternary Research*, v. 27, p. 248-262.
- Oviatt, C.G., Currey, D.R., and Sack, D., 1992, Radiocarbon chronology of Lake Bonneville, eastern Great Basin, USA: *Palaeogeography, Palaeoclimatology, Palaeoecology*, v. 99, p. 225-241.
- Phillips, F.M., Campbell, A.R., Kruger, C., Johnson, P., Roberts, R., and Keyes, E., 1992, A reconstruction of the water balance in western United States lake basins to climatic change: New Mexico Water Resources Research Institute Technical Completion Report, n. 269, v. 1.
- Phillips, F.M., Zreda, M.G., Smith, S.S., Elmore, D., Kubik, P.W., and Sharma, P., 1990, Cosmogenic chlorine-36 chronology for glacial deposits at Bloody Canyon, Eastern Sierra Nevada: *Science*, v. 248, p. 1529-32.
- Picard, M.D., and High, L.R., Jr., 1972, Criteria for recognizing lacustrine rocks, *in* Rigby, J.K., and Hamblin, W.K., eds., *Recognition of ancient sedimentary environments*: Society of Economic Paleontologists and Mineralogists Special Publication 16, p. 108-145.
- Picard, M.D., and High, L.R., Jr., 1981, Physical stratigraphy of ancient lacustrine deposits, *in* Ethridge, F.G., and Flores, R.M., eds., *Recent and nonmarine depositional environments: models for exploration*: Society of Economic Paleontologists and Mineralogists Special Publication 31, p. 233-259.

- Porter, S.C., Pierce, K.L., and Hamilton, T.D., 1983, Late Wisconsin mountain glaciation in the western United States, *in* Wright, H.E., Jr., ed., Late-Quaternary Environments of the United States, v.1, the Late Pleistocene: Minneapolis, University of Minnesota Press, p. 71-111.
- Roberts, S.M., Spencer, R.J., Yang, W., Krouse, H.R., Lowenstein, T.K., Ku, T.L., and Luo, S., 1994, Paleoclimate of Death Valley, California between 100 and 200 thousand years b.p.: Geological Society of America abstracts with programs, v. 26, n. 7, p. A-170.
- Rogers, D.B., 1993, Saline groundwater circulation and solute balance at Mono Basin, California [Ph.D. thesis]: University of California, Santa Cruz, 226 p..
- Roselle, G.T., Baumgartner, L.P., and Valley, J.W., 1994, Fluid-flow in the Ubehebe Peak contact aureole, Last Chance Mts., California: Geological Society of America Abstracts with Programs, v. 26, p. 225.
- Ruddiman, W.F., Sancetta, C.D., and McIntyre, A., 1977, Glacial/interglacial response rate of subpolar North Atlantic waters to climatic change: The record in ocean sediments: Philosophical Transactions of the Royal Society of London, Series B 280, p. 119-142.
- Ruddiman, W.F., and Wright, H.E., Jr., 1987, Introduction, *in* Ruddiman, W.F., and Wright, H.E., Jr., eds., North America and Adjacent Oceans During the Last Deglaciation: Boulder, Colorado, Geological Society of America, Inc., p. 1-12.
- Sarmiento, R., and Kirby, R.A., 1962, Recent Sediments of Lake Maracaibo: Journal of Sedimentary Petrology, v. 32, no. 4, p. 698-724.

- Sarna-Wojcicki, A.M., Meyer, C.E., and Wan, E., in press, Tephra layers, position of the Matuyama-Brunhes boundary, and effects of Bishop ash eruption on Owens Lake sediments: core OL-92: submitted to Geological Society of America Special Paper.
- Sharp, R.P., 1972, Pleistocene glaciation, Bridgeport Basin, California: Geological Society of America Bulletin, v. 83, p. 2233-2260.
- Smith, G.I., 1984, Paleohydrologic regimes in the southwestern Great Basin, 0-3.2 my ago, compared with other long records of "global" climate: Quaternary Research, v. 22, p. 1-17.
- Smith, G.I., 1993, Core OL-92 from Owens Lake, southeast California, 1.0 Introduction: U.S. Geological Survey Open-File Report 93-683, p. 1-5.
- Smith, G.I., in press, Stratigraphy, lithology, and sedimentary structures of Owens Lake core OL-92: submitted to Geological Society of America Special Paper.
- Smith R.S.U., 1976, Late-Quaternary pluvial and tectonic history of Panamint Valley, Inyo and San Bernardino Counties, California, Ph.D. dissertation, California Institute of Technology, 295 p.
- Smith, G.I., and Bischoff, J.L., in press, Core OL-92 from Owens Lake: Project rationale, geologic setting, drilling procedures, and summary: submitted to Geological Society of America Special Paper.
- Smith, G.I., Bischoff, J.L., and Bradbury, J.P., in press, Paleoclimatic interpretation of the Owens Lake sedimentary record from core OL-93: submitted to Geological Society of America Special Paper.

- Smith, G.I., and Pratt, W.P., 1957, Core logs from Owens, China, Searles, and Panamint basins, California: U.S. Geological Survey Bulletin, B 1045-A, p. 1-62.
- Smith, G.I., and Street-Perrott, F.A., 1983, Pluvial Lakes in the Western United States, *in* Wright, H.E., Jr., ed., Late Quaternary Environments of the United States: Minneapolis, University of Minnesota Press, p. 190-211.
- Spaulding, W.G., and Graumlich, L.J., 1986, The last pluvial climatic episodes in the desert of southwestern North America: *Nature*, v. 320, p. 441-444.
- Stamm, J.F., 1991, Modeling local paleoclimates and validation in the southwest United States, Ph.D. thesis, Kent State University, Kent, Ohio, 325 p.
- Stine, S., 1994, Extreme and persistent drought in California and Patagonia during mediaeval time: *Nature*, v. 369, p. 546-549.
- Stuiver, M., 1970, Oxygen and carbon isotope ratios of fresh-water carbonates as climatic indicators: *Journal of Geophysical Research*, v. 75, p. 5247-5257.
- Summerfield, M.A., and Hulton, N.J., 1994, Natural controls of fluvial denudation rates in major world drainage basins: *Journal of Geophysical Research*, v. 99, p. 13,871-13,883.
- Surdam, R.C., 1977, Zeolites in closed hydrologic systems, *in* Mumpton, F.A., ed., Mineralogy and geology of natural zeolites: Mineralogical Society of America Short Course Notes, v. 4, p. 65-91.
- Talbot, M.R., 1990, A review of the palaeohydrological interpretation of carbon and oxygen isotope ratios in primary lacustrine carbonates: *Chemical Geology*, v. 80, p. 261-279.

- Thompson, R.S., Benson, L., and Hattori, E.M., 1986, A revised chronology for the last Pleistocene lake cycle in the central Lahontan Basin: *Quaternary Research*, v. 25, p. 1-9.
- Torresan, M.E., 1987, A review and comparison of the hydrophotometer and pipette methods in the analysis of fine-grained sediment: U.S. Geological Survey Open-File Report 87-514, 38 p.
- Veizer, J., and Hoefs, J., 1976, The nature of O^{18}/O^{16} and C^{13}/C^{12} secular trends in sedimentary rocks: *Geochimica et Cosmochimica Acta*, v. 40, p. 1387-1395.
- Vorster, P., 1985, A water balance forecast model for Mono Lake, California, Masters Thesis, California State University, Hayward, 350p.
- Waite, R.B., Jr., 1980, About forty last-glacial Lake Missoula jökulhlaups through southern Washington: *Journal of Geology*, v. 88, p. 653-679.
- Waite, R.B., Jr., 1985, Case for periodic, colossal jökulhlaups from Pleistocene glacial Lake Missoula: *Geological Society of America Bulletin*, v. 96, p. 1271-1286.
- Wentworth, C.K., 1922, A scale of grade and class terms for clastic sediments: *the Journal of Geology*, v. 30, n. 5, p. 377-392.
- Winograd, I.J., Coplen, T.B., Landwehr, J.M., Riggs, A.C., Ludwig, K.R., Szabo, B.J., Kolesar, P.T., and Revesz, K.M., 1992, Continuous 500,000-year climate record from vein calcite in Devils Hole, Nevada: *Science*, v. 258, p. 255-260.